Molecular Actions of Pyrethroids on Ion Channels in the Maize Weevil, *Sitophilus zeamais*

Rubia Aparecida de Araujo

Thesis submitted to the University of Nottingham for the degree of

Doctor of Philosophy

August 2010

Abstract

Previous studies on the mechanism of action of pyrethroids have confirmed that voltage-gated sodium channels (VGSC) in the axon membrane are the major target site of these compounds. The use of pyrethroids to control maize weevils, *Sitophilus zeamais,* a major pest of stored maize in Brazil, has led to the occurrence of resistance. The work described here seeks to establish whether changes in VGSC of *S.zeamais* can explain pyrethroid resistance.

The *S. zeamais* homologue of the *Drosophila para* VGSC was identified using degenerate primers and sequenced. Resistance mutations were examined by sequencing the IIS4-IIS6 region of the gene from laboratory strains of susceptible and resistant insects, revealing one amino acid replacement (T929I). The T929I mutation has been identified in other insects but always associated with a second mutation together producing a highly resistant phenotype. The occurrence of T929I in isolation is rare. DNA-based diagnostic assays were designed to screen weevils for the T929I mutation and analyse Brazilian field populations revealing a low frequency of heterozygous individuals carrying the mutation.

The effect of the T929I mutation on VGSC function was investigated using whole cell patch clamping on cultured neurons isolated from thoracic ganglia of wild-type and resistant weevils. Inward currents were recorded by depolarizing the neuron to test potentials in the range -70mV to +70mV in 10mV increments for 25ms from a holding potential of -80mV. Current amplitudes were similar in cells from resistant weevils however other changes

were apparent, notably a significant depolarizing shift in the voltage-dependence of activation of sodium currents in the resistant animals ($P<0.05$). Mutant neurons are also less sensitive to deltamethrin than the wild types.

Acknowledgments

I specially would like to thank my supervisor, Dr Ian Duce, for receiving me in his laboratory and making me feel at home since the beginning of my PhD. Thank you so much for your support and guidance.

I am really grateful to Dr Ian Mellor, for his patience and valuable advice during the course of my research and in the writing up process.

Thanks to my colleagues at Rothamsted Research: Dr Martin Williamson, Dr Chis Bass, Professor Lin Field, Dr Emyr Davies, Dr Mirel Puinean, Dr Joanna Amey, for their advice and friendship.

I also would like to thank my MSc supervisor, Dr Raul Narciso Carvalho Guedes, my source of inspiration, for his endless encouragement and supervision.

All the other members of the laboratory: Professor Peter Usherwood, Tim Smith, Paul, David and Mark.

All my friends in and outside Nottingham, especially Eugenio, for his priceless advice; Nicoleta and Tina, for the wonderful time we spent in Nottingham; and Charu, for all her support and precious friendship.

All my colleagues from Derby Hall: particularly Professor Charles and John.

To Michal, for all his love, affection and encouragement during the final stage of my PhD.

To all my family, specifically my mums Judite and Gorete, without whom I could not have done this.

Lastly, I would like to thank CAPES Foundation, Ministry of Education of Brazil, for the financial support.

Abbreviations

4-AP	4-amino-pyridine
ATP	adenosine-5’-triphosphate
ATX	sea anemone toxin II
bp	base pair
C	celsius
cDNA	complementary deoxyribonucleic acid
DDT	dichloro diphenyl tricloroethane
DMSO	dimethylsulphoxide
DNA	deoxyribonucleic acid
dNTP	deoxynucleotide triphosphate
dsDNA	double-stranded deoxyribonucleic acid
DTT	dithiothreitol
EC_{50}	half maximal effective concentration
EDTA	ethylene diamine tetra-acetic acid
EGTA	ethylene glycol tetraacetic acid
FBS	foetal bovine serum
h	hour
HRM	high resolution melt
Hz	hertz
Kdr	knockdown resistance
kHz	kilohertz
M	molar
MΩ	megaohm
mg	milligram
min	minute

ml	millilitre
mm	millimeter
mM	millimolar
ms	millisecond
mV	millivolts
µg	microgram
µl	microlitre
µM	micromolar
ng	nanogram
nm	nanometer
nM	nanomolar
pA	picoampere
PCR	polymerase chain reaction
RFLP	restriction fragment length polymorphism
RH	relative humidity
RNA	ribonucleic acid
rpm	revolutions per minute
RT-PCR	reverse transcription polymerase chain reaction
s	second
SAC	stretch-activated channel
SDS	sodium dodecyl sulphate
SEM	mean ± standard error of the mean
SDW	sterile de-ionized water
SNP	single nucleotide polymorphism
ssDNA	single-stranded deoxyribonucleic acid
TAE	tris acetate EDTA
TBE	tris borate EDTA
TEA	tetraethylammonium
T_M	temperature of melting

TRP	transient receptor potential
TTX	tetrodotoxin
U	unit
UV	ultraviolet
V	volts
V_{50}	voltage at '50% level' of given parameter
V_h	holding potential
V_{rev}	reversal potential
V_t	test potential
w/v	weight per volume

Content

Chapters **Page**

1. Introduction

1.1. Insecticides 14

1.2. Pyrethroids 17

1.2.1. Pyrethrum flowers and the chemical study of natural pyrethrins 17

1.2.2. Development of synthetic pyrethroids 19

1.2.2.1. Characteristics and classification 20

1.2.2.2. Site of action 22

1.3. Voltage-gated sodium channels 24

1.3.1. Sodium channels derived from mammalian systems 24

1.3.2. Insect sodium channels 29

1.3.3. Effect of pyrethroids on sodium channels 31

1.4. Insecticide resistance 35

1.4.1. Pyrethroid insensitivity to the target site 35

1.4.2. Real-time PCR for detection of mutant insects in the field 40

1.5. The maize weevil 43

1.5.1. Biology 44

1.5.2. Control 45

1.5.3. Insecticide resistance in *S. zeamais* 46

1.6. Aims and Objectives 47

2. Materials and Methods

2.1. Maize weevil populations 50

2.2. Molecular biology 54

2.2.1. RT-PCR analysis of *S. zeamais* sodium channel gene sequences 54

2.2.1.1. Total RNA extraction 54

2.2.1.2. cDNA synthesis 54

2.2.1.3. PCR protocol 55

2.2.1.4. Gel electrophoresis 57

2.2.1.5. Purification of PCR products 57

2.2.1.6. DNA sequencing 58

2.2.2. Insecticide bioassay to select resistant individuals 58

2.2.3. Extraction of genomic DNA and analysis of gene fragments 59

2.2.4. Diagnostic assays for insecticide resistance 60

2.2.4.1. Preparation of 96 sample reference plate 60

2.2.4.2. Taqman SNP genotype assay 61

2.2.4.3. High Resolution Melt (HRM) assay 62

2.2.4.4. PCR RFLP (Restriction Fragment Length Polymorphism) 64

2.3. Light and electron microscopy 65

2.4. Neurons of *S. zeamais* 66

2.4.1. Isolation of nervous cells and short term culture 66

2.4.2. Coating Petri dishes 68

2.5. Whole-cell patch-clamping 69

2.5.1. Basic properties of ion channels 73

2.5.2. Pyrethroid treatment of sodium channels 74

2.6. Voltage protocols 74

2.7. Data analysis 78

3. Identification of a Super-*kdr* Mutation in the *Sitophilus zeamais para* Sodium Channel Gene Associated with Pyrethroid Resistance.

3.1. Introduction 80

3.2. RT-PCR analysis of the IIS4-IIS6 region of the *S. zeamais para* sodium channel gene sequences 83

3.2.1. Extraction of total RNA, cDNA synthesis and amplification 83

3.2.2. Purification of PCR product 86

3.2.3. Maize weevil *para* sodium channel gene from cDNA 87

3.3. Design of the maize weevil-specific *para* primers 89

3.4. Selecting resistant individuals 91

3.5. Genomic DNA extraction and gene fragment analysis 92

3.5.1. Amplification of genomic DNA and purification of PCR products 92

3.5.2. *Para* IIS4-IIS6 sodium channel gene from maize weevil genomic DNA 93

3.5.3. Super-*kdr* mutation in the maize weevil *para* sodium channel gene 95

3.6. Discussion 97

4. Diagnostic assays for detection of the super-*kdr* mutation in field-collected populations of *Sitophilus zeamais* from Brazil

4.1. Introduction 105

4.2. Diagnostic assays for insecticide resistance 107

4.2.1. Taqman assay 107

4.2.2. High Resolution Melt (HRM) 111
4.2.3. PCR RFLP (Restriction Fragment Length Polymorphism) 115
4.3. Discussion 117

5. Electrophysiological Characterization of Voltage-Gated Ion Channels in Maize Weevils

5.1. Introduction 121
5.2. Understanding the organization of the cells in the thoracic ganglia is important for isolation of neurons 123
5.2.1. Light microscopy 124
5.2.2. Transmission electron microscopy 125
5.3. Ion channels are induced by depolarization 127
5.4. Electrophysiological studies require efficient cell adhesion to the surface of the Petri dish 131
5.4.1. Con A promotes adhesion without affecting the inward current 132
5.5. TTX blocks the inward currents 134
5.6. Outward currents in *S. zeamais* neurons are highly resistant to blockade 137
5.6.1. Conventional potassium channel blockers do not completely block outward currents in *S. zeamais* neurons 137
5.6.2. Red Sea soft coral toxin does not inhibit the persistent outward current 140
5.6.3. Persistent outward current is unaffected by other cation channel blockers 144
5.7. Discussion 147

6. Electrophysiological Investigation of Super-*kdr* Resistance in *Sitophilus zeamais* and the Action of Pyrethroids

6.1. Introduction 154

6.2. Super-*kdr* sodium channels show a depolarising shift in the activation voltage 156

6.3. Deltamethrin causes a hyperpolarising shift in the activation voltage in wild-type sodium channels 158

6.4. Sodium channel sensitivity to deltamethrin is reduced by the super-*kdr* mutation 161

6.5. Fast inactivation 165

6.6. Discussion 170

7. Conclusions and Future Directions

7.1. Molecular characterization of the maize weevil *para* sodium channel gene 178

7.2. Resistance management and maize weevil control 179

7.3. *S. zeamais* neurons form a heterogeneous population 182

7.4. Electrophysiological characterization of sodium channels from maize weevil neurons 184

References 188

Appendix 217

Chapter 1

Introduction

1.1. Insecticides

There are approximately 1,000,000 species of insects in the natural world. About 10,000 species are crop-eating, with 700 causing most of the insect damage to crops worldwide – both in the field and in storage (Ware, 1994). It is believed that primitive human ancestors used mud and dust spread over their skin to repel biting and tickling insects, a practice that resembles the habits of water buffalo, pigs and elephants (Mariconi, 1985; Ware, 1994). These materials were the first ones that could be classed as insect control agents (repellents). During human history other materials have been used to control insects, including gall from a green lizard to protect apples from worms and rotting, extracts of pepper and tobacco, hot water, soapy water, whitewash, vinegar, turpentine, fish oil, brine and many others (Takayama, 2008). Some decades ago, the insecticide supply was limited to agents such as pyrethrum, sulphur, arsenicals, petroleum oils, cryolite, nicotine and hydrogen cyanide gas. However, the Second World War launched the "Chemical Era" with the introduction of synthetic organic insecticides, with DDT as the flagship (Ray, 2010).

Since then, a number of classes of synthetic insecticides have been discovered and developed based on different mechanism of actions:

a) Organochlorines: neurotoxic insecticides including the cyclodienes and hexachlorocyclohexane which act to block chloride channels and DDT which targets the voltage-gated sodium channels in the axon membrane. These chemicals, which were acknowledged as very useful

insecticides, are now widely banned due to their high persistence in the environment and they have been reported to affect human health, agriculture and the environment (Smith, 2010; Ray, 2010).

b) Organophosphates: neurotoxic insecticides which act on synapses by inhibiting the enzyme acetylcholinesterase. This group replaced the organochlorines in many applications. They are generally the most toxic of all pesticides to vertebrate animals (Chambers *et al*., 2001).

c) Carbamates: they also inhibit the enzyme acetylcholinesterase and share some of the adverse effects on the vertebrate nervous system (Ecobichon, 2001).

d) Pyrethroids: neurotoxic insecticides with the same site of action as DDT, i.e., the voltage-gated sodium channels in the axon membrane. As this class of insecticide is the topic of this study, it will be considered in more detail (Temple & Smith, 1996, Ray, 2010).

e) Neonicotinoids: the most recently introduced major class of insecticides act as agonists of nicotinic acetylcholine receptors and are now in widespread use (Jeschke & Nauen, 2005).

f) A range of other synthetic insecticides have been developed and have made a variable contribution to crop protection and public and animal health worldwide including: i. Organosulphurs: work as inhibitors of ATP synthesis; ii. Formamidines: act as agonists of octopamine receptors; iii. Cartap derived from nereistoxin: inhibits acetylcholine receptors; iv. Oxadiazines such as indoxacarb: block voltage-gated sodium channels; v. Phenylpyrazoles such as fipronil: blocks chloride

channels; vi. Fluorinated sulphonamides, Thioureas and Chlorfenapyr: act on respiratory metabolism; vii. Spirocyclic tetronic acid: inhibit lipid synthesis; viii. Juvenoids: synthetic analogues of juvenile hormone; ix. Acylureas: insect growth regulators (McAteer et al., 2008; Pfeiffer, 2008).

g) Synergists: many commercial formulations of synthetic insecticides contain synergists such as piperonyl butoxide which synergise the actions of the toxicant by inhibiting enzymes responsible for breakdown of the insecticide (Casida & Quistad, 1998; Ishaaya & Horowitz, 1998; Blasi, 1999).

Natural products may also provide a commercially important source of insecticides, particularly when their production can be linked to biotechnological methods or expression in genetically modified plants. They can be divided into 4 groups: 1. Botanicals: nicotine, rotenone, sabadilla, azadirachtin, ryania, limonene, pyrethrum and pyrethrins; 2. Animal origin: juvenoids and anti-juvenile hormone; 3. Microbials: milbemycin, avermectins, spinosyns, toxin of *Bacillus thuringiensis* and viral insecticides; 4. Inorganic: sulphur and fumigants (Isman, 2005; Dhadialla et al., 2005; Khachatourians, 2009; Gonzalez-Coloma *et al.*, 2010).

1.2. Pyrethroids

Pyrethroid insecticides have been used in agricultural and home formulations for more than 30 years and account for approximately one quarter of the worldwide insecticide market (Casida and Quistad 1998). The study of pyrethroid chemistry started about 1910, and since then, has involved two main periods. In the first period, the chemical structure of natural pyrethrins was elucidated, and based on knowledge gained a number of synthetic pyrethroids were invented in the second period.

1.2.1. Pyrethrum flowers and the chemical study of natural pyrethrins

Pyrethrum flowers belong to the genus *Tanacetum* or *Chrysanthemum*, with two kinds of species, one with white flowers and other with red flowers. However, only white flowers *Tanacetum* (*Chrysanthemum) cinerariaefolium* (Vis) contain the insecticidal active components (Katsuda, 1999). It is believed that pyrethrum was discovered in 1694 in the former Yugoslavia, but only in the 1840s was the insecticidal activity of this plant confirmed. Thereafter, pyrethrum cultivation started in United States of America and Japan, with the latter leading the production of these flowers for many decades.

The insecticidal active component from pyrethrum flowers was separated by Fujitani (1909) and called 'pyrethron'. In the following years, other

researchers (Yamamoto, 1923, 1925; Staudinger & Ruzicka, 1924; LaForge & Barthel, 1945) modified the chemical structure of this pyrethron and discovered the natural pyrethrins, with six active ingredients: pyrethrins-I, -II, cinerins-I,-II, and jasmolins-I,-II (Figure 1-1). These are ester compounds formed from acid and alcohol moieties. After the chemistry of natural pyrethrins was clarified, a model for the development of synthetic compounds became available. Pyrethrin and its synthetic derivatives were all called pyrethroids.

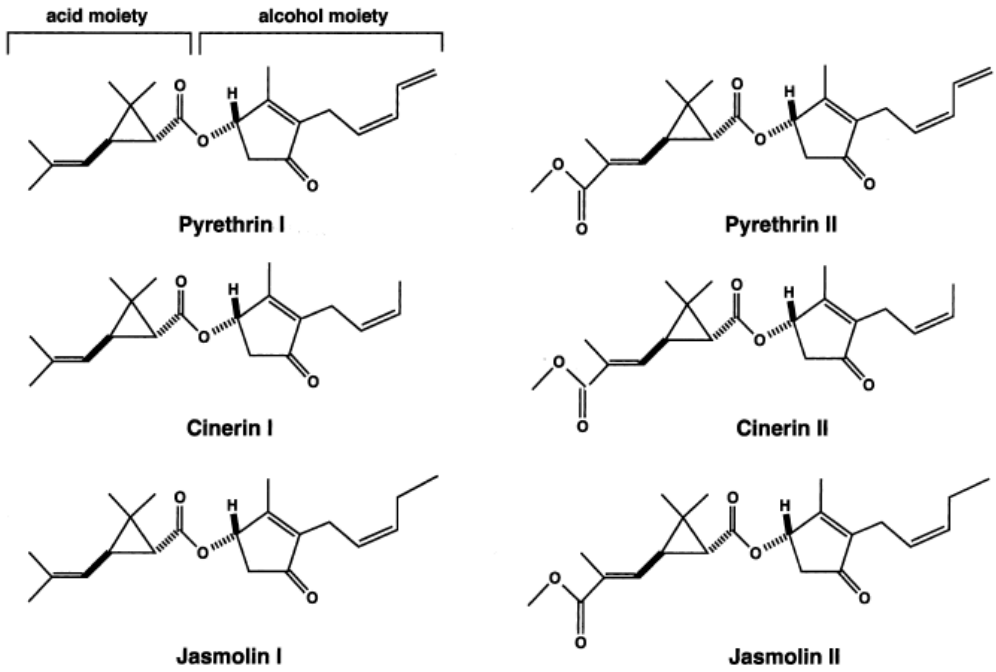

Fig.1-1: Structures of the six natural pyrethrins.

1.2.2. Development of synthetic pyrethroids

Many useful compounds were derived from the structural modification of the natural pyrethrin-I, but the major investigation was made by Schechter in 1949 (Naumann, 1990). He synthesized allethrin, the first non-natural pyrethroid to be commercialized. This compound was structurally simpler than pyrethrin-I but more effective against house flies.

The revolution in the development of synthetic pyrethroids was made mostly by Michael Elliott's team at Rothamsted Research and later by researchers in Japan. Elliot's started work on pyrethroids in 1948 and, in 1962, he showed that pyrethrin-I was the most insecticidal component of pyrethrum extracts and pyrethrin-II had superior *knockdown* activity to pyrethrin-I (Khambay & Jewess, 2005). In 1962, Elliot's discovered resmethrin, which was over 50-fold more effective than pyrethrin-I against house flies and other insect species, but lacked the photostability that is necessary for use in agriculture (Casida, 2010). In the 1970s, enhanced photostability was achieved with the insecticides permethrin, cypermethrin and deltamethrin, discovered by Elliot's, and fenvalerate discovered by Sumitomo (Casida, 2010). The last three compounds have an α–cyano group in the 3-phenoxybenzyl moiety and are referred to as type-II pyrethroids with enhanced insecticidal activity compared to natural pyrethrins and also lower mammalian toxicity (Khambay, 2002). All these pyrethroids contain common structural features: an acid moiety, a central ester bond, and an alcohol moiety.

The discovery of the photostable pyrethroids encouraged agrochemical companies to invest in research and led to the discovery of many pyrethroids with different properties. Other commercially successful pyrethroids include tralomethrin, flumethrin, kadethrin, acrinathrin, prallethrin, bifenthrin, cyfluthrin, empenthrin, transfluthrin and tefluthrin. The last phase of Elliot's pyrethroid research focused on non-esters, based in part on earlier findings of weakly active compounds (Berteau & Casida, 1969). In the 1980s, very effective alkene, ether (etofenprox) and silylalkyl (silafluofen) pyrethroids were being successfully commercialized, with etofenprox dominating the rice insecticide pyrethroid market where low fish toxicity was required (Casida, 2010).

The development of synthetic pyrethroids is the result of modification of the structure of the natural pyrethrins in order to increase photostability while retaining their potent and rapid insecticidal activity and relatively low acute vertebrate toxicity. Although in the early stages of this process the natural pyrethrins were used as the templates, subsequent stages employed synthetic pyrethroids with desirable insecticidal activity, stability, and other properties as the templates for further design of new compounds.

1.2.2.1. Characteristics and classification

Synthetic pyrethroids are sold commercially in a variety of formulations for both agricultural and home use (Shafer & Meyer, 2004). The reason for pyrethroids' popularity is their photostability, i.e., they do not undergo photolysis (splitting in the presence of ultraviolet light). They also have minimal volatility, provide extended residual effectiveness, have limited

persistence in the field, high insecticidal activity and low mammalian toxicity (Martinez-Galera *et al*., 2003). Such characteristics make pyrethroids useful for household use, and those compounds with improved chemical stability are valuable agrochemicals (Katsuda, 1999).

Originally, pyrethroids were classified into two groups based on the initiation of either the T (whole body tremor) or CS (choreoathetosis with salivation) intoxication syndrome after intravenous or oral administration to rats at sub lethal doses (Verschoyle & Aldridge, 1980). The T-syndrome consisted of aggressive sparring, sensitivity to external stimuli, fine tremor progressing to whole body tremor and prostration. The CS syndrome was comprised initially of pawing and burrowing behaviour followed by profuse salivation, coarse whole body tremor progressing to sinuous writhing (choreoathetosis), increased startle response and terminal clonic seizures. Apparently, the CS syndrome was associated with pyrethroids that posses the α-cyano group in the 3-phenoxybenzyl moiety (Verschoyle & Aldridge, 1980). These findings were confirmed by Lawrence & Casida (1982) in 29 pyrethroids administered intracerebrally to mice. In order to permit generalization to *in vitro* systems and insect models, these authors classified the synthetic pyrethroids into two broad groups: Type I (Figure 1-2), with the absence of an α-cyano group and corresponding to the T-syndrome; and Type II (Figure 1-2), with the presence of an α-cyano group and corresponding to the CS syndrome (Gammon *et al*., 1981; Gammon, 1985). However, some pyrethroids do not fit neatly into these schemes because they produce signs related to both syndromes (Verschoyle & Aldridge 1980; Soderlund *et al*. 2002).

A

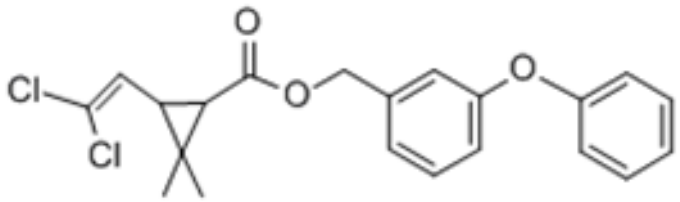

Permethrin

B

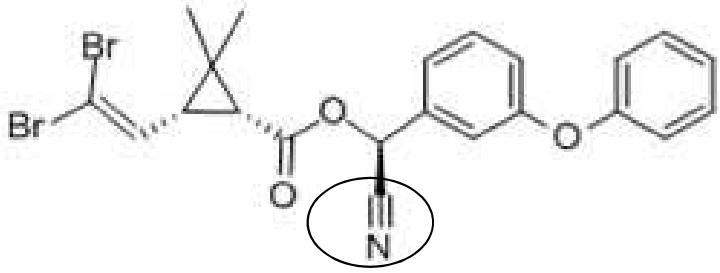

Deltamethrin

Fig.1-2: Structures that are typical of (A) type I and (B) type II pyrethroids with the α–cyano group encircled.

1.2.2.2. Site of action

Pyrethroids are neurotoxic insecticides and act as nerve poisons, i.e., act directly in neurons disrupting nerve conduction in both invertebrates and vertebrates (Khambay & Jewess, 2005). They affect both the peripheral and central nervous systems of insects, modifying the kinetics of voltage-gated sodium channels, which mediate the transient increase in the sodium

permeability of the nerve membrane that triggers the nerve action potential (Soderlund & Bloomquist, 1989; Bloomquist, 1993).

Pyrethroids induce various symptoms in nerve preparations, including hyperactivity, tremors, incoordination, convulsions followed by paralysis and death. From these symptoms, only the initial ones can be linked to neurophysiological measurements and then only for Type I pyrethroids (Khambay & Jewess, 2005). These compounds induce repetitive firing in sensory nerve axonal preparations accompanied by occasional large bursts of action potentials in the ganglia (Nakagawa *et al*., 1982; Narahashi, 2002; Soderlund *et al*., 2002). On the other hand, Type II pyrethroids initially cause much less visible activity in insects, convulsions and rapid paralysis being the main symptoms (Khambay & Jewess, 2005). They cause slow depolarization of nerve membranes leading to block of nerve conduction (Khambay & Jewess, 2005), a sub lethal effect known as *knockdown*. Type II pyrethroids kill insects at a much lower concentration than the Type I compounds (Khambay & Jewess, 2005).

Quicker penetration to the target and better *knockdown* rates are achieved with pyrethroids of higher lipophilicity. However, such compounds may not promote a satisfactory kill because they may dissociate from the target (Davies *et al*., 2007). Type I pyrethroids (e.g., permethrin) are good *knockdown* insecticides due to their ability to induce repetitive firing in axons. Type II pyrethroids (e.g., deltamethrin) causes a convulsive phase which results in a satisfactory kill because depolarization of the nerve axons and terminals is irreversible (Bloomquist, 1996). The duration of modified sodium currents by Type I chemicals lasts only tens or hundreds of milliseconds, while

those of Type II pyrethroids last for several seconds or longer, explaining the different physiological effects in both types of pyrethroids (Davies *et al*., 2007).

Another interesting feature of pyrethroid insecticides is that they display a negative temperature coefficient, i.e., they are more effective in both toxicity and *knockdown* rates when they are applied at lower ambient temperatures. This may be one of the factors that contribute towards their low mammalian toxicity (Davies *et al*., 2007).

Pyrethroids also have the potential to act, not only on sodium channels but also at other sites in excitable tissues. Some studies have shown that pyrethroids act on isoforms of voltage-gated calcium channels, thereby contributing to the release of neurotransmitters and hence pyrethroid-induced toxicity (Hildebrand *et al*., 2004; Symington & Clark, 2005). Moreover, pyrethroids may also act at voltage-gated chloride channels (Ray *et al*., 1997) and nicotinic acetylcholine receptors (Ray, 2001). Although other putative target sites for pyrethroid action have been identified *in vitro*, these targets do not appear to play a major role in pyrethroid toxicity.

1.3. Voltage-gated sodium channels

1.3.1. Sodium channels derived from mammalian systems

The structure and function of voltage-gated sodium channels was elucidated during the last two decades after extensive molecular analysis of mammalian sodium channels (Catterall, 2000; Yu & Catterall, 2003; Goldin,

2001, 2003). Mammalian sodium channels consist of a large pore-forming transmembrane α-subunit, which is approximately 260 kDa associated with auxiliary β-subunits (Catterall, 2000). Expression of the pore-forming α-subunit alone in *Xenopus* oocytes or mammalian cell lines is sufficient to confer on the membrane the ability to produce and inward sodium current in response to a depolarizing stimulus. The β-subunits modify the kinetics and voltage-dependence of channel gating. They are also involved in channel localization and interaction with cell adhesion molecules, extracellular matrix, and intracellular cytoskeleton (Catterall *et al*., 2005).

The α-subunit contains four homologous domains (I to IV), connected by intracellular linkers, each domain consisting of six transmembrane segments (S1 to S6) connected by intracellular and extracellular loops (Liu *et al*., 2002) (Figure 1-3). The four positively charged S4 segments function as voltage sensors. In response to membrane depolarization, the S4 segments move outward to initiate activation (i.e., channel opening) (Catterall, 2000). Transmembrane segments S5 and S6 of each domain and the membrane-reentrant P-loops connecting the S5 and S6 segments that dip into the transmembrane region form the narrow outer pore and ion selectivity filter (Catterall, 2000). Amino acids D, E, K, and A in the loop connecting S5 and S6 of domains I, II, III, and IV, respectively, are the key determinants of ion selectivity (Dong, 2007). The short intracellular loop connecting homologous domains III and IV (IFM motif) serves as the inactivation gate, folding into the channel structure and blocking the pore from the inside during sustained depolarization of the membrane (Catterall *et al*., 2005). Several residues in the intracellular loop connecting S4 and S5 are believed to be part of the docking receptor for the inactivation gate (Dong, 2007).

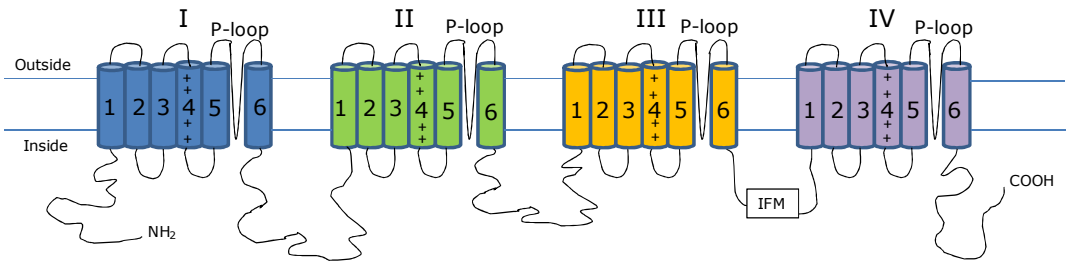

Fig. 1-3: The transmembrane topology of the voltage-gated sodium channel. The pore-forming α-subunit consists of a single polypeptide chain with four internally homologous domains (I to IV), each having six transmembrane segments (S1 to S6). The voltage-dependence of channel activation is thought to derive from the movement of the four positively charged (+) S4 segments. Figure adapted from Schuler *et al*., 1998.

Sodium channels are responsible for action potential initiation and propagation in excitable cells, including nerve, muscle, and neuroendocrine cell types (Catterall *et al*., 2005). They are also expressed at low levels in non-excitable cells, where their physiological role is unclear.

In response to a depolarization, the sodium channel undergoes a conformational change to allow a selective influx of sodium through the pore. During a depolarization the permeability for sodium rises rapidly and then decays as the channel converts to inactivated, non conducting states in which it remains until the membrane is repolarized and then the channel deactivates (Figure 1-4) (Catterall, 2000).

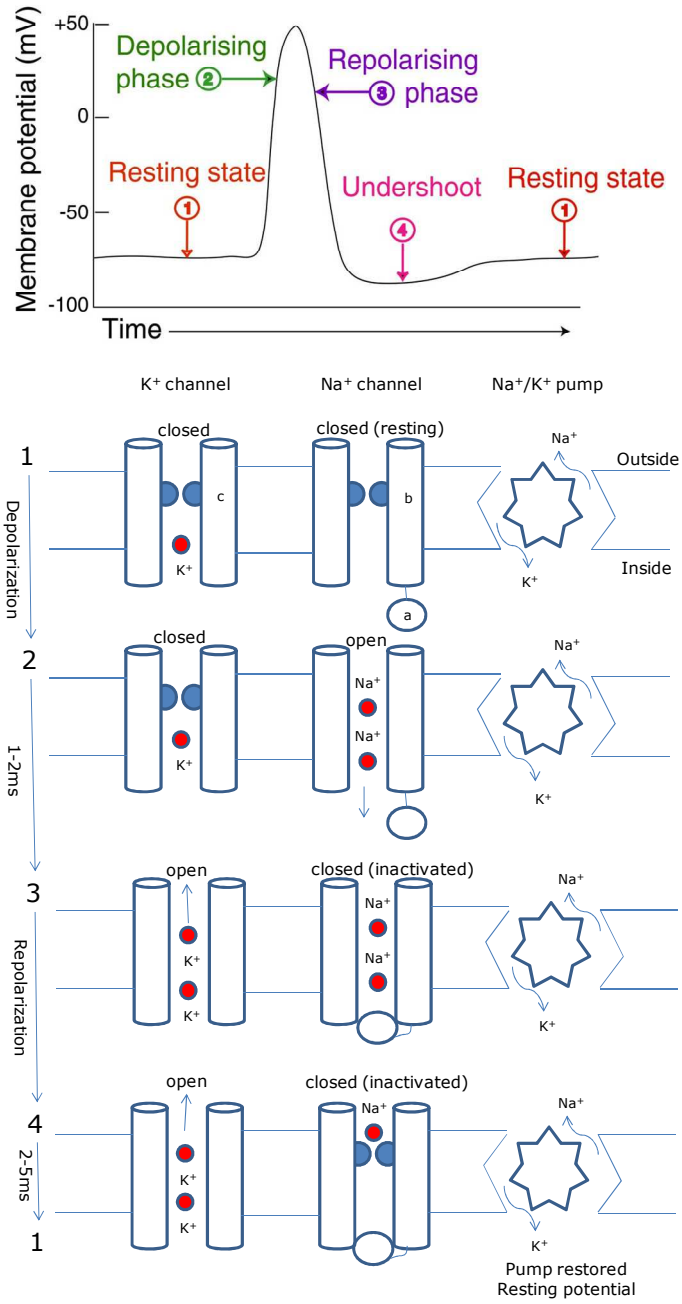

Fig. 1-4: Initiation and generation of an action potential. The extracellular fluid surrounding the axonal membrane contains a high concentration of sodium ions (Na^+) and a low concentration of potassium ions (K^+), while the reverse is true for the inside of the nerve cell. At resting potential (1) the axonal membrane is moderately permeable to K^+ but not Na^+. This makes the inside of the cell negative with respect to the outside, the difference in potential being around -60 mV. Nerve stimulation makes the axonal membrane permeable to Na^+ due to the sodium channel opening (2). This causes the inside of the axon to become positive and generates the rising phase of the action potential. Sodium channel inactivation (3) is accompanied by an efflux of K^+ as a result of voltage-gated potassium channels opening and generates the falling phase of the action potential. The generation of the action potential results in sequential depolarization of other regions of the axon, resulting in a wave of depolarization along the axon. The ATP driven Na^+/ K^+ pump maintains the ion gradient across the axonal membrane (4) and helps to restore the resting potential. Figure adapted from Davies *et al.*, 2007.

Figure 1-4 shows that the sodium channel is closed at resting potential because the activation-gate of the 'b-gate' (voltage-dependent) blocks the sodium channel pore. Membrane depolarization causes conformational changes at the 'b-gate', involving movements in IS4 and IIS4 and lateral rotation of the pore forming S6 segments. The channel opens for a few milliseconds, allowing influx of sodium. This activation leads to closing of the 'a-gate' within 1-2 miliseconds (fast-inactivation). Now the intracellular mouth of the pore is blocked and the channel is in an inactivated state. Inactivation is coupled to activation and is faster from the open state but has little, or no, voltage dependence. A reversal of the conformation change at the 'b-gate' which closes the channel pore (deactivation) is caused by membrane repolarization. Both gates are now closed (since the inactivation (a) gate is still blocking the pore), but the conformational changes of the 'b-gate' forces the 'a-gate' to reopen within a period of 2-5ms, bringing the channel back to the closed state. Sodium channels do not follow only this pattern during the generation of an action potential (Davies *et al*., 2007). Channels may hop the activation state and go directly to an inactivated state by a voltage-dependent process called closed-state inactivation. A channel also may re-open without first inactivating (Hille, 2001).

At least nine different sodium channel α-subunits ($Na_v1.1$ to $Na_v1.9$) have been identified in mammals (Goldin *et al*., 2000; Catterall *et al*., 2003). These sodium channel isoforms exhibit distinct expression patterns in the central and peripheral nervous systems, and skeletal and cardiac muscle (Goldin, 1999). $Na_v1.1$, $Na_v1.2$, $Na_v1.3$, and $Na_v1.6$ are predominantly expressed in the central nervous system, whereas $Na_v1.7$, $Na_v1.8$, and $Na_v1.9$ are expressed in the peripheral nervous system. $Na_v1.4$ and $Na_v1.5$ are

expressed in skeletal and cardiac muscles, respectively. Mammalian sodium channel α-subunit isoforms also exhibit distinct electrophysiological properties (Goldin, 2001; Dib-Hajj *et al*., 2002; Yu & Catterall, 2003). Selective expression of different sodium channel genes (with unique gating properties) contributes to the specialized function of sodium channels in various mammalian tissues and cell types (Yu & Catterall, 2003).

1.3.2. Insect sodium channels

Previously, two sodium channel-like genes from insects, *DSC1* and *para* were isolated from *Drosophila melanogaster*. *DSC1* was originally isolated from a *Drosophila* genomic DNA library using an eel sodium channel probe (Salkoff *et al*., 1987), and *para* was identified using temperature-sensitive paralysis phenotypes displayed by mutant alleles in *Drosophila* (Loughney *et al*., 1989).

Later, a *DSC1* orthologous gene was identified from German cockroach (*Blatella germanica*) and named *BSC1* (Liu *et al*., 2001). Like sodium channel α-subunits, *DSC1* and *BSC1* have four homologous domains, each having six transmembrane segments. Until very recently, *DSC1* and *BSC1* had been predicted to encode a voltage-gated sodium channel based on their overall similarity of deduced amino acid sequence and domain organization to eel and mammalian sodium channel proteins (Littleton & Ganetzky, 2000). However, another study showed that *BSC1* and *DSC1* encode a novel family of calcium-selective cation channels, not sodium channels (Zhou *et al*., 2004). The biological role of *DSC1* and *BSC1* channels in insects remains to be determined. Nevertheless, a previous investigation showed that partially

reduced expression of the *DSC1* gene was correlated with certain olfactory defects in *D. melanogaster* (Kulkarni *et al*., 2002), suggesting a role of *DSC1* in olfaction.

The overall structure and amino acid sequence of the *para* sodium channel shares a high similarity with those of mammalian sodium channel α-subunits. The structural features that are critical for mammalian sodium channel function, including residues crucial for sodium channel selectivity, are conserved in the *para* sodium channel (Loughney *et al*., 1989). Most importantly, subsequent functional expression and characterization in *Xenopus* oocytes conclusively demonstrated that the *para* gene encodes a sodium channel (Feng *et al*., 1995; Warmke *et al*., 1997). Except for significant sequence similarities with the *DSC1* channel protein and limited sequence similarity with putative calcium channel α1 subunits, *para* is not similar to any other genes in the *Drosophila* genome (Littleton & Ganetzky, 2000). Therefore, it seems that *para* is the only gene that encodes voltage-gated sodium channel in *Drosophila* and apparently in other insect species as well.

Para orthologous genes have been isolated from several medically or agriculturally important insect pest species (Soderlund & Knipple, 2003). However, in most cases, only partial cDNA clones were obtained. Full-length cDNA clones are available only for three *para* orthologous channels: *Vssc1* from house fly *Musca domestica* (Ingles *et al*., 1996, Williamson *et al*., 1996), $BgNa_v$ from the German cockroach *Blatella germanica* (Dong, 1997) and $VmNa_v$ from the mite *Varroa destructor* (Wang *et al*., 2003a). The availability of the full-length clones made it possible to successfully express these *para* orthologues in *Xenopus* oocytes and to demonstrate that these genes indeed

encode functional sodium channels (Ingles *et al*., 1996; Tan *et al*., 2002a, Song *et al*., 2004).

1.3.3. Effects of pyrethroids on sodium channels

The primary mode of action of DDT and pyrethroids in both insects and mammals is the disruption of sodium channel function. Although DDT is still used in developing countries for controlling disease vectors, this insecticide was banned from use in crop protection (Davies et al., 2007; van den Berg, 2009). For this reason, this study focused only on the effect of pyrethroid insecticides, which are extensively used for controlling both agriculture pests and disease vectors in many countries.

Many *in vivo* and *in vitro* studies on mechanism of action and metabolism of pyrethroids have been carried out on mammalian systems because of the interest in toxicology of these insecticides to mammals and the expertise present in many laboratories for electrophysiology on mammalian neurons and muscles (Khambay & Jewess, 2005). However, these studies may not be relevant to insects since there are differences in metabolism, amino acid sequences and also pharmacological properties of the sodium channel protein (Khambay & Jewess, 2005). Another difficulty is that mammals have several genes expressing different sodium channel isoforms, which exhibit differential responses to the two types of pyrethroids, Type I and Type II (Tatebayashi & Narahashi, 1994; Soderlund *et al*., 2002). Furthermore, each gene can express splice variants with varying pharmacological and biophysical

properties (Tan *et al*., 2002a). In insects, sodium channels are encoded by only one gene, which can also express splice variants. It is possible therefore that although insect channels have a common pyrethroid binding site, splice variants might exhibit differences in their responses to pyrethroids (Khambay & Jewess, 2005).

The effects of pyrethroids on sodium channels and on whole nerve excitability have been explored using: crude synaptosomal preparations (Bloomquist & Soderlund, 1988; Eells *et al*., 1992), membrane preparations from non-mammalian species, (Vijverberg & van den Bercken, 1979; Lund & Narahashi, 1982), primary culture of mammalian neurons (Tabarean & Narahashi, 1998; Song *et al*., 1996), standard cell lines such as N1E-115 neuroblastoma cells (Burr & Ray, 2004), and heterologous expression systems such as human embryonic kidney (HEK) cells (Hildebrand *et al*., 2004), and oocytes from *Xenopus laevis* (Vais *et al*., 2001).

Collectively, these studies show that pyrethroids slow the activation, or opening of sodium channels. They also slow the rate of sodium channel inactivation (or closing) and shift the voltage-dependence of activation (or opening) to more hyperpolarized potentials (Narahashi, 1996). Therefore, sodium channels open at more hyperpolarized potentials (i.e., after smaller depolarizing changes in membrane potential) and are held open longer, allowing more sodium ions to cross and depolarize the neuronal membrane. The prolonged channel opening is evidenced by a large tail current associated with repolarization under voltage-clamp conditions (Dong, 2007). In general, Type II compounds delay the inactivation of sodium channels considerably longer than do Type I compounds. Type I pyrethroids prolong channel opening

only long enough to cause repetitive firing of action potentials (repetitive discharge), whereas Type II compounds hold open the channels for such long periods of time that the membrane potential eventually becomes depolarized to the point at which generation of action potentials is not possible (depolarization-dependent block) (Figure 1-5). These differences in prolongation of channel open times are assumed to contribute to the differences in the T and CS syndromes after exposure to Type I and Type II pyrethroids, respectively (Ray, 2001).

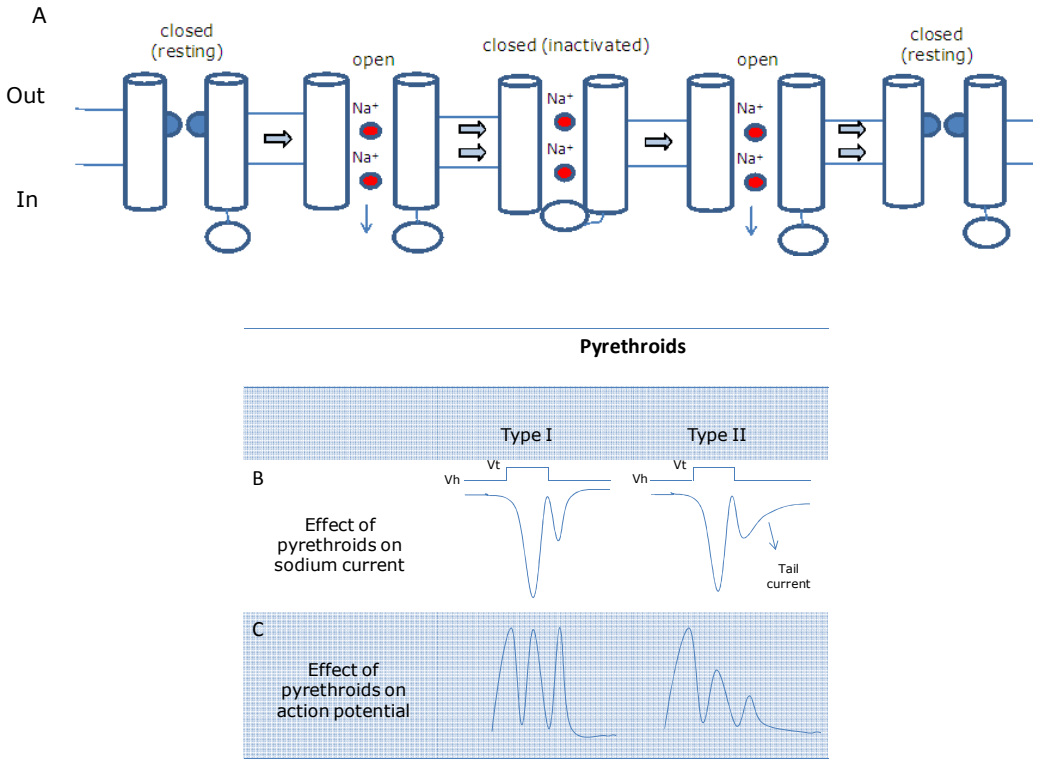

Fig. 1-5: Pyrethroid effects on neuronal excitability. This schematic represents (A) pyrethroid effects on individual channels, (B) whole cell sodium currents and (C) action potentials. (A) Pyrethroids inhibit the function of two different gates that control sodium flux through sodium channel, delaying inactivation (indicated by double arrows between states) of the channel and allowing continued sodium flux (open). (B) If sodium current through an entire cell is measured, pyrethroid-modified sodium channels remain open when depolarization ends (sodium current), resulting in a tail current. (C) Sodium channels modified by type I compounds (action potential) depolarize the cell membrane above the threshold for action potential generation, resulting in a series of action potentials (repetitive firing). Type II compounds cause greater membrane depolarization, diminishing the sodium electrochemical gradient and subsequent action potential amplitude. Eventually, membrane potential becomes depolarized above the threshold for action potential generation (depolarization-dependent block). V_h: holding potential, V_t: test potential. Figure adapted from Shafer *et al.*, 2005.

1.4. Insecticide resistance

Insecticide resistance is associated with intensive insecticide exposure during insect pest control (Georghiou & Taylor, 1977; Roush & Mckenzie, 1987; Mckenzie, 1996). The evolution of resistance by an insect pest to a particular insecticide involves a number of possible mechanisms, including a) reduced penetration; b) behavioral resistance c) increased excretion; d) metabolic resistance (detoxification enzyme); and e) target site modifications (McKenzie, 1996).

Elevated detoxifying enzyme production (P-450 mono-oxygenases, esterases, glutathione S-transferases) and target site modification are the most common mechanisms of resistance to pyrethroids. In general, P450 monooxygenases can mediate resistance to all classes of insecticides whereas esterases can mediate resistance to organophosphates, carbamates and pyrethroids which contain ester-bonds (Verhaeghen *et al*., 2009).

1.4.1. Pyrethroid insensitivity to the target site

The intensive use of pyrethroids has led to the occurrence of widespread resistance in many insect species and this is now a serious risk to their sustained, effective use in many pest control programs (Khambay & Jewess, 2005).

Because the two insecticides have a common mode of action, ie they modify the kinetics of sodium channels, the earlier development of resistance among insect pests to DDT was also likely to confer resistance to pyrethroids. The common resistance mechanism that did emerge, so called *knockdown* resistance (*kdr*), was first recognized in houseflies by Busvine in 1951 (Busvine, 1951). Previous studies have shown that *kdr* resistance is caused by modifications (point mutations) in the *para*-type sodium channel protein (Figure 1-6), making this protein less responsive to the toxic effect of pyrethoids (Miyazaki *et al*., 1996; Williamson *et al*., 1996; Dong, 1997). It was also demonstrated that *kdr* resistance caused a 10-20 fold reduction in target-site sensitivity to these compounds and is probably the most important of numerous resistance mechanisms described in insect species (Hemingway & Ranson, 2000). This type of resistance has now been reported in many important agricultural pests and disease vectors, and in many cases, is accompanied by a second resistance trait designated super-*kdr* (Figure 1-6) which confers much greater resistance to pyrethroids (Farnham *et al*., 1987) (A list of *kdr* and super-*kdr* mutations identified in different insect species is provided in Chapter 3). Several *kd*r and super-*kdr* mutations are grouped on the S4-S5 linker and S5 or S6 of domain II, or in the corresponding linker/segments of domains I and III of the sodium channel protein (Figure 1-6).

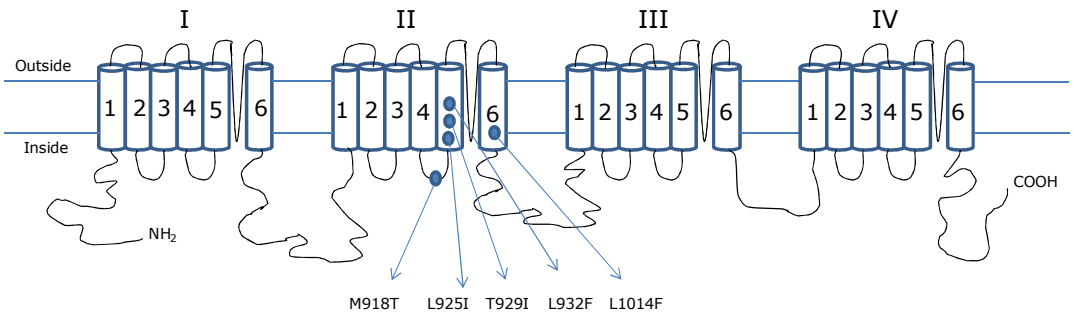

Fig. 1-6: Transmembrane topology of the sodium channel. The pore-forming α-subunit consists of a single polypeptide chain with four homologous domains (I to IV), each having six transmembrane helices (S1 to S6). The identity and location of mutations associated with resistance (*kdr* and super-*kdr*) are shown (•) with residues numbered according to the sequence of the housefly sodium channel. Figure adapted from Schuler *et al*., 1998.

Although DDT had not been used for many years, the introduction and intensive use of pyrethroids was able to select *kdr* insects and reduce their efficacy against these pest species within a very short time period. The first cases of such cross-resistance were documented in the mid-1970s in houseflies in Europe (Keiding, 1975). By 1980 over 200 insect pests were documented as having resistance to DDT (Georghiou, 1990), many of which have also been reported as showing cross-resistance to pyrethroids.

The characterization of mutations in an *in vivo* expression system, such as the *Xenopus* oocyte system, significantly improves our understanding of the molecular basis of the *kdr* mechanism and the molecular interaction between pyrethroid insecticides and sodium channels (Liu *et al*., 2000).

Functional assays using insect sodium channels expressed in *Xenopus* oocytes show that *kdr* and super-*kdr* mutations reduce sodium channel sensitivity to pyrethroids and therefore represent a major mechanism of pyrethroid resistance in diverse insect pest species. The electrophysiological analyses of *kdr* mutant channels in oocytes quantified the effects of *kdr* mutations on channel gating and pyrethroid binding. Vais *et al*. (2000a) showed that *kdr* and super-*kdr* mutations shift both the voltage-dependence of activation and steady-state inactivation towards more positive potentials (Smith *et al*., 1997; Lee *et al*., 1999b) and promote closed-state inactivation (Vais *et al*., 2000a), whereby 70-80% of the sodium channels never open. These mutations also reduce the binding affinity for open channels (Vais *et al*., 2000a, 2003).

A three-dimensional model of the pore region of the housefly sodium channel (O'Reilly *et al*., 2006) has facilitated the prediction (through ligand docking simulations) of a putative pyrethroid-binding pocket on the sodium channel (Figure 1-7). This model highlights the role of the IIS4-S5 linker and the IIS5 and IIIS6 helices in pyrethroid binding and supports the involvement of several amino acid residues that could be part of the pyrethroid binding site and may contribute to the different sensitivities between insect and mammalian sodium channels.

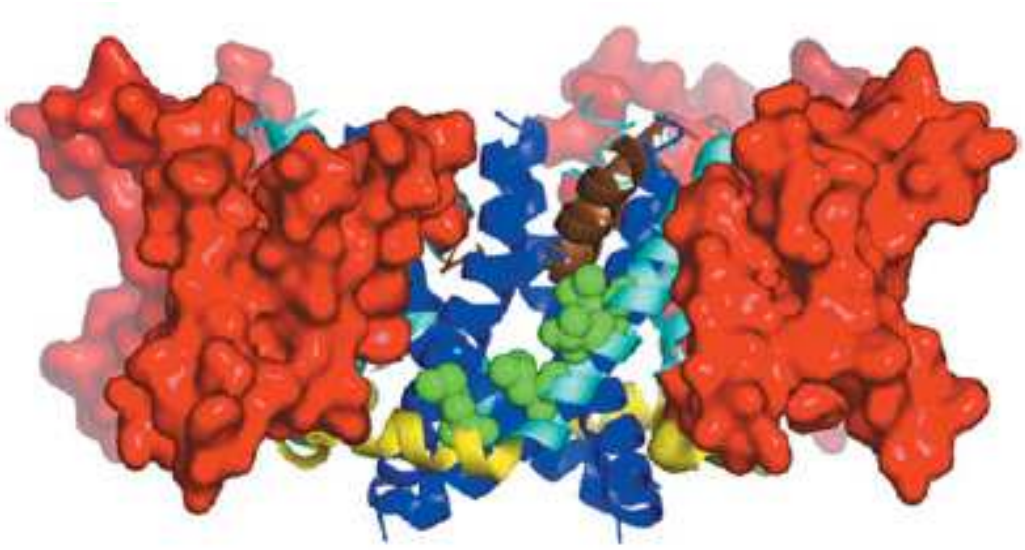

Fig. 1-7: Model of the activated-state of the house fly voltage-gated sodium channel. The four voltage sensor domains are shown in surface representation (**red**). The S4-S5 linkers, the S5 helices, the pore helices and the S6 helices are shown in cartoon (**yellow**, **cyan**, **brown** and **blue** respectively). Amino acid residues implicated in pyrethroid binding in various pest species are shown in space fill (**green**) (O'Reilly *et al*., 2006). The Biochemical Society, London, UK.

A previous study of resistance factors (RF) (Khambay *et al*., 1994) demonstrated that *kdr* is equally effective against all pyrethroids and DDT, with essentially uniform resistance (mean RF = 14) across the whole range of structural variation. Therefore, the modification involved is likely to be in a region where the ion conductance properties of the sodium channel are modified. In contrast, the effect of super-*kdr* was found to be sensitive to pyrethroid structure, with the highest degree of resistance observed with the more toxic Type II pyrethroids (e.g. permethrin RF = 56; deltamethrin RF =

560). Hence, super-*kdr* is likely to be at the real binding site for the pyrethroid insecticides and to involve a change that rejects large cyclic side chains in the alcoholic component, whereas variations in the acid, link and spacer components have little effect (Davies *et al*., 2007).

1.4.2. Real-time PCR for detection of mutant insects in the field

The ineffective application of insecticides, which wastes time and money and results in environmental problems, could be prevented by resistance monitoring (Anstead *et al*., 2004). This type of monitoring requires rapid high-throughput tests for the presence of resistance mechanisms. Conventionally, *kdr*-type mutations were only able to be detected by a full bioassay on live insects (Field *et al*., 1997) or DNA sequencing (Eleftherianos *et al*., 2002) both of which take several days to produce useful results. More recently, high-throughput assays based on real-time PCR have been developed for detection of *kdr* and super-*kdr* mutations, providing a resistance profile on the same day that samples are collected. These include real-time PCR using either Taqman probes (Taqman assay, Figure 1-8) or Eva Green dye (High Resolution Melt – HRM, Figure 1-9) (Bass *et al*., 2007a).

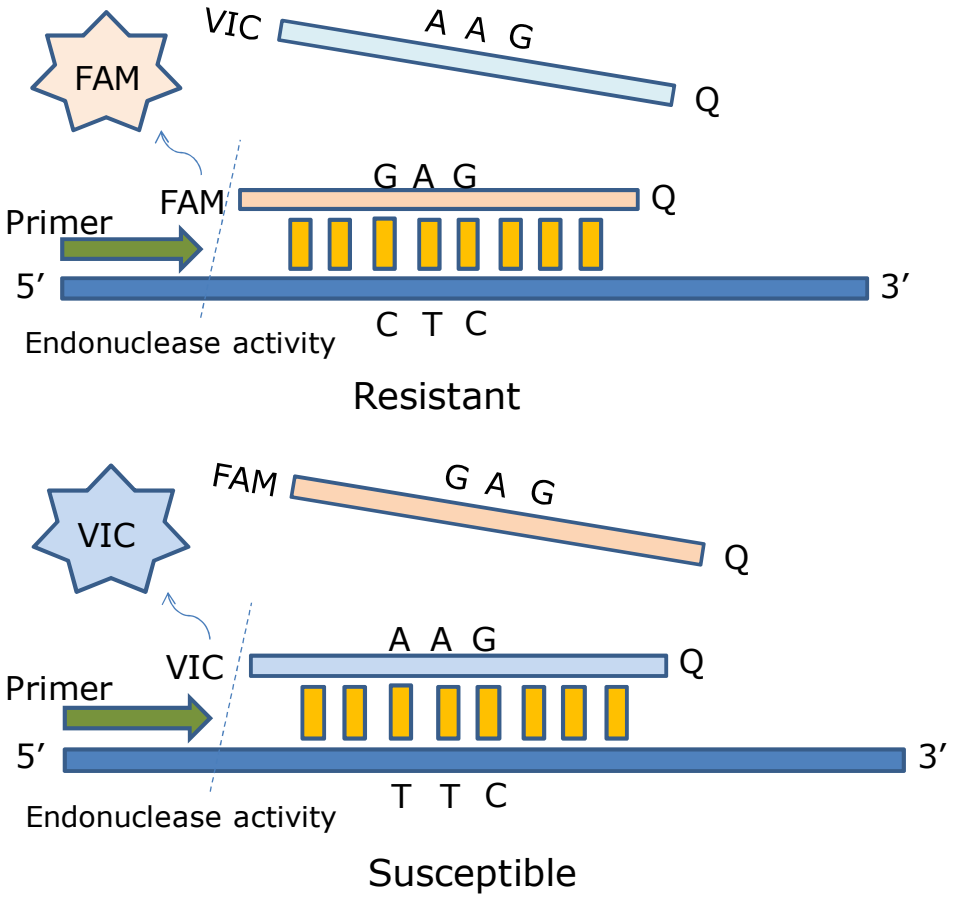

Fig. 1-8: The principle of the Taqman assay. Taqman probes were designed for susceptible and resistant alleles, each carrying a different dye (VIC for susceptible and FAM for resistant). During amplification, each probe specifically binds to its complementary PCR product. DNA polymerase then cleaves the reporter dye from the attached probe, which results in increased fluorescence of the reporter dye, as it is separated from the quencher. This cleavage occurs every cycle resulting in an increase of fluorescence proportional to the amount of PCR product and enabling the genotype to be scored. Figure adapted from Anstead *et al*., 2004.

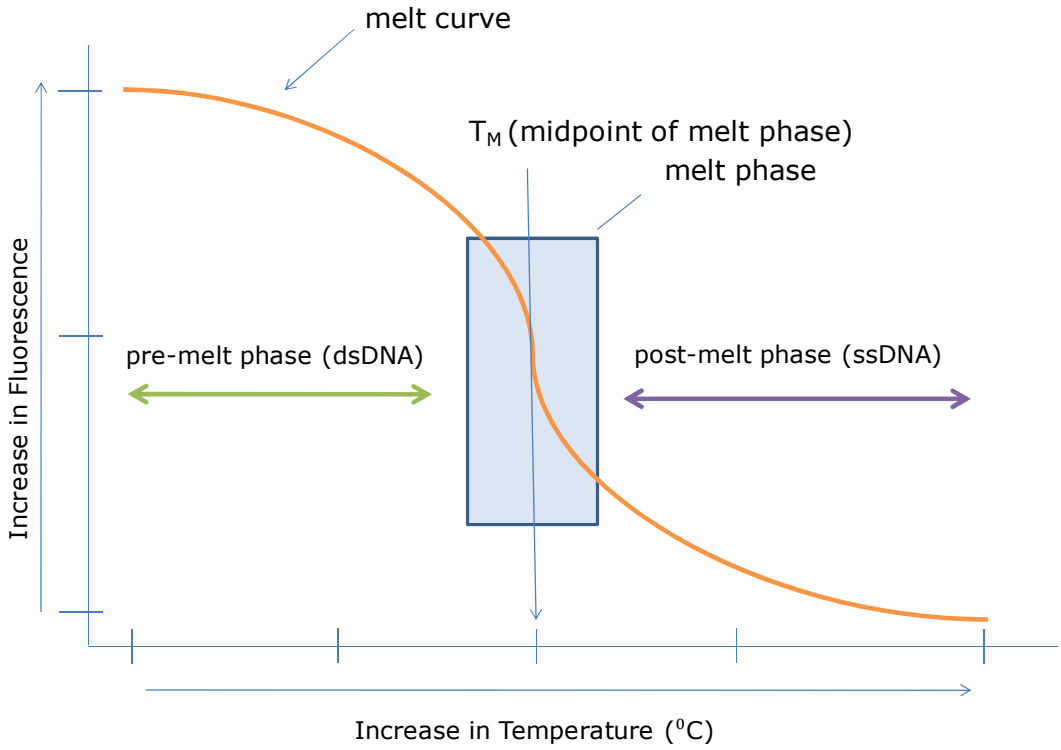

Fig. 1-9: Principle of a typical HRM plot. The melt curve (orange) plots the transition from high fluorescence of the initial pre-melt phase through the sharp fluorescence decrease of the melt phase to basal fluorescence at the post-melt phase. DNA amplification (PCR) is carried out in the presence of a double-stranded (dsDNA) intercalating fluorescent dye (Eva Green). The dye does not interact with single-stranded DNA (ssDNA) but actively intercalates with dsDNA and fluoresces brightly in this state. Initially, fluorescence is high in the melt analysis because the sample starts as dsDNA, but fluorescence decreases as Eva Green is released from dsDNA as it dissociates (melts) into ssDNA. The midpoint of the melt phase, at which the rate of change in fluorescence is greatest, defines the temperature of melting (T_M) of the particular DNA fragment under analysis. Figure adapted from CorProtocol™ 6000-1-July06.

These two methods are based on real-time PCR with the amplification being monitored through the fluorescence of dsDNA-specific dyes or sequence-

specific probes, depending on the assay (Wilhelm & Pingoud, 2003). The first dye used for this purpose was ethidium bromide (Higuchi *et al*., 1993, Wittwer *et al*., 1997). In melting curve analysis, DNA samples are characterized according to their dissociation behavior as they change from dsDNA to ssDNA with increasing temperature (CorProtocol™ 6000-1-July06).

The most important advantage of real-time PCR compared to other methods for genotyping is the significantly higher reliability of the results compared to the conventional PCR. In the real-time PCR, the whole amplification profile is known and individual reactions deviating in their profile of amplification efficiency can be easily identified (Wilhelm & Pingoud, 2003). More details about Taqman and HRM assays are given in Chapter 4.

1.5 The maize weevil

The maize weevil, *Sitophilus zeamais* Motschulsky (Coleoptera: Curculionidae) is one of the most serious cosmopolitan pests in tropical and sub-tropical regions of stored cereal grain, especially of maize (*Zea mays*, L.), (Throne, 1994) (See Appendix I). The infestation starts in the field before harvest and continues throughout the storage period (USDA, 1980; Rees, 1996). The strong flying ability (Hagstrum *et al*., 1996) and destructive power of this species accounts for a great part of the 15% loss in total weight recorded in stored grains at the farm level in Brazil (Santos *et al*., 1990). For many years, insecticides have provided the main control method against these insects, due to the lack of appropriate control alternatives (White & Leesch, 1996; Fragoso *et al*., 2003; Ribeiro *et al*., 2003).

1.5.1 Biology

The complete development time for the life cycle of *S. zeamais* average 36 days (range 33-45) at 27±1ºC, and 69±3% relative humidity (RH) (Sharifi & Mills, 1971). Most eggs are deposited in the endosperm, but 28% are in or around the germ. The maximum daily rate of fecundity (6.7 eggs per female in 24h), duration of development and number of progeny produced are optimal at 30ºC and 75% RH (Throne, 1994). The lower limit for development from egg to adult weevils is 15.6ºC and the upper limit is 32.5ºC at 75% RH (Throne, 1994).

S. zeamais is an internal feeder whose adults attack whole grains and whose larvae feed and develop entirely within grains (Storey, 1987), contributing to the deterioration of the quality and quantity of stored grains. The female drills a hole into the kernel, deposits the egg, and then secretes a mucilaginous plug to enclose the egg as the ovipositor is withdrawn. The plug rapidly hardens, leaving a small raised area above the seed surface, which provides the only external evidence that the kernel is infested. Eggs may be laid anywhere in the kernel, but few are laid in the embryo. Sometimes, more than one egg may be laid in a single grain but it is rare for more than one larva to develop to maturity, because of cannibalism (Longstaff, 1981). Not all excavated holes are used for oviposition, some are abandoned and others are expanded into feeding holes (Campbell, 2002).

There are four larval instars, all of which remain within the grain. Immediately on hatching, the first instar feeds by burrowing through the tissues of the grain. At the end of the fourth instar the larva uses a mixture of

frass and larval secretion to close off the end of the burrow, to form a pupal cell. Under normal development conditions, weevil larvae allow their frass to accumulate around them inside the grain in which they are feeding. However, if the carbon dioxide level exceeds 5%, the fourth instar larva makes a small hole in the grain and ejects much of the frass. The larva then assumes a prepupal form for a short period before transforming into the pupa (Longstaff, 1981).

When the adult has developed, it remains inside the grain for several days before emerging, with the time varying with temperature (Longstaff, 1981). During this time, its cuticle hardens and matures. Adults emerge and females move to a surface above the food to release sex pheromone. Males are attracted to this pheromone for mating (Mason, 2003).

1.5.2 Control

DDT was the most widely used insecticide to protect stored maize in Brazil until its prohibition in 1985 (Mariconi, 1963; Gallo *et al*., 1970, 1978; Guedes, 1993), even though in 1970, DDT resistance in *S. zeamais* had already been detected in a field population from Capinopolis, State of Minas Gerais (Mello, 1970). When organochlorines were discontinued, the use of organophosphorus compounds, especially malathion, for control of stored grain insects greatly increased (Guedes *et al*., 1995). However, malathion use decreased after control failures in stored grain and the sudden development of resistance in several stored grain insects pests all over the world (Champ & Dyte, 1978; Badmin, 1990; Guedes, 1990). Thus, this compound was replaced by another organophosphate pirimiphos-methyl, and the pyrethroids

deltamethin and permethrin which showed great efficiency against *S. zeamais* (Braga *et al*., 1991; Guedes *et al*., 1995). Despite the initial success of deltamethrin, Santos (1988) reported control failures with this compound when used on maize weevil populations in the State of Parana and Rio Grande do Sul. However these populations were successfully controlled by the organophosphorus insecticides malathion and pirimiphos-methyl. Other pyrethroids were also tested against these same populations but none of them was effective.

1.5.3 Insecticide resistance in *S. zeamais*

Previous studies on pyrethroids frequently pointed to a close relationship between pyrethroid resistance and DDT resistance in *Musca domestica* (Busvine, 1951; Milani & Travaglino, 1957), ticks and *Pulex irritans* (Plapp, 1976), mosquitoes (Priester & Georghiou, 1980; Malcolm & Wood, 1982; Halliday & Georghiou, 1985), *Haematobia irritans* (Byford *et al*., 1985), *Blatella germanica* (Cochran, 1987) and predacious mites (Scott *et al*., 1983). Cross-resistance between DDT and pyrethroids was reported in *Spodoptera littoralis* (Gammon, 1980; Riskallah *et al*., 1983), and in stored grain pests, the phenomenon was verified in *Sitophilus oryzae* by Heather (1986). Both DDT and pyrethoids have sodium channels as the primary target site. For this reason, cross-resistance between these two compounds occurs when resistant insects show modification in their site of action (*kdr* resistance) as the main resistance mechanism.

Resistance has been evident in many field populations of insect species that infest stored products (Champ & Dyte, 1976; Badmin, 1990; Pacheco *et al*., 1990; Guedes *et al*., 1995, 1996; Subramanyam & Hagstrum, 1996) and *S. zeamais* is not an exception, with some reports of resistance to DDT and pyrethroids by the early 1990s (Guedes *et al*., 1995)**.** The over-reliance on insecticides for maize weevil control caused insecticide resistance to develop in Brazilian populations of this pest species, sparking environmental and economic concerns in the country (Guedes *et al*., 1995; Ribeiro *et al*., 2003). Investigations of pyrethroid resistance mechanisms in *S. zeamais* relied upon *in vivo* contact bioassays with synergists and biochemical assays for detoxification enzymes (Ribeiro *et al*., 2003; Fragoso *et al*., 2007). According to these investigations, target site modification is the prevailing insecticide resistance mechanism in some Brazilian populations of *S. zeamais* with secondary involvement of enhanced detoxification by glutathione S-transferases.

1.6 Aims and Objectives

The overall aim of this study was to gain an understanding of the molecular mechanism underlying pyrethroid resistance in maize weevils. This was achieved by addressing the following objectives:

1. PCR amplification and sequence analysis of target fragments of the maize weevil *para* sodium channel gene to identify possible mutations involved in conferring resistance to pyrethroid insecticides.

2. Development of diagnostic assays to detect the mutations identified in (1) in individual weevils, and to use these to screen field-collected maize weevil populations.

3. Electrophysiological characterization of ion channels from maize weevil neurons in order to optimize the methodology for subsequent sodium current recordings.

4. Electrophysiological characterization of maize weevil *para* sodium channel protein aiming to investigate if the mutation identified in (1) alters the biophysical properties of the mutant channels as well as the sensitivity to pyrethroids.

Chapter 2

Materials and Methods

2.1 Maize weevil populations

Three Brazilian populations of *S. zeamais* were obtained from the Ecotoxicology Laboratory of the Federal University of Viçosa, Minas Gerais, Brazil. The standard susceptible population was originally collected in Sete Lagoas (SL) County (state of Minas Gerais) and provided by the National Center of Maize and Sorghum from the Brazilian Agricultural Research Corporation (EMBRAPA Milho e Sorgo). This population has been maintained for nearly 20 years without insecticide exposure and its susceptibility to pyrethroids and organophosphates is well known (Guedes *et al*., 1994, 1995; Fragoso *et al*., 2003; Ribeiro *et al*., 2003; Araújo *et al*., 2008a). The other two populations are both pyrethroid-resistant (> 100-fold resistant, when performing insecticide bioassays) (Guedes *et al*., 1994, 1995; Ribeiro *et al*., 2003; Oliveira *et al*., 2007; Araújo *et al*., 2008a). The first was collected in Jacarezinho (JA) County (state of Parana) in the late 1980s and the inheritance of deltamethrin resistance was found to be sex-linked (Guedes *et al*., 1994, 1995; Ribeiro *et al*., 2003). The other resistant population was collected in Juiz de Fora (JF) County (state of Minas Gerais) in 1999 (Guedes *et al*., 1995; Fragoso *et al*., 2003). The JF population shows a fitness disadvantage in the absence of pyrethroids, unlike the JA population (Fragoso *et al*., 2005; Oliveira *et al*., 2007). Another twelve field-collected strains of maize weevil obtained from the same laboratory in Brazil were additionally used in the diagnostic study. These populations were collected in 2007 from different Brazilian states (Figure 2-3) and the level of resistance to pyrethroids is not known.

All populations were maintained in jars on whole maize grains (13% moisture content) at a temperature 25 ± 2ºC, a RH of 70 ± 5% and a photoperiod of 12h light 12h dark (Figure 2-1). The adult maize weevil can be seen in Figure 2-2.

Fig. 2-1: Population of *S. zeamais* maintained on whole maize grains.

Fig. 2-2: *S. zeamais,* adult length 3 - 3.5mm.

Fig. 2-3: Location of the 12 field-collected strains of maize weevil in Brazil: Machado (1), Espírito do Santo do Pinhal (2), Guarapuava (3), Nova Era (4), Sacramento (5), Rio Verde (6), Piracicaba (7), Viçosa (8), Sao João (9), Votuporanga (10), Linha Barreirinha (11) and Sao José do Rio Pardo (12).

2.2 Molecular biology

2.2.1 RT-PCR analysis of S. *zeamais* sodium channel gene sequences

2.2.1.1 Total RNA extraction

Total RNA was extracted from adult weevils (50 - 100mg) by using a tight-fitting pestle in a 1.5ml eppendorf tube and grinding to a fine powder in liquid nitrogen. One RNA sample was produced for each population. The samples were homogenized in 1ml of TRIzol Reagent (Invitrogen) according to the manufacturer's instructions. Samples were frozen at -80ºC until needed.

2.2.1.2 cDNA synthesis

The IIS4-IIS6 region of the *S. zeamais para* sodium channel gene was initially amplified by reverse transcriptase-mediated PCR (RT-PCR). First strand cDNA was synthesized from total RNA (1 - 5µl) using Superscript II Reverse Transcriptase (Life Technologies). RNA (2µl; 1-5 µg/µl) was mixed with 1µl oligo-dT primer (50 ng/µl) and 4.5µl nuclease-free water, and denatured at 70ºC for 10min before cooling on ice. To this, 1.5µl 10mM dNTP mix, 3µl first strand buffer, 1.5µl 0.1M DTT and 0.75µl Superscript II enzyme (200 U/µl) were added and the reaction was incubated at 37ºC for 15min, 42ºC for 40min and then heated for 5min at 95ºC. The cDNA was stored at -20ºC and used as a template for PCR.

2.2.1.3 PCR protocol

The cDNA fragments served as a template to amplify the IIS4-IIS6 coding sequence of the *para* gene. Two rounds of PCR were carried out in sterile 0.2ml plastic tubes containing 2µl template DNA, 100ng of each degenerate sodium channel primer (DgN2 and DgN3 for the primary PCR and DgN1 and DgN4 for the secondary PCR) (Martinez-Torres *et al*., 1997) (Table 2-1), 12.5µl Master Mix (buffer, dNTP and Taq Polymerase) and sterile distilled water to 25µl. The thermal conditions for both PCRs were: denaturation at 94ºC for 1min followed by 30 cycles of 94ºC for 45s, 50ºC for 45s (annealing) and 72ºC for 1min 15s (elongation), and final extension at 72ºC for 10min. PCR reactions were performed using a thermal cycler with heated lid (Eppendorf Mastercycler Gradient, Techne Progene, Techne Genius or Hybaid Omnigene). Samples were stored at -20ºC.

Table 2-1: Oligonucleotide primer sequences used to PCR amplify DNA from the IIS4-IIS6 domain of the maize weevil *para* sodium channel gene.

Primer name	Sequence[a]
Domain II degenerate primers[b]	
DgN1	GCNAARTCNTGGCCNAC
DgN2	GCNAARTCNTGGCCNACNYT
DgN3	YTTRTTNGTNTCRTTRTCRGG
DgN4	TTNGTNTCRTTRTCRGCNGTNGG
DgSeq1	TNCCNMGNTGGAAYTTYAC
DgSeq2	RAARTCNGTRAARTTCCANC
S. zeamais specific primers[c]	
Sz1	ACCCTGAACTTATTGATATCC
Sz2	TGAACTTATTGATATCC
Sz3	GAGCGGACAAACTTGAAGATC
Sz4	CTTGAAGATCCAAAGTTGCTC
Sz8	ATGGAATACAAGAGACATCTC

[a]All primers are shown 5'-3'. [b]Degenerate primers based on conserved sequences in domain II and used for amplification in a range of species. [c]Primers based upon the *S. zeamais* sequence. Degenerate bases are represented using standard IUB codes: R=A+G, Y=C+T, M=A+C, N=A+C+G+T.

2.2.1.4 Gel electrophoresis

The concentration, size and quality of RNA and DNA samples were established by agarose gel electrophoresis. PCR products (6µl) were mixed with 2µl of sterile distilled water and 2µl of 1x loading buffer (95% formamide; 0.025% xylene cyanol; 0.025% bromophenol blue; 18mM EDTA; 0.025% SDS), and loaded onto 1.5% agarose gel. Electrophoresis was carried out in 1x TAE buffer (40mM Tris-acetate, 1mM EDTA, pH 8.0) and run at 100V for 1 - 1.5h. An appropriate size marker, GeneRuler 100bp, was run alongside the RNA/DNA samples. Gels were post-stained in ethidium bromide solution (0.5 µg/ml) for 20min at room temperature and de-stained for 20min in distilled water. RNA/DNA fragments were visualized on a UV transilluminator and photographed using a Kodak Digital Science DC290 Zoom camera. Images were analyzed using the Kodak 1D gel imaging software v3.5.4.

2.2.1.5 Purification of PCR products

PCR products were purified by recovery of DNA from agarose gel and ethanol precipitation. For recovery of DNA from agarose gels, the gel slices containing the DNA fragments of the expected size (417bp) were excised with a clean sterile scalpel blade and the DNA recovered from 1.5% agarose gel using the QIAquick gel extraction kit (Qiagen) according to manufacturer's recommendations. For ethanol precipitation, PCR products (25µl) were mixed with 40µl 4M ammonium acetate and 200µl 100% ethanol and centrifuged at 13,000rpm at room temperature for 20min. The supernatant was removed

and the pellet washed with 75% ethanol, re-centrifuged for 5min, air-dried and re-suspended in 10µl of nuclease-free water.

2.2.1.6 DNA sequencing

Sequencing was carried out using the BigDye Terminator v1.1 Cycle Sequencing kit™ (Applied Biosystems) in reactions containing 50ng PCR product, 25ng sequencing primers (DgSeq1, DgSeq2, DgN1 and DgN4) (Table 2-1), 4µl ready-reaction mix, 2µl 2.5x Big Dye reaction buffer (200mM Tris-HCl pH 9; 5mM $MgCl_2$) and sterile water to a total volume of 20µl. The sequencing reaction was run through 25 cycles of 96ºC for 1min, 96ºC for 30s, 50ºC for 30s and 60ºC for 4min in a thermal cycler. To remove incorporated dye terminators prior to electrophoresis, products were precipitated with 2µl of sodium acetate and 50µl 100% ethanol for 10min at room temperature before centrifugation for 15min at 13,000rpm. The supernatant was discarded and the pellet washed in 70% ethanol, re-centrifuged for 5min, air-dried and re-suspended in 20µl Hi Di formamide. Samples were run on an ABI 310 Automated DNA Sequencer (PE Applied Biosystems) and the sequences were aligned and analyzed using Vector NTI software (Invitrogen Corp).

2.2.2 Insecticide bioassay to select resistant individuals

Insecticide bioassay followed methods adapted from studies on *Rhyzopertha dominica* (F.) (Coleoptera: Bostrichidae) (Guedes *et al*., 1996,

1997; Guedes & Zhu, 1998), using 17ml scintillation vials. DDT (Sigma-Aldrich) was dissolved in acetone and four different concentrations (16, 32, 40 and 50mg/ml) were prepared. Aliquots of 340µl of each concentration (three repetitions) were applied to the scintillation vials. Once the acetone evaporated, twenty insects from each resistant population (JA and JF) were placed into the vials. Acetone was used as control. Following 48h of exposure, dead insects were collected from the lower concentration and live insects were collected from the higher concentration (resistant). Genomic DNA was extracted from these insects and direct sequencing of the IIS4-IIS6 region of the sodium channel *para* gene was carried out. DDT was chosen for the bioassay due to the cross-resistance in pyrethroid-resistant insects and enhanced detoxification enzyme activity in the resistant populations (JA and JF) in the presence of pyrethoids (Fragoso *et al*., 2007).

2.2.3 Extraction of genomic DNA and analysis of gene fragments

Corresponding *para* IIS4-IIS6 gene fragments were PCR amplified from maize weevil genomic DNA using weevil specific primers designed from the cDNA sequence. Genomic DNA was extracted from individual weevils using 200µl of DNAzol reagent (Molecular Research Center Inc.) for each extraction and following the manufacturer's instruction. Samples were stored at -20ºC until required. Gene fragments were amplified in a two-step nested PCR with the designed primers (Table 2-1). The primary PCR reaction (25µl) contained 2µl cDNA, 100ng of each primer (Sz1 and Sz3) (Table 2-1), 12.5µl of Master Mix (buffer, dNTP and Taq Polymerase) and 8.5µl of sterile de-ionized water

(SDW). The secondary reaction (25µl) contained 1µl primary PCR product, 100ng of each primer (Sz2 and Sz4) (Table 1), 12.5µl of Master Mix and 9.5µl of SDW. PCR reaction conditions (cycles and temperatures) were as described for RT-PCR analysis. After ethanol precipitation, the *para* gene fragments (493bp) were directly sequenced using the internal primer, Sz8 (20ng) (Table 2-1) and The Big Dye Terminator v1.1 Cycle Sequencing Kit™. The sequencing reaction conditions also were the same as described in section 2.2.1.6 and all sequences were analyzed using Vector NTI software (Invitrogen Corp).

2.2.4 Diagnostic Assays for insecticide resistance

2.2.4.1 Preparation of 96 sample reference plate

Maize weevil field populations from 12 different sites in Brazil (Figure 2-3) were used in all diagnostic assays. The fluorescence-based assays (Taqman SNP genotyping and High Resolution Melt) were performed on a standard 96 well test plate comprised of individual weevil genomic DNAs from the field populations. Twenty insects were screened from each strain. DNA was extracted from a single maize weevil using DNAzol reagent (Molecular Research Center, Inc) at one fifth the recommended volume for each extraction, and afterwards re-suspended in 50µl sterile water. The concentration of DNA in a 2µl sample was determined by absorption at 260nm using a NanoDrop spectrophotometer (NanoDrop Technologies). Genotyping was carried out in blind trials and any samples of ambiguous genotype were sequenced. Genomic DNA from individuals of known genotype was used for the initial optimization of the assay and as a positive control when the field-

collected populations were screened. Water blank was used as a negative control.

2.2.4.2 TaqMan SNP genotype assay

The nucleotide alignments of the *S. zeamais* domain II sodium channel gene sequence from JA and JF and a conserved region around the super-*kdr* site were selected for primer/probe design. Forward and reverse primers and two minor groove binding (MGB) probes (Applied Biosystems) were designed using the Primer Express™ Software Version 2.0. Primers weevil-TtoV Forward (5'-ACCATGGGTGCCTTGGG-3') and weevil-TtoV Reverse (5'-GCATACCCATCACGGCGAATATAAA-3') were standard oligonucleotides with no modification. The probe weevil-TtoVV2 (5'-ACAACACAAAGGTCAGGTT-3') was labeled with VIC (reporter dye) at the 5' end for the detection of the wild-type allele and the probe weevil-TtoVM2 (5'-ACAACACAAAGATCAGGTT-3') was labeled with 6-FAM (reporter dye) for detection of the super-*kdr* allele. Each probe also carried a 3' non-fluorescent quencher and a minor groove binder at the 3' end. The minor groove binder gives more precise allelic discrimination by raising the melting temperature (T_M) between matched and mis-matched probes (Afonina *et al*., 1997). The primers, weevil-TtoV Forward and weevil-TtoV Reverse, and the probe weevil-TtoVV2 were used in the assay with probe weevil TtoVM2 for super-*kdr* detection. A diagram with the position of the primers and probes at the TaqMan assay is shown in Figure 2-4.

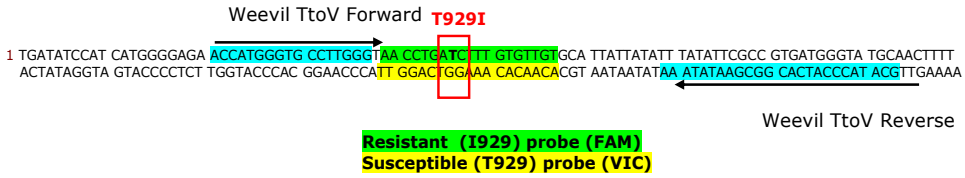

Fig. 2-4: *S. zeamais para* sodium channel gene fragment with the location of the primers and probes designed for the T929I TaqMan assay.

PCR reactions (20µl) contained 2µl of genomic DNA, 10µl of SensiMix DNA kit (Quantace), 900nM of each primer and 200nM of each probe. Samples were run on a Rotor-Gene 6000™ (Corbett Research) using the temperature cycling conditions of: 95ºC for 10min followed by 42 cycles of 95ºC for 10s and 60ºC for 45s. The increase in VIC and FAM fluorescence was monitored in real time by acquiring each cycle on the yellow (530nm excitation and 555nm emission) and green channel (470nm excitation and 510nm emission) of the Rotor-Gene respectively. For each assay, fluorescence values of the negative controls were averaged and subtracted from the raw data to correct for background fluorescence. The endpoint values of fluorescence for each dye were then plotted against each other in bivariate scatter plots that gave a clear clustering of the samples and enabled easy scoring of the genotypes.

2.2.4.3 High Resolution Melt (HRM) assay

HRM assay for super-*kdr* detection was performed following the methods in previous reports (CorProtocol™ 6000-1-July06; Krypuy *et al*., 2006; Vezenegho *et al*., 2009). Two primers were designed (super-*kdr* F1 5'-

TATTGATATCCATCATGGGGAGAA-3' and super-*kdr* R3 5'-CAATATATTACCCCAGTAGTTTTTGCCG-3') and their positions on the maize weevil *para* sodium channel gene fragment are shown in Figure 2-5. PCR reactions contained 2µl of genomic DNA, 10µl of Sensimix HRM kit (reaction buffer, heat-activated Taq DNA polymerase, dNTPs, 6mM $MgCl_2$ and stabilizers) (Quantace), 200nM of each primer (super-*kdr* F1 and super-*kdr* R3) and 1µl of EvaGreen Dye (fluorescent intercalating dye), made up to 25µl with sterile distilled water. Samples were run on a Rotor-Gene 6000 (HRM)^{TM} (Corbett Research) using temperature cycling conditions of: 1 cycle of 95ºC for 10min followed by 45 cycles of 95ºC for 10s and 60º for 20s. This was immediately followed by a melt step of 70 - 80ºC rising by 0.1ºC and pausing for 2s per step. The increase in Eva Green fluorescence was monitored in real time during the PCR and the subsequent decrease during the melt phase by acquiring each cycle-step to the green channel (470nm excitation and 510nm emission) of the Rotor-Gene. Genotypes were scored by examining normalized and difference melt plots using the Rotor-Gene Software. The Sensimix HRM kit was stored at -20ºC and the Eva Green tube was wrapped in aluminum foil to protect the solution against light exposure.

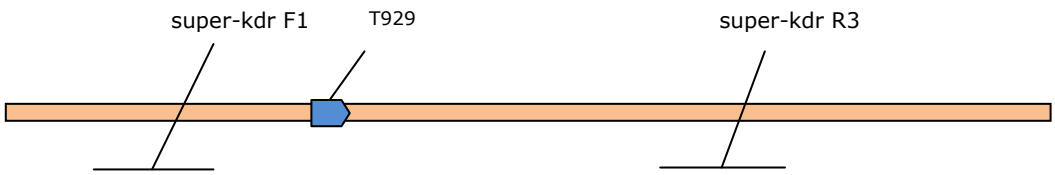

Fig. 2-5: Schematic diagram of the maize weevil *para* sodium channel gene fragment (180bp) with the T929I mutation position and the location of the primers designed for the HRM assay.

2.2.4.4 PCR RFLP (Restriction Fragment Length Polymorphism)

The same genomic DNAs used for the optimization of the Taqman and HRM were used for the optimization of the PCR. For the negative control we used a water blank. Two primers, F2 (5'-GAACTTATTGATATCCATCATGGGGAGAACC-3') and F5 (5'-CTGATGGTCAGGAAATCTGTCCACATT-3'), were designed to allow the amplification of the DNA fragment with the T929I mutation. PCR amplification was carried out in a final volume of 20µl. Each reaction contained 1.5µl of template DNA, 100ng of each primer, 10µl of PCR mix and 6.5µl of sterile distilled water. An initial denaturation step at 95ºC for 1min was followed by 40 cycles of denaturation at 94ºC for 20s, annealing at 55ºC for 17s and extension at 72ºC for 25s, with a final extension step of 72ºC for 7min. Amplified products were visualized by 2% (w/v) agarose gel electrophoresis in 1x TBE buffer (89mM Tris Base , 89mM Borate and 2mM EDTA; pH 8.0), stained with ethidium bromide (0.5µg/ml) and photographed under UV transillumination.

Para sodium channel gene sequences of all individuals with known genotype were aligned and scanned with NEBcutter V2.0 (http://tools.neb.com/NEBcutter2/). Finally, the enzyme Mbo I was selected producing the best genotype-specific restriction pattern. Digestion was performed by incubating 10µl of PCR product with 2.5U of the enzyme, 10µl of 10x enzyme-buffer, in a final reaction volume of 30µl, at 37ºC for 4h. Restriction products were then separated by 2% agarose gel electrophoresis in TBE buffer, stained with ethidium bromide and visualized under a UV transilluminator.

2.3 Light and Electron Microscopy

Thoracic ganglia were fixed for 2h in 2.5% glutaraldehyde in phosphate buffer (0.15M), washed in the same buffer for 4 - 10min and left overnight in the fridge. The ganglia were post-fixed for 1 - 2h in 1% osmium tetroxide in the same buffer, washed three times in distilled water, serially dehydrated in ethanol (30%, 50%, 70%, 90% for 5min and 100% for 1h), infiltrated with Spurr's low viscosity epoxy resin and left in the fridge overnight. The ganglia were embedded in fresh resin overnight at 60ºC.

For Light Microscopy, 0.5µm thick sections were collected, baked for 5min at 80ºC, stained with 1% Toluidine Blue in 1% Borate solution for 1 - 2min and washed with distilled water to rinse off excess stain (Mercer, 1963). The sections were examined under a light microscope at a magnification of 40-1000x.

For Transmission Electron Microscopy, silver/gold sections (0.07nm thick) were cut on a Reichert-Jung Ultracut using a diamond knife and collected on 300 mesh copper grids. Sections, stained with Reynolds Lead Citrate and 5% Uranyl Acetate in distilled water for 10 - 15min each, were observed with a Jeol 1010 transmission electron microscope.

2.4 Neurons of *S. zeamais*

2.4.1 Isolation of nervous cells and short term culture

Adults were ventrally glued with Superglue in a Petri dish and the thorax was cut open with a scalpel (Figure 2-6). After removing the digestive tract, the thoracic ganglia were exposed in the ventral side of the thorax, removed and maintained in Ca^{2+}/Mg^{2+}-free Rinaldini's saline (135mM NaCl, 2.5mM KCl, 0.4mM NaH_2PO_4, 1.25mM $NaHCO_3$, 0.5mM Glucose, 5mM HEPES, pH 7.2 with NaOH) (Schneider & Blumenthal, 1978). For each experiment, aproximatelly fourty thoracic ganglia were removed from 15 weevils. To isolate the neurons, the thoracic ganglia were separated and the neural sheath surrounding the ganglia was disrupted mechanically prior to treatment with 0.5 mg/ml collagenase (Clostridiopeptidase A) (Sigma-Aldrich) and 2 mg/ml dispase (Sigma-Aldrich) (in Ca^{2+}/Mg^{2+}-free Rinaldini's saline) for 1h at room temperature (21-23ºC). The enzyme treatment was performed in a plastic 1ml centrifuge-tube placed in a laminar air-flow cabinet and terminated by washing the ganglia several times with Ca^{2+}/Mg^{2+}-free Rinaldini's saline. After centrifuging, the pellet was then re-suspended in modified Schneider's culture medium (85% Schneider's *Drosophila* medium (Gibco GBL), 15% foetal bovine

serum (FBS), plus 100 U/ml penicillin and 100 µg/ml streptomycin). The individual neurons were isolated into the culture media by gently triturating the ganglia with the flame polished tip of a Pasteur pipette. After trituration, the ganglia were allowed to settle to the bottom of the centrifuge-tube and the supernatant was placed directly onto 35mm Petri dishes (Nunc, Roskilde) coated with 0.01% Poly-L-lysine (Sigma-Aldrich) or 40 mg/ml Concanavalin A (Con A, Sigma-Aldrich) and/or 1 mg/ml Laminin (Sigma-Aldrich), depending on the experiment (see section 2.4.2). Ganglia left at the bottom of the centrifuge tube were re-suspended in modified Schneider's medium and the procedure was repeated. The dishes were left overnight at 18ºC to allow neurons to settle down and stick to the surface of the dish (Figure 2-6).

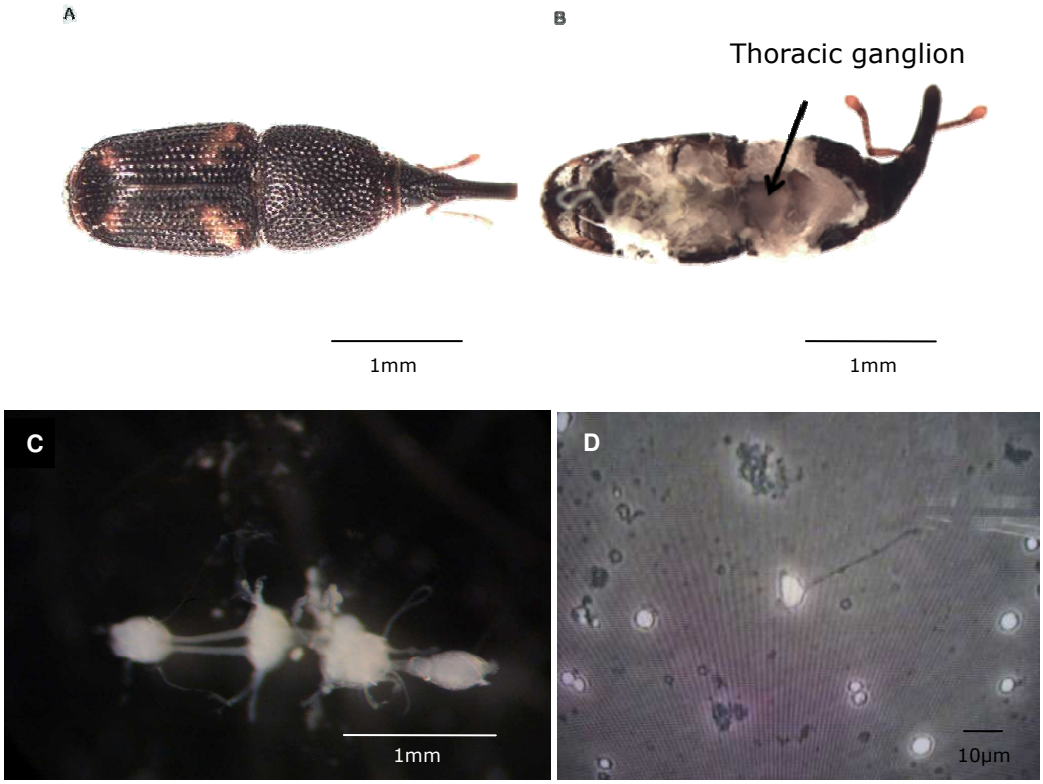

Fig. 2-6: Neurons were isolated from thoracic ganglia of *S. zeamais*. (A) Maize weevils were ventrally glued in Petri dishes. (B) The thorax was cut open to expose the thoracic ganglion (black arrow). (C) Ganglia were removed and maintained in Rinaldini's saline. (D) Neuronal soma and proximal axon isolated from thoracic ganglia by enzyme treatment and trituration followed by overnight culture at 18ºC.

2.4.2 Coating Petri dishes

Four different coating treatments were performed (Poly-L-lysine, Con A, Laminin and Con A with Laminin), with the aim of selecting the best substrate which would attach the maize weevil neurons to the surface of the Petri dish

without interfering with the sodium channel activity. Petri dishes (35mm) (Nunc, Roskilde) coated with 0.5ml 0.01% Poly-L-lysine solution (Sigma-Aldrich) were left for 1h at room temperature, washed with sterile distilled water and left overnight to dry-out in a sterile tissue culture hood. In different treatments, 40µl of 40 mg/ml Con A (Sigma-Aldrich) and/or 16µl of 1 mg/ml Laminin (Sigma-Aldrich) were mixed with 4ml of sterile distilled water to make up a stock solution. 1ml aliquots of this solution were added to 35mm dishes and left for 2h at 37ºC in a humid environment. The dishes were then rinsed with a stream of sterile water and left overnight to air-dry in a sterile tissue culture hood (Hayashi & Hildebrand, 1990).

2.5 Whole-cell patch-clamping

Dishes with *S. zeamais* neurons were used as static baths, filled with house fly ringer (140mM NaCl, 5mM KCl, 0.75mM $CaCl_2$, 4mM $NaHCO_3$, 1mM $MgCl_2$, 5mM HEPES, pH 7.2 with NaOH) and placed on the stage of an inverted microscope. Patch pipettes (5 - 10MΩ) were pulled from borosilicate glass capillaries (World Precision Instruments, Florida) using a P-97 Flaming/Brown Micropipette Puller (Sutter Instrument Co., USA) and filled with house fly pipette saline (140mM KCl, 1.1mM EGTA, 2mM $MgCl_2$, 0.1mM $CaCl_2$, 5mM HEPES, pH 7.2 with KOH). Patch pipettes were not polished. Currents were recorded using the whole-cell configuration of the patch clamp technique (Figure 2-7). Pipettes were introduced into the bath saline with the internal pipette saline under a slight positive pressure to prevent the tip from blocking. Patch seals were improved if this pressure was released before establishing

cell contact. Having made contact with the cell, a giga-ohm seal was attained by gentle suction. Further suction was applied to enter the whole-cell configuration. Changes in cell capacitance indicated that whole-cell mode had been achieved (Figure 2-8). A series of voltage steps was applied to the cells by changing the holding potential using voltage protocols controlled by WCP software (Dr John Dempster, University of Strathclyde). Experiments were performed using an Axopatch 200 patch-clamp amplifier (Axon Instruments, USA). Data acquisition and control of the amplifier was also performed using WCP software run on a PC via a National Instruments analog-to-digital interface (PCI-6014). An oscilloscope (Gould) allowed for monitoring of cell contact, seal quality and entry into the whole cell configuration (Figure 2-8). Whole cell capacitance compensation was performed using the Axopatch 200 and leak current subtraction performed using WCP software. The filtering rate was 5kHz and the sampling rate was 50kHz for peak currents and 1.28kHz for tail current experiments.

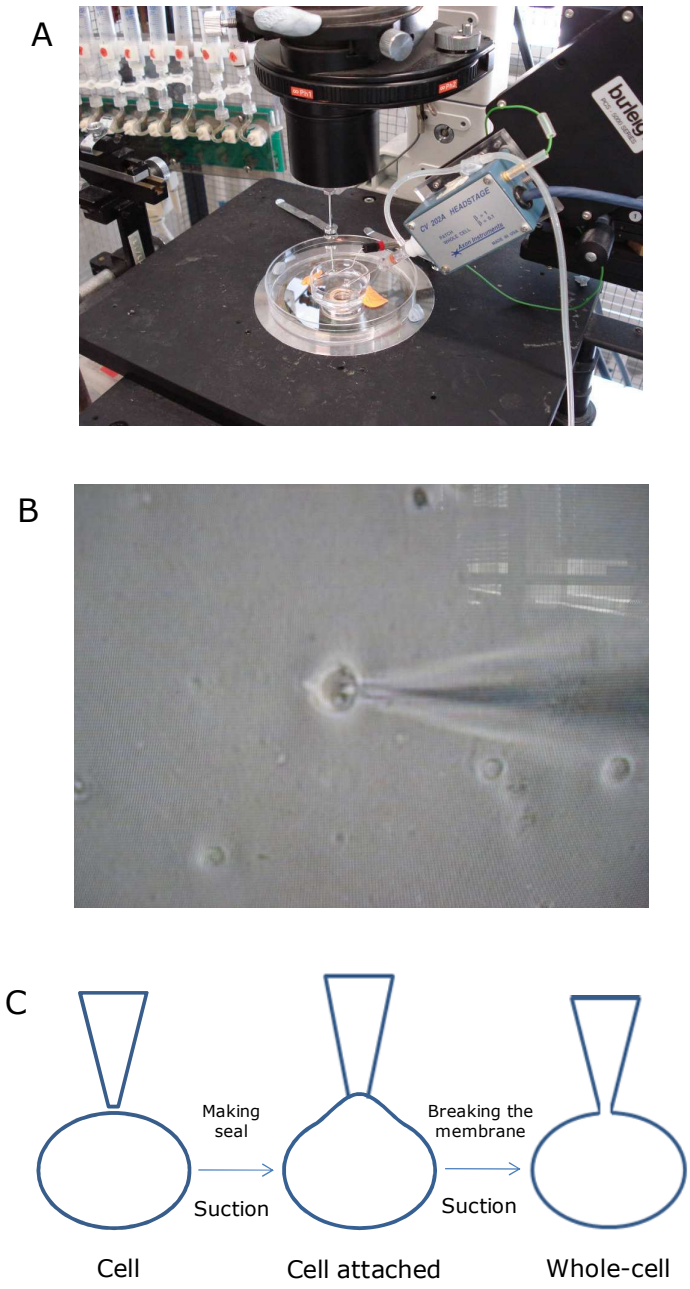

Fig. 2-7: Picture illustrating the whole-cell patch-clamp technique, (A) the amplifier head stage and pipette holder, (B) microscope view of the pipette on a neuron, (C) the whole-cell configuration.

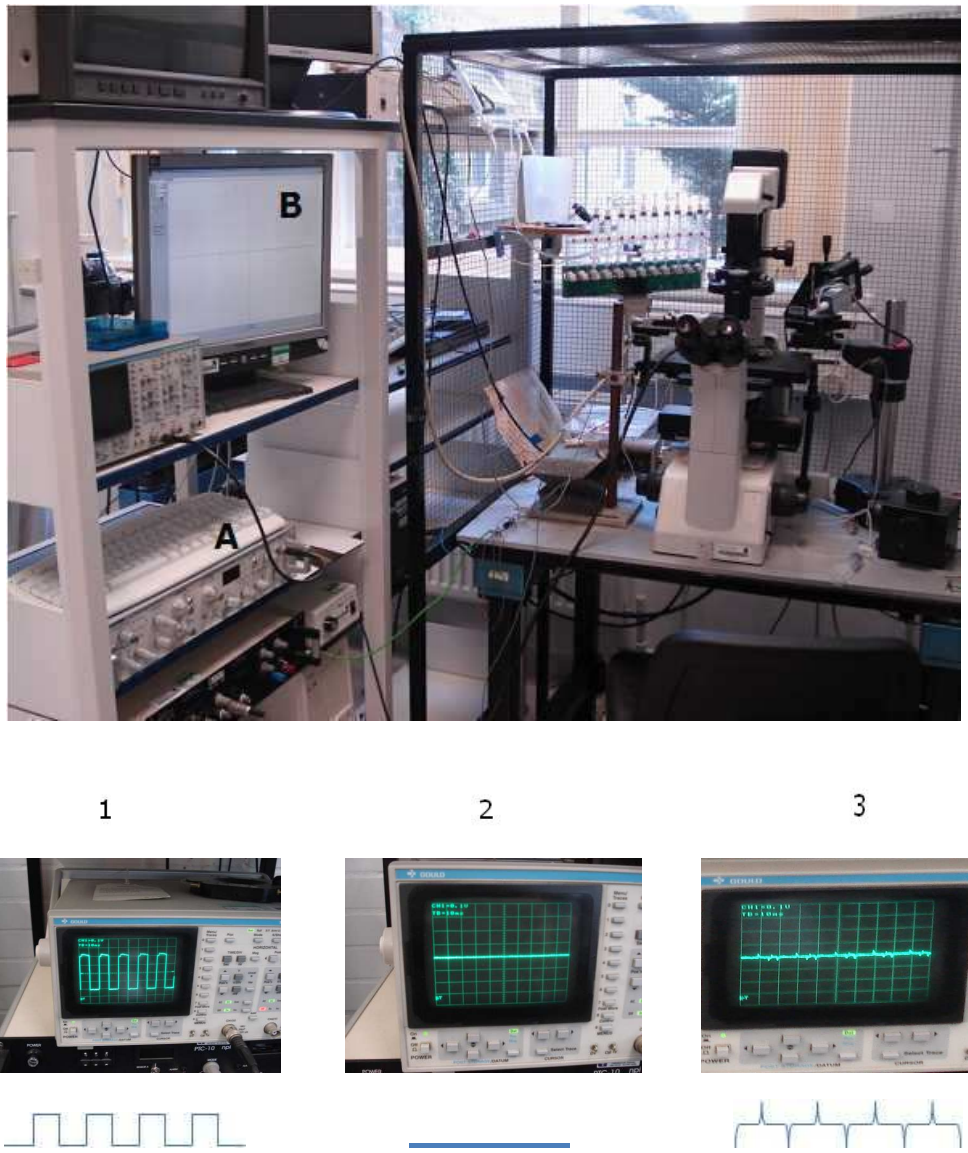

Fig. 2-8: Pictures illustrating the experimental apparatus used to record voltage-gated ion currents in isolated neurons. Currents were detected using a patch-clamp amplifier (A). A generator (built into Axopatch 200) was used to apply square voltage pulses to the patch electrode and enabled the formation of a giga-ohm seal to be monitored. Voltage protocols and data acquisition were controlled by the computer (B).

2.5.1 Basic properties of ion channels

The basic properties of ion channels from maize weevils were investigated and ion currents from different channels were separated by external/internal ion substitution and/or external natural toxin application.

Initially, blockers were omitted from the bathing and pipette saline, but later, the salines were supplemented with different types of ion channel blockers, according to the aim of each experiment. Some ion channel blockers tested during this study were: Co^{2+}(1mM) (Sigma-Aldrich), Cs^{+}(140mM) (Sigma-Aldrich), TEA (tetraethylammonium) (30mM) (Sigma-Aldrich), 4-AP (4-amino-pyridine) (1mM) (Sigma-Aldrich), amiloride (5mM) (Sigma-Aldrich), Gd^{3+} (5mM) (Sigma-Aldrich) and ruthenium red (100μM) (Sigma-Aldrich). In other experiments, some natural toxins were also tested as ion channel blockers, including trigonelline hydrochloride (3-carboxy-1-methyl pyridinium) (Fluka) and TTX (tetrodotoxin) (Sigma-Aldrich). Co^{2+} was used with the intention of blocking voltage-gated calcium channels; Cs^{+}, TEA, 4-AP and trigonelline to block voltage-gated potassium channels; amiloride and Gd^{3+} to block stretch-activated channels (SACs); ruthenium red to block TRP (transient receptor potential) channels; and TTX to block voltage-gated sodium channels. Trigonelline hydrochloride, from a Red Sea soft coral toxin, was dissolved in sterile distilled water to generate a stock solution of 1M and serial dilutions were made to achieve the required concentrations. The toxin was applied by direct addition to the bath in a 100-fold dilution to obtain the final concentrations 0.1mM and 1mM. TTX was also dissolved in distilled water

and the final concentrations in the bath solution were 10nM and 100nM. Experiments were performed at room temperature (21-23ºC).

2.5.2 Pyrethroid treatment of sodium channels

Deltamethrin ((S)-α-cyano-3-phenoxybenzyl(1R,3R)-3-(2,2-dibromovinyl)-2,2dimethylcyclopropanecarboxylate) was obtained from Bayer CropScience. A stock solution of 10^{-1}M deltamethrin was prepared in DMSO and a range of serial dilutions was undertaken to achieve concentrations in the range 10^{-2} to 10^{-6}M. The final concentration of DMSO when applied in the bath solution was not higher than 0.1%. Control experiments showed no effect of 0.1% DMSO on resting membrane potential and sodium channel current. Deltamethrin was introduced to the bath solution to provide a final 1000-fold dilution, and after 3min, the final concentrations, 10^{-5} to 10^{-9}M, were tested. Experiments were undertaken at room temperature (21-23ºC). Recordings were taken before and after application of deltamethrin.

2.6 Voltage protocols

Current-voltage relationships were determined by stepping the cell to test potentials (V_T) in the range -70 to +70mV in 10mV increments for 25ms from a holding potential of -80mV.

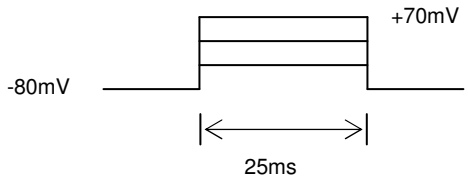

(voltage protocol 1)

Peak current in response to each V_T was measured and plotted against the test potential. The data were then normalized and the largest current in a series was ranked as 1 or 100% and all other currents in that series were represented as a proportion of that maximum. The normalized data allow populations of cells to be compared before being fitted with a modified Boltzmann equation (Equation 1).

Equation 1: $I_{peak} = I_{\max} \times ((V_T - V_{rev}) / (1 + \exp(-(V_T - V_{50}) / K)))$

Where I_{peak} is the normalized peak current elicited by V_T, I_{max} is the maximum peak current elicited by the pulse series, V_T is the test potential, V_{rev} is the reversal potential (determined from the extrapolated I-V curve), V_{50} is the voltage at which half of the maximal current response is elicited, and *k* is the slope function in mV.

The voltage-dependence of activation was calculated by transforming the data to give conductance (Equation 2).

Equation 2: $G = I_{peak} / (V_T - V_{rev})$

Where G is the conductance, I_{peak} is the current evoked by V_T, V_T is the test potential and V_{rev} is the reversal potential (obtained from the fit of Equation 1 to the current-voltage relationship).

Conductance was plotted against V_T and the data fitted with the Boltzmann sigmoidal function giving the conductance-voltage relationship of the channels (Equation 3).

Equation 3: $G = 1/(1 + \exp(V_{50} - V_T / K))$

Where the parameters are the same as those in Equations 1 and 2, but V_{50} is now the voltage for half maximum conductance.

'Fast inactivation' of the channel was also investigated using the voltage protocol 1. A single exponential decay (equation 4) was fitted to the decaying phase of the inward sodium currents attained through the step depolarization protocol.

Equation 4: $I(t) = a0 + a\exp(-t/\tau)$

Where I(t) is the current at time t, a_0 is the plateau current following decay, a is the span of the exponential component and τ is the time constant of the decay. The time constant (τ) values were plotted against their corresponding V_T.

A different protocol was created to study a particular characteristic of sodium channels affected by pyrethroids, known as the tail current. Because pyrethroids slow channel inactivation and deactivation, the tail current characteristic is the most evident effect of these compounds (Vais *et al*., 2001). Deltamethrin, a type II pyrethroid insecticide, preferentially targets the open channels; hence modification by this compound is increased by a number of conditioning pulses (Vais *et al*., 2000a). The protocol was designed to elicit 100 conditioning pulses (5ms, 66Hz) to 0mV from the holding potential of -

80mV with 10ms intervals (sufficient time for recovery from open state inactivation), followed by a single 15s repolarization pulse to -80mV. With repolarization after depolarization, it is expected the channel is rapidly closed, so any residual current indicates pyrethroid modification of the channel. This protocol promotes a good measure and visualization of channel sensitivity.

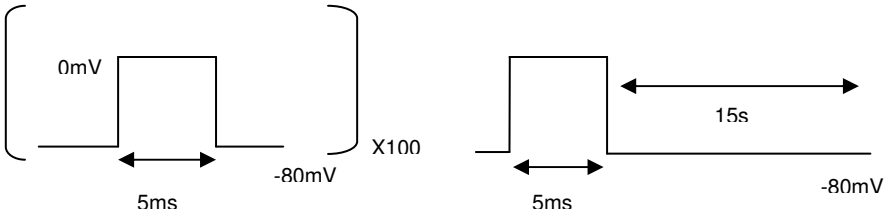

(voltage protocol 2)

Previous studies quantified the sensitivity to pyrethroids through calculating an estimate of the percentage of modified sodium channels (M) with Equation 5 (Tatebayashi & Narahashi, 1994; Vais *et al*., 2000a; Vais *et al*., 2001).

Equation 5: $M(\%) = \{[I_{tail} / (V_{tail} - V_{rev})] / G_{\max}\} \times 100$

Where M is percentage modification, I_{tail} is the peak amplitude of the tail current recorded at the membrane potential V_{tail} (-80mV), V_{rev} is the reversal potential and G_{max} is the maximum sodium conductance of the cell. V_{rev} and G_{max} are obtained through applying the modified Boltzmann function (Equation 1) to the I-V data for the individual cell tested.

M was obtained for different deltamethrin concentrations. The percentage of modification (M) was plotted against deltamethrin concentration

and fitted with a sigmoidal concentration-response function to estimate EC_{50} values.

2.7 Data Analysis

The data were recorded and analysed by WinWCP: Strathclyde Electrophysiology Software V4.0.0 (Dr John Dempster, University of Strathclyde, UK). The peak currents were plotted and conductance data was transformed using Graphpad Prism 5 software on the PC (Graphpad software inc, La Jolla, CA). All graphs were created using Graphpad Prism 5. Results are shown as a mean ± standard error of the mean (SEM). All curve fitting was performed using Graphpad Prism 5 and statistical analysis used the F-test in the same software.

Chapter 3

Identification of a Super-*Kdr* Mutation in the *Sitophilus zeamais para* Sodium Channel Gene Associated with Pyrethroid Resistance

3.1 Introduction

Knockdown resistance *(kdr)* is a recessive trait in insects that causes nerve insensitivity to pyrethroids and DDT (Soderlund & Bloomquist, 1990). The molecular basis of *kdr* resistance was unclear until the cloning of sodium channel genes (homologous to the *Drosophila para* gene) from a number of insects (Park & Taylor, 1997; Miyazaki *et al*., 1996; Williamson *et al*., 1996; Dong, 1997) and identification of several point mutations that are associated with resistance to pyrethroids in these insects (Soderlund, 2005).

The most common *kdr* mutation is a leucine (L) to phenylalanine (F), histidine (H) or serine (S) substitution at position 1014 (housefly sodium channel numbering) in domain II segment 6 (IIS6), associated with moderate levels of pyrethroid resistance. The L1014F mutation was initially identified in house flies, *Musca domestica* (Miyazaki *et al*., 1996; Williamson *et al*., 1996) and the equivalent mutation has now been described in a range of other insect species including German cockroaches, *Blattella germanica* (Miyazaki *et al*., 1996; Dong, 1997; Dong *et al*., 1998); diamondback moths, *Plutella xylostella* (Schuler *et al*., 1998); peach-potato aphid, *Myzus persicae* (Martinez-Torres *et al*., 1999a); mosquitoes, *Anopheles gambiae* (Martines-Torrez *et al*., 1998; Ranson *et al*., 2000), *Culex pipiens* (Martinez-Torres *et al*., 1999b) and *Culex quinquefasciatus* (Xu *et al*., 2005); horn flies, *Haematobia irritans* (Guerrero *et al*., 1997); Colorado potato beetles, *Leptinotarsa decemlineata* (Lee at al., 1999); western flower thrips, *Frankliniella occidentalis* (Forcioli *et al*., 2002); onion thrips, *Thrips tabaci* (Toda & Morishita, 2009); codling moths, *Cydia pomonella* (Brun-Barale *et al*., 2005); and cat fleas, *Ctenocephalides felis*

(Bass *et al*., 2004). The L1014S substitution has been described in *C. pipiens* (Martinez-Torres *et al*., 1999b) and *A. gambiae* (Ranson *et al*., 2000) and the L1014H mutation in tobacco budworm, *Heliothis virescens* (Park and Taylor, 1997).

Additional amino acid substitutions in the sodium channel associated with an enhanced level of resistance to pyrethroids and DDT (termed super-*kdr*) have also been described in insects. These secondary mutations are often found to co-exist with the *kdr* mutation. In house flies displaying the super-*kdr* trait, a methionine (M) to threonine (T) mutation (M918T) in the linker connecting domain II segment 4 and segment 5 is present in addition to the L1014F mutation in domain IIS6 (Williamson *et al*., 1996; Miyazaki *et al*., 1996). Both M918T and L1014F are also found together in horn fly strains, exhibiting high levels of resistance to pyrethroids (Guerrero *et al*., 1997). Another super-*kdr* type mutation is T929I, a threonine to isoleucine substitution found in domain IIS5, in a highly resistant strain of *P. xylostella* (Schuler *et al*., 1998). The T929I mutation was subsequently shown to significantly reduce sensitivity of the *para* sodium channel to pyrethroids (Vais *et al*., 2001). Mutations at the same position have also been reported in three other insect species, a T918C substitution was identified in western flower thrips (Forcioli *et al*., 2002) and a T929V substitution was described in a pyrethroid-resistant cat flea (Bass *et al*., 2004) and whitefly, *Bemisia tabaci* populations (Alon *et al*., 2006; Roditakis *et al*., 2006). As for the original super-*kdr*, these mutations are frequently found in combination with the L1014F *kdr* mutation and confer enhanced levels of resistance up to 1000-fold for certain pyrethroids (Soderlund & Knipple, 2003; Vais *et al*., 2001). However some exceptions to this rule have been described and include

pyrethroid-resistant head lice, *Pediculus capitis,* which showed a T929I substitution together with two different mutations, M827I and L932F (Lee *et al*., 2000, 2003; Tomita *et al*., 2003; Yoon, 2006), pyrethroid resistant whitefly, where the T929V and L925I substitutions can be found as single mutations (Roditakis *et al*., 2006) and a pyrethroid-resistant strain of onion thrips, which carried a T929I change independently of other *kdr*-type mutations (Toda & Morishita, 2009).

In German cockroach, mutations (D58G, E434K, C764R and P1888L) were identified outside of domain II in combination with the L1014F substitution (Liu *et al*., 2000). Although these mutations are associated with high levels of resistance their role in pyrethroid resistance remains to be established.

A number of insect species displaying *kdr*-type resistance, including *H. virescens*, *Aedes aegypti* and cattle ticks, *Boophilus microplus* and *Rhipicephalus microplus*, carry alternative *kdr*-type mutations to the L1014F/H/S substitutions in IIS6, revealing, instead, a V421M substitution in IS6, F1269C change in IIIS6 and L190I replacement in IIS4-S5 (Park *et al*., 1997, Kawada *et al*., 2009, Morgan *et al*., 2009) of the sodium channel.

The *kdr* and super-*kdr* mutations identified in the *para*-type sodium channel gene of a range of different insect species have been shown to confer moderate to high levels of pyrethroid resistance and their detection is an essential part of pest resistance management. This chapter describes the identification of a mutation in domain IIS5 of the sodium channel that is associated with resistance to pyrethroids in the maize weevil, *S. zeamais*. The C-T change at amino acid position 929 of the *para*-type sodium channel gene

results in a T to I substitution in the sodium channel protein of resistant insects and is likely to be responsible for the high levels of pyrethroid resistance of these resistant *S. zeamais* populations.

3.2 RT-PCR analysis of the IIS4-IIS6 region of the *S. zeamais para* sodium channel gene sequences

3.2.1 Extraction of total RNA, cDNA synthesis and amplification

Total mRNA was extracted from adult maize weevils from one susceptible (SL) and two pyrethroid-resistant populations (JA and JF) and reverse transcribed to cDNA. Degenerate primers were designed from highly conserved sequences of invertebrate *para* sodium channel (domain II) which encompass the region where most of the mutations conferring *kdr* and *super-kdr* resistance to pyrethorids are located (Martinez-Torres *et al*., 1997) (Figure 3-1). These were used in nested PCR (see section 2.2.1.3, Chapter 2), to amplify a 417bp fragment covering the IIS4-IIS6 region (Figure 3-2).

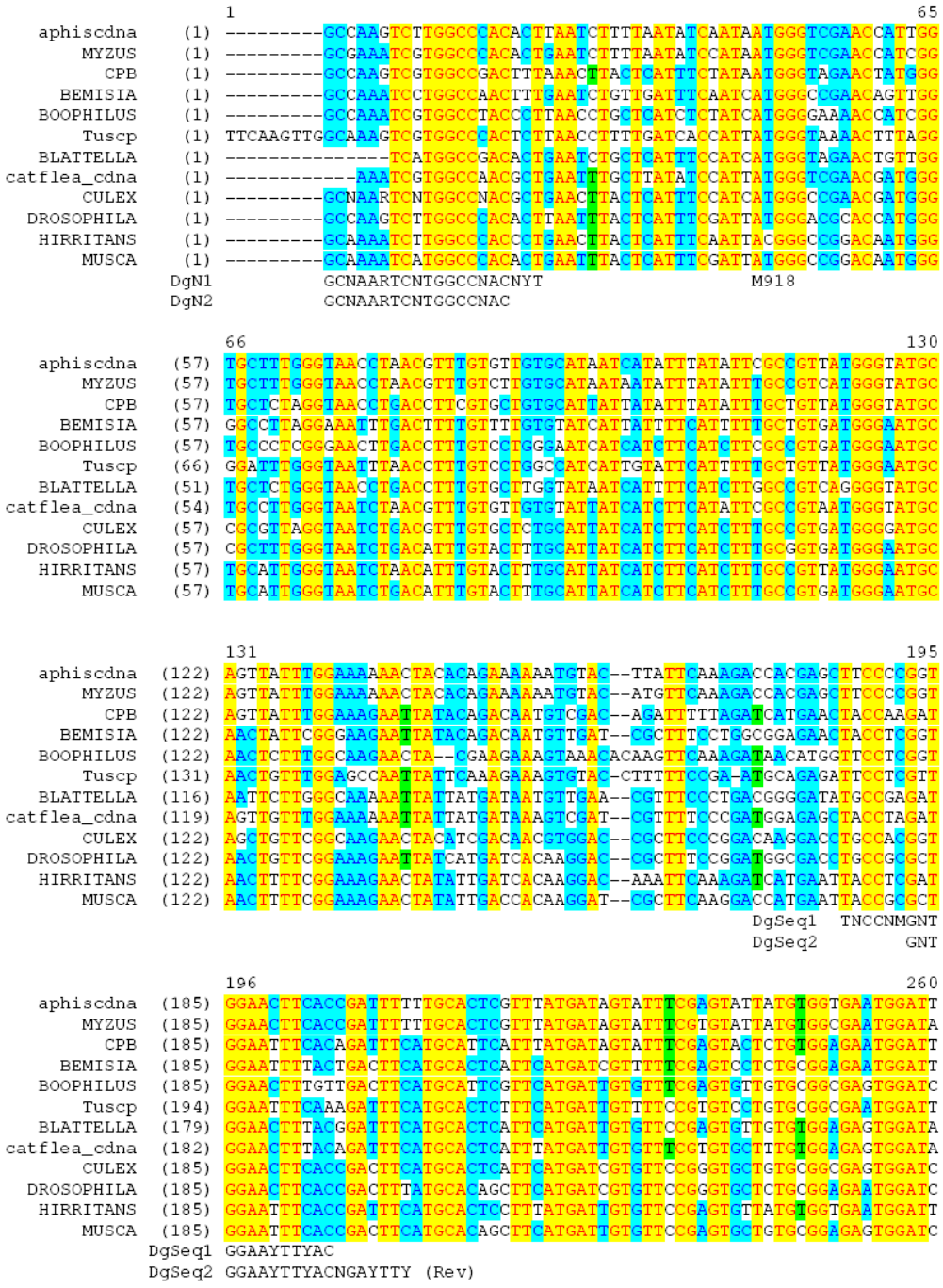
1 65
aphiscdna (1) ---------GCCAAGTCTTGGCCCACACTTAATCTTTTAATATCAATAATGGGTCGAACCATTGG
MYZUS (1) ---------GCGAAATCGTGGCCCACACTGAATCTTTTAATATCCATAATGGGTCGAACCATCGG
CPB (1) ---------GCCAAGTCGTGGCCGACTTTAAACTTACTCATTTCTATAATGGGTAGAACTATGGG
BEMISIA (1) ---------GCCAAATCCTGGCCAACTTTGAATCTGTTGATTTCAATCATGGGCCGAACAGTTGG
BOOPHILUS (1) ---------GCCAAATCGTGGCCTACCCTTAACCTGCTCATCTCTATCATGGGGAAAACCATCGG
Tuscp (1) TTCAAGTTGGCAAAGTCGTGGCCCACTCTTAACCTTTTGATCACCATTATGGGTAAAACTTTAGG
BLATTELLA (1) ---------------TCATGGCCGACACTGAATCTGCTCATTTCCATCATGGGTAGAACTGTTGG
catflea_cdna (1) ------------AAATCGTGGCCAACGCTGAATTTGCTTATATCCATTATGGGTCGAACGATGGG
CULEX (1) ---------GCNAARTCNTGGCCNACGCTGAACTTACTCATTTCCATCATGGGCCGAACGATGGG
DROSOPHILA (1) ---------GCCAAGTCTTGGCCCACACTTAATTTACTCATTTCGATTATGGGACGCACCATGGG
HIRRITANS (1) ---------GCAAAATCTTGGCCCACCCTGAACTTACTCATTTCAATTACGGGCCGGACAATGGG
MUSCA (1) ---------GCAAAATCATGGCCCACACTGAATTTACTCATTTCGATTATGGGCCGGACAATGGG
DgN1 GCNAARTCNTGGCCNACNYT M918
DgN2 GCNAARTCNTGGCCNAC
66 130
aphiscdna (57) TGCTTTGGGTAACCTAACGTTTGTGTTGTGCATAATCATATTTATATTCGCCGTTATGGGTATGC
MYZUS (57) TGCTTTGGGTAACCTAACGTTTGTCTTGTGCATAATAATATTTATATTTGCCGTCATGGGTATGC
CPB (57) TGCTCTAGGTAACCTGACCTTCGTGCTGTGCATTATTATATTTATATTTGCTGTTATGGGTATGC
BEMISIA (57) GGCCTTAGGAAATTTGACTTTTGTTTTGTGTATCATTATTTTCATTTTTGCTGTGATGGGAATGC
BOOPHILUS (57) TGCCCTCGGGAACTTGACCTTTGTCCTGGGAATCATCATCTTCATCTTCGCCGTGATGGGAATGC
Tuscp (66) GGATTTGGGTAATTTAACCTTTGTCCTGGCCATCATTGTATTCATTTTTGCTGTTATGGGAATGC
BLATTELLA (51) TGCTCTGGGTAACCTGACCTTTGTGCTTGGTATAATCATTTTCATCTTGGCCGTCAGGGGTATGC
catflea_cdna (54) TGCCTTGGGTAATCTAACGTTTGTGTTGTGTATTATCATCTTCATATTCGCCGTAATGGGTATGC
CULEX (57) CGCGTTAGGTAATCTGACGTTTGTGCTCTGCATTATCATCTTCATCTTTGCCGTGATGGGGATGC
DROSOPHILA (57) CGCTTTGGGTAATCTGACATTTGTACTTTGCATTATCATCTTCATCTTTGCGGTGATGGGAATGC
HIRRITANS (57) TGCATTGGGTAATCTAACATTTGTACTTTGCATTATCATCTTCATCTTTGCCGTTATGGGAATGC
MUSCA (57) TGCATTGGGTAATCTGACATTTGTACTTTGCATTATCATCTTCATCTTTGCCGTGATGGGAATGC
131 195
aphiscdna (122) AGTTATTTGGAAAAAACTACACAGAAAAATGTAC--TTATTCAAAGACCACGAGCTTCCCCGGT
MYZUS (122) AGTTATTTGGAAAAAACTACACAGAAAAATGTAC--ATGTTCAAAGACCACGAGCTTCCCCGGT
CPB (122) AGTTATTTGGAAAGAATTATACAGACAATGTCGAC--AGATTTTTAGATCATGAACTACCAAGAT
BEMISIA (122) AACTATTCGGGAAGAATTATACAGACAATGTTGAT--CGCTTTCCTGGCGGAGAACTACCTCGGT
BOOPHILUS (122) AACTCTTTGGCAAGAACTA--CGAAGAAAGTAAACACAAGTTCAAAGATAACATGGTTCCTCGGT
Tuscp (131) AACTGTTTGGAGCCAATTATTCAAAGAAAGTGTAC-CTTTTTCCGA-ATGCAGAGATTCCTCGTT
BLATTELLA (116) AATTCTTGGGCAAAAATTATTATGATAATGTTGAA--CGTTTCCCTGACGGGGATATGCCGAGAT
catflea_cdna (119) AGTTGTTTGGAAAAAATTATTATGATAAAGTCGAT--CGTTTTCCCGATGGAGAGCTACCTAGAT
CULEX (122) AGCTGTTCGGCAAGAACTACATCGACAACGTGGAC--CGCTTTCCCGGACAAGGACCTGCCACGGT
DROSOPHILA (122) AACTGTTCGGAAAGAATTATCATGATCACAAGGAC--CGCTTTCCGGATGGCGACCTGCCGCGCT
HIRRITANS (122) AACTTTTCGGAAAGAACTATATTGATCACAAGGAC--AAATTCAAAGATCATGAATTACCTCGAT
MUSCA (122) AACTTTTCGGAAAGAACTATATTGACCACAAGGAT--CGCTTCAAGGACCATGAATTACCGCGCT
DgSeq1 TNCCNMGNT
DgSeq2 GNT
196 260
aphiscdna (185) GGAACTTCACCGATTTTTTGCACTCGTTTATGATAGTATTTCGAGTATTATGTGGTGAATGGATT
MYZUS (185) GGAACTTCACCGATTTTTTGCACTCGTTTATGATAGTATTTCGTGTATTATGTGGCGAATGGATA
CPB (185) GGAATTTCACAGATTTCATGCATTCATTTATGATAGTATTTCGAGTACTCTGTGGAGAATGGATT
BEMISIA (185) GGAATTTTACTGACTTCATGCACTCATTCATGATCGTTTTTCGAGTCGTCTGCGGAGAATGGATT
BOOPHILUS (185) GGAACTTTGTTGACTTCATGCATTCGTTCATGATTGTGTTTCGAGTGTTGTGCGGCGAGTGGATC
Tuscp (194) GGAATTTCAAAGATTTCATGCACTCTTTCATGATTGTTTTCCGTGTCCTGTGCGGCGAATGGATT
BLATTELLA (179) GGAACTTTACGGATTTCATGCACTCATTCATGATTGTGTTCCGAGTGTTGTGTGGAGAGTGGATA
catflea_cdna (182) GGAACTTTACAGATTTCATGCACTCATTTATGATTGTGTTTCGTGTGCTTTGTGGAGAGTGGATA
CULEX (185) GGAACTTCACCGACTTCATGCACTCATTCATGATCGTGTTCCGGGTGCTGTGCGGCGAGTGGATC
DROSOPHILA (185) GGAACTTCACCGACTTTATGCACAGCTTCATGATCGTGTTCCGGGTGCTCTGCGGAGAATGGATC
HIRRITANS (185) GGAATTTCACCGATTTCATGCACTCCTTTATGATTGTGTTCCGAGTGTTATGTGGTGAATGGATT
MUSCA (185) GGAATTTCACCGACTTCATGCACAGCTTCATGATTGTGTTCCGAGTGCTGTGCGGAGAGTGGATC
DgSeq1 GGAAYTTYAC
DgSeq2 GGAAYTTYACNGAYTTY (Rev)

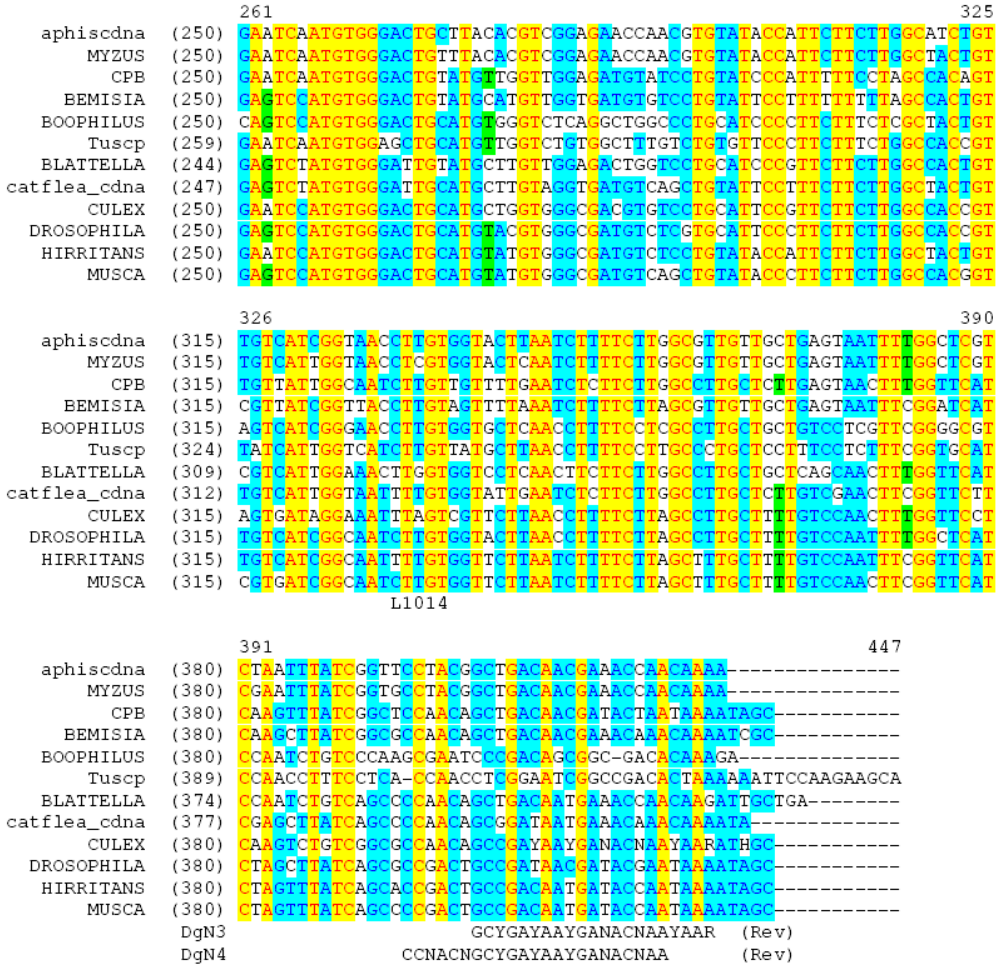

Fig. 3-1: Sequences of invertebrate *para* sodium channel gene (domain II) with the respective positions of the degenerate primers (DgN1, DgN2, DgN3, DgN4, DgSeq1 and DgSeq2).

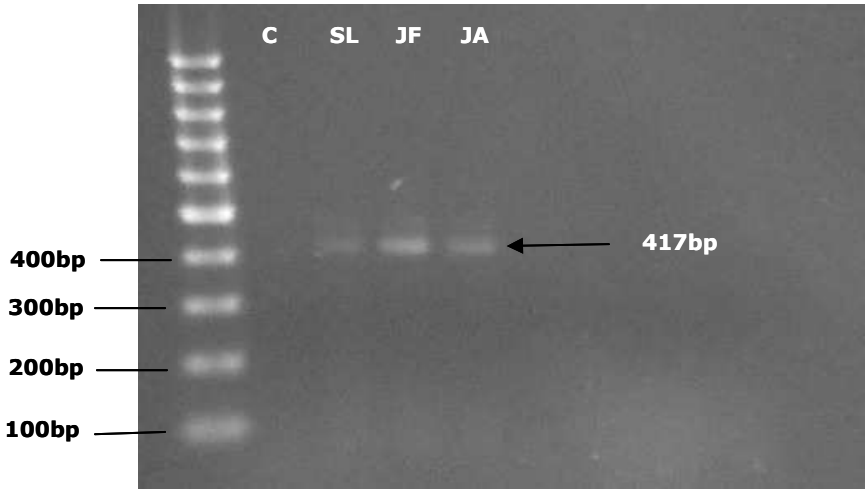

Fig. 3-2: Amplified *para* IIS4-IIS6 gene fragments from cDNA of three maize weevil populations after electrophoresis on a 1.5% agarose gel with a 100bp ladder. C = control (sterile distilled water); SL = Sete Lagoas (susceptible population); JF = Juiz de Fora and JA=Jacarezinho (both resistant populations).

3.2.2 Purification of PCR products

After amplification, PCR products were recovered from agarose gels. Purification was performed using the QIAquick gel extraction kit (Qiagen) (see section 2.2.1.5, Chapter 2) and recovery was confirmed by running an aliquot on a second agarose gel (Figure 3-3).

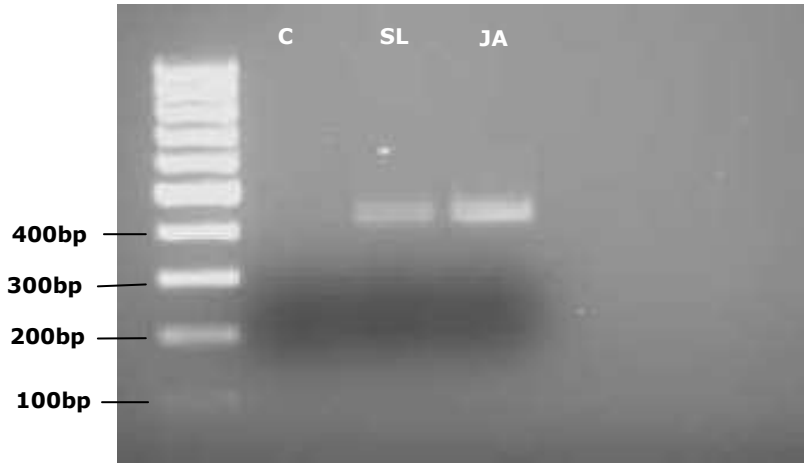

Fig. 3-3: Purified PCR products after electrophoresis on a 1.5% agarose gel with a 100bp ladder. C = control (sterile distilled water); SL = Sete Lagoas (susceptible population) and JA=Jacarezinho (resistant population).

3.2.3 Maize weevil *para* sodium channel gene from cDNA

cDNA was sequenced directly using the sequencing primers DgSeq1, DgSeq2, DgN1 and DgN4 (see section 2.2.1.6, Chapter 2) and the desired fragment of the maize weevil *para* sodium channel coding sequence was obtained. As expected the partial *S. zeamais* gene shows highest sequence identity with the *para* gene of other coleopterans such as the Colorado potato beetle (*Leptinotarsa decemlineata*) (80%) and the red flour beetle (*Tribolium castaneum*) (79%) (Figure 3-4). Examination of the cDNA sequences from resistant and susceptible strains did not reveal any mutations previously associated with *kdr* and/or super-*kdr* in other insect species.

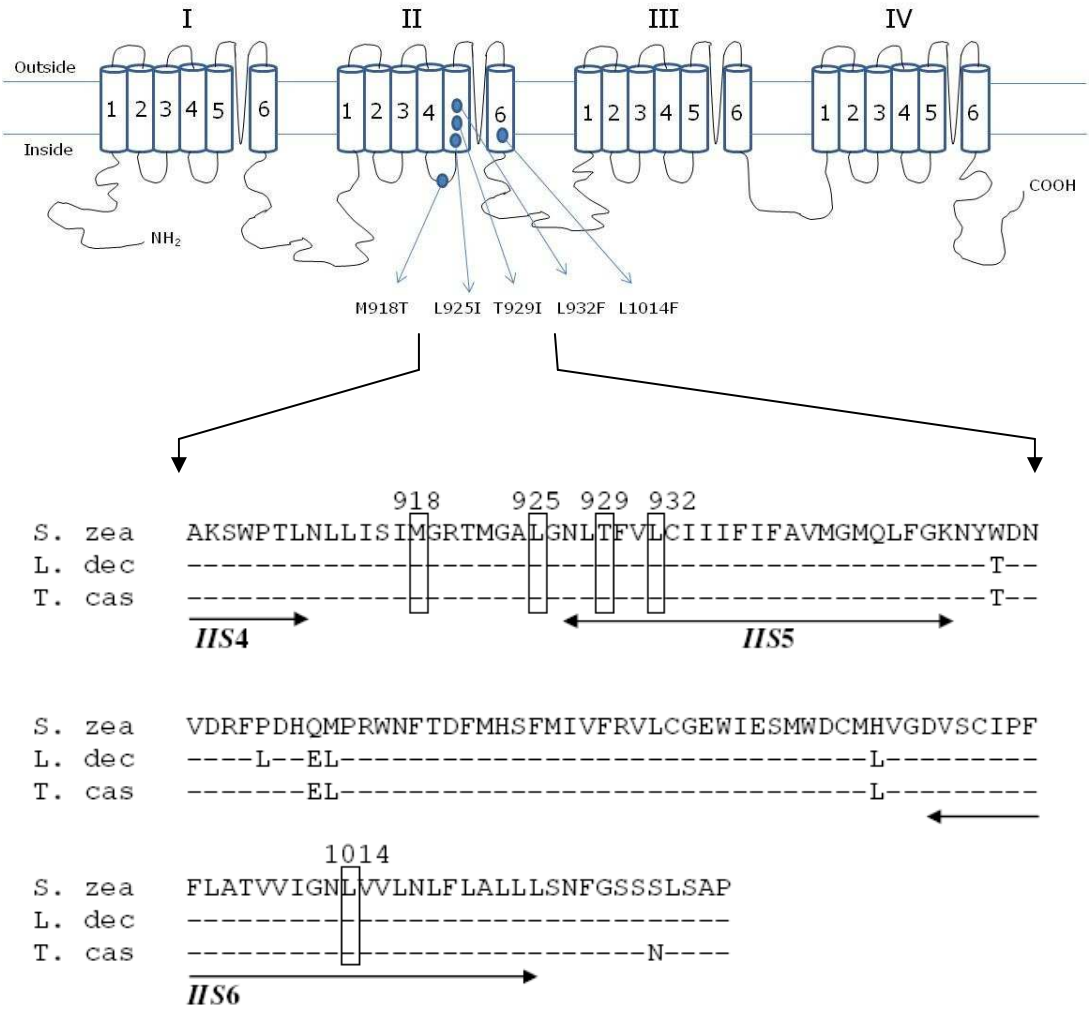

Fig. 3-4: (Top) Diagram of the sodium channel showing the four main domains (I-IV) and six transmembrane segments (S1-S6) within each domain (figure adapted from Schuler *et al*., 1998); (Bottom) Alignment of the maize weevil sodium channel sequence with the corresponding region from red flour beetle (*Tribolium castaneum*) (NP_001159380) and Colorado potato beetle (*Leptinotarsa decemlineata*) (AAD22957). Transmembrane segments (S4, S5, S6) are indicated by arrows under the sequence. The positions of previously reported mutations (M918T, L925I, T929I, L932F and L1014F) are boxed.

3.3 Design of the maize weevil-specific *para* primers

In a further attempt to identify *kdr*-type mutations and also to characterize introns within the genomic DNA encoding the IIS4-IIS6 region of the sodium channel, maize weevil-specific *para* primers were designed and used to amplify the *para* gene from genomic DNA (Figure 3-5). In total eight primers were designed, four forward (Sz1, Sz2, Sz5 and Sz6) and four reverse (Sz4, Sz3, Sz7 and Sz8) (see table 2-1, Chapter 2).

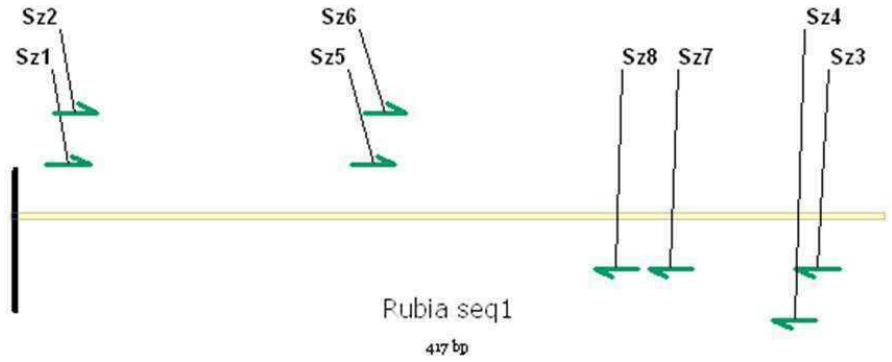

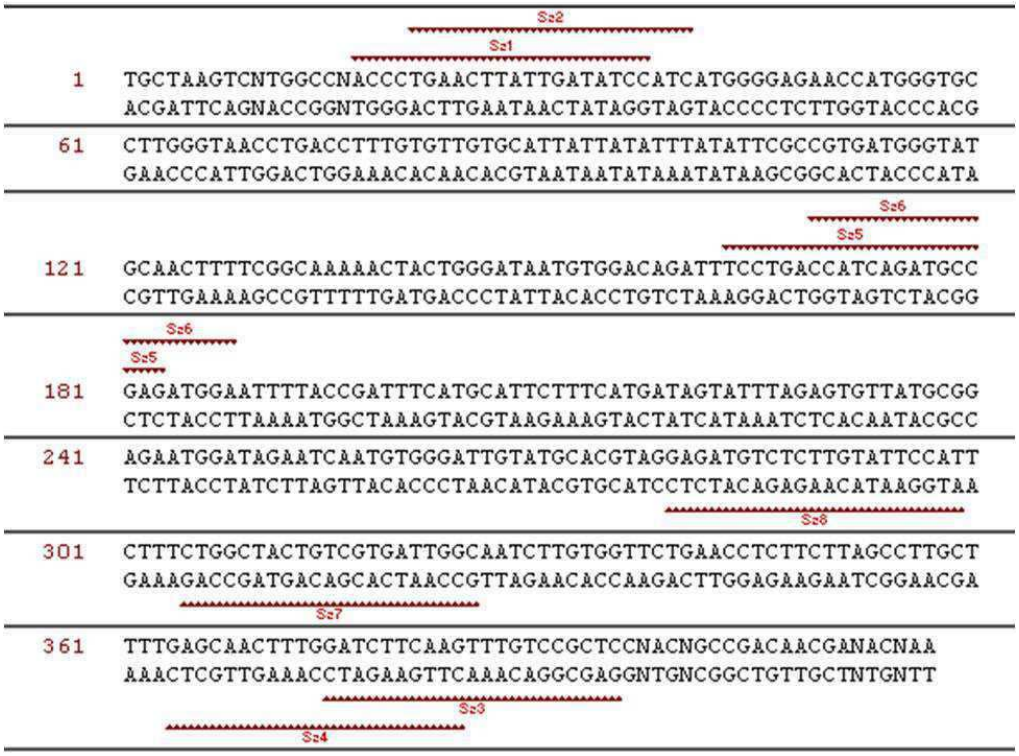

Fig. 3-5: Schematic diagram and sequence of the maize weevil *para* sodium channel gene with the respective positions of specific *para* primers, Sz1 to Sz8. Sz=*Sitophilus zeamais*.

3.4 Selecting resistant individuals

In the initial experiment, the fragments obtained were amplified using RNA extracted from a pool of adults as the template. The resistant populations, JA and JF, had not been subjected to selection with pyrethroids for a long period of time. Consequently, these populations may be comprised of both susceptible and resistant insects. Previous studies using synergists (diethyl maleate, piperonyl butoxide and triphenyl phosphate) suggested that the underlying mechanism of resistance in these strains as "target-site" modification conferring cross-resistance between DDT and pyrethroids (Guedes *et al*., 1994, 1995; Ribeiro *et al*., 2003). Enhanced glutathione S-transferase activity was however observed in the JA and JF populations when compared to the pyrethroid-susceptible population (SL) (Fragoso *et al*., 2003, 2007). For this reason both populations were challenged with DDT.

Four different concentrations of DDT were used to select highly resistant individuals from the JA and JF populations, and after 48h of exposure, dead insects from the lowest concentration and live insects from the highest concentration were collected for extraction of DNA and PCR analysis.

3.5 Genomic DNA extraction and gene fragment analysis

3.5.1 Amplification of genomic DNA and purification of PCR products

The *para* IIS4-IIS6 gene fragments were PCR amplified from genomic DNA (see section 2.2.3, Chapter 2) using maize weevil-specific *para* primers (Figure 3-6).

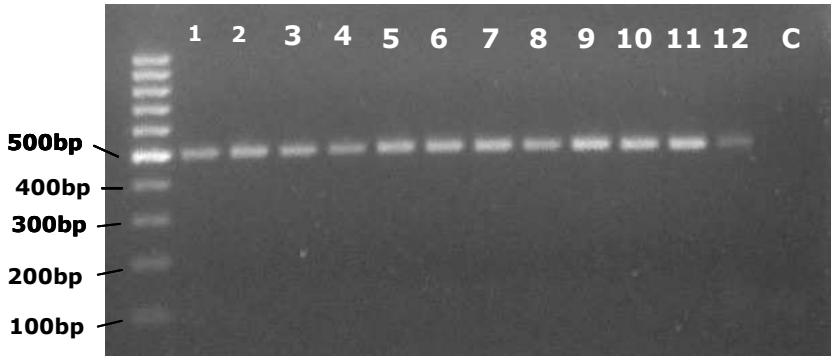

Fig. 3-6: Amplified *para* IIS4-IIS6 gene fragments from genomic DNA after running on a 1.5% agarose gel with a 100bp ladder. Genomic DNA was extracted from individuals selected with DDT. 1, 2, 3 = live (DDT resistant phenotype) and 4, 5, 6 = dead insects (DDT susceptible phenotype) from JA population; 7, 8, 9 = live (DDT resistant phenotype) and 10, 11, 12 = dead insects (DDT susceptible phenotype) from JF population; C = control (sterile distilled water).

Following amplification, PCR products were precipitated with ethanol and directly sequenced using primer Sz8 (see section 2.2.3 Chapter 2).

3.5.2 *Para* IIS4-IIS6 sodium channel gene from maize weevil genomic DNA

Genomic DNA was also used to determine the position and size of the introns within the IIS4-IIS6 region of the maize weevil *para* gene. Figure 3-7 shows the complete sequence of the *para* IIS4-IIS6 gene (493bp) of an individual from JA population and reveals the presence of two introns. The size of both introns is small, 57bp (5') and 44bp (3'), and they appear to be highly conserved in sequence across the three strains used in this study.

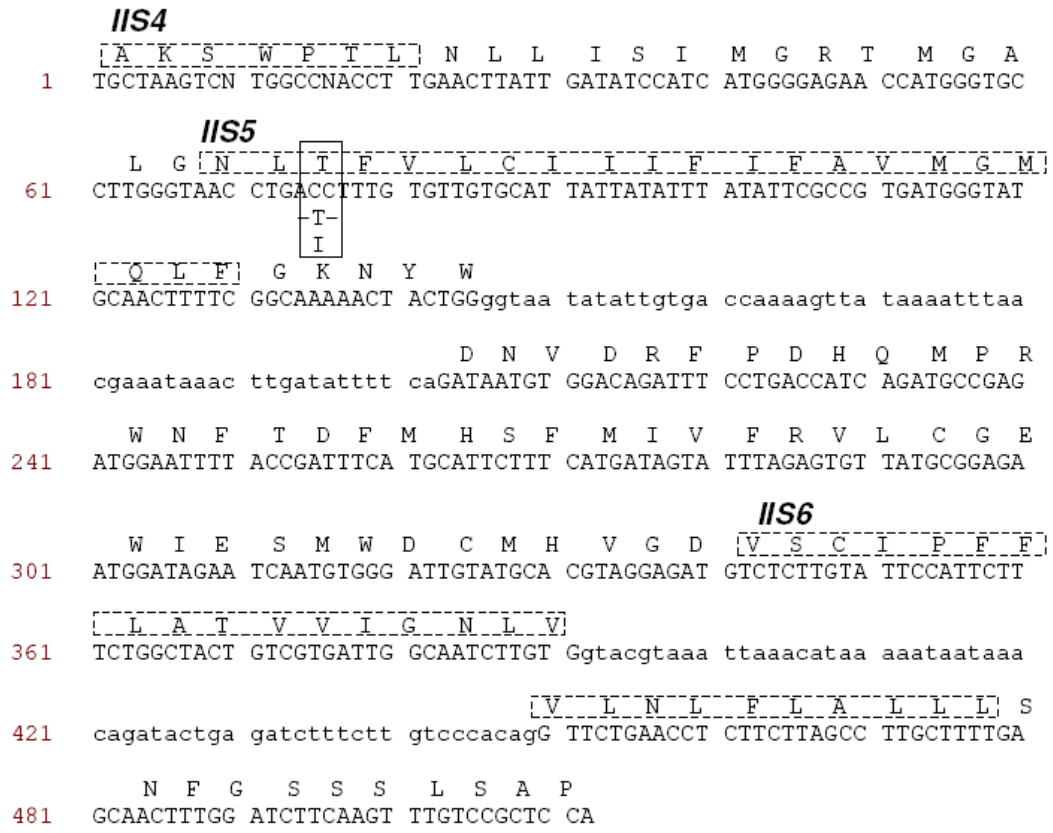

Fig. 3-7: Nucleotide and predicted amino acid sequence of the IIS4-IIS6 region of the maize weevil *para* sodium channel gene. Intron sequences are shown lowercase. Transmembrane segments (S4, S5, S6) are indicated by hashed boxes. The position of the T929I mutation is boxed.

3.5.3 Super-*kdr* mutation in the maize weevil *para* sodium channel gene

The re-amplification of the maize weevil *para* sodium channel gene from genomic DNA allowed us to characterize this region of the gene from multiple individuals of the resistant populations and compare the obtained sequences with those generated from individuals of the susceptible strain. This revealed a single nucleotide substitution (ACC to ATC) at the start of the domain IIS5 transmembrane segment causing a threonine to isoleucine substitution at residue 929 (housefly numbering) in individuals of the resistant strains (Figure 3-8).

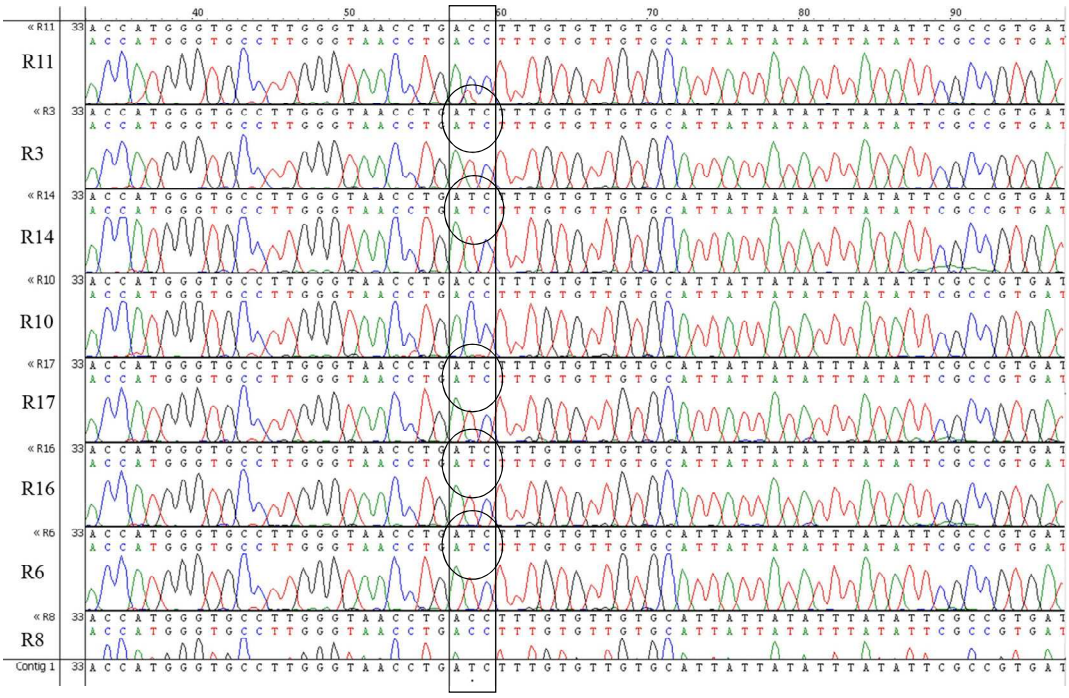

Fig. 3-8: Partial nucleotide sequence chromatograms showing the super-*kdr* mutation site (T929I) of the *para* sodium channel gene from maize weevil strains. The sense strand sequences are shown in each chromatogram. The 929 position is boxed and the T929I mutation is circled. R= individual from resistant population (R11, R10, R8: dead insects; R3, R14, R17, R16, R6: live insects).

Genotyping of individuals from the DDT selection experiment showed that the occurrence of the T929I mutation correlated strongly with resistance. All the live weevils selected with the bioassay had the nucleotide sequence ATC, encoding the resistant (Ile) amino acid, while all the dead ones had the nucleotide sequence ACC, encoding the susceptible (Thr) amino acid.

In total, twenty three insects from the two resistant populations (JA and JF) were genotyped and the frequency of the T929I mutation between dead

and alive adults was analyzed (Table 3-1). From 12 live insects, 11 individuals were homozygous for the T929I mutantion (5 from JA and 6 from JF) and a single individual was heterozygous (JA strain). In contrast, from 11 dead insects, 8 individuals were homozygous for the wild-type allele (T929) (3 from JA and 5 from JF) and 3 were heterozygous for the T929I mutation (2 from JA and 1 from JF).

Table 3-1: Frequency of the T929I mutation (I929) between dead and alive weevils from the resistant populations (JA and JF).

Genotype	DDT selection of maize weevils from resistant populations			
	JA		JF	
	Alive	Dead	Alive	Dead
Homozygous resistant (I929)	5	0	6	0
Heterozygous	1	2	0	1
Homozygous susceptible (T929)	0	3	0	5

3.6 Discussion

Pyrethroid and DDT resistance in many agricultural pests and disease vectors has been shown to be due to a variety of point mutations in the voltage gated sodium channel genes which modify the amino acid sequence of the sodium channel protein (Davies *et al*., 2007; Dong, 2007).

In this study, the sequence of the domain IIS4-IIS6 of the *para* sodium channel gene was initially obtained from maize weevil cDNA and used to design specific primers for amplification of the same region from genomic

DNA. Sequence analysis of selected DDT resistant and susceptible weevils revealed a super-*kdr* type mutation, a threonine to isoleucine substitution in the IIS5 trans-membrane segment of the sodium channel gene, equivalent to residue T929 in the housefly *para* gene sequence. This amino acid substitution was only found in DDT selected individuals from two laboratory resistant populations, JA and JF, which have been previously reported to be strongly resistant to a range of insecticides, including DDT and pyrethoids (Guedes *et al*., 1994, 1995; Ribeiro *et al*., 2003; Oliveira *et al*., 2007; Araújo *et al*., 2008a).

The T929I mutation occurs 11 residues downstream of the methionine to threonine (M918T) substitution of super-*kdr* house flies, which is strongly implicated in enhancing levels of pyrethroid resistance in that species (Williamson *et al*., 1996; Vais *et al*., 2001). The T929I has been previously identified in diamondback moth (Schuler *et al*., 1998), human head lice (Lee *et al*., 2000), thrips (*Thrips tabaci*) (Toda and Morishita 2009) and as novel variations, T929V in cat flea (Bass *et al*., 2004) and white fly (Alon *et al*., 2006; Roditakis *et al*., 2006) and T929C in the Western Flower thrips (Forcioli *et al*., 2002). In diamondback moth, the T929I mutation in combination with L1014F is associated with a high resistance phenotype to pyrethroids (similar to the super-*kdr* phenotype of houseflies) (Schuler *et al*., 1998). Functional expression studies of insect sodium channels in *Xenopus laevis* oocytes have showed that this super-*kdr* mutation reduces sodium channel sensitivity to deltamethrin by over 10,000-fold when combined with the *kdr* substitution (Vais *et al*., 2001, 2003).

Two lines of evidence suggest that the T929I substitution confers resistance to pyrethroids and DDT in maize weevil. Firstly, the mutation was identified in the homozygous genotype in 11 out of 12 maize weevils that survived exposure to DDT but not in those that were killed by this insecticide. Secondly, previous studies using site-directed mutagenesis have demonstrated that this mutation (independently of any other mutation) reduces channel sensitivity to deltamethrin by 100-fold (Usherwood *et al*., 2007).

Both resistant populations (JA and JF) carried the super-*kdr* I929 allele in the absence of the *kdr* F1014 allele. The identification of this mutation alone in maize weevils demonstrates that this mutation can be selected independently of the more frequently occurring L1014F mutation. Thus, weevils carrying the I929 allele are viable and this result shows that additional mutations such as L1014F are not necessarily required to avoid any functional impairment of the sodium channel incurred by having *super-kdr* alone, as has been suggested previously for T929I (Schuler *et al*., 1998) and the original super-*kdr* mutation M918T (Lee *et al*., 2000; Tan *et al*., 2002b). In this respect, T929I in maize weevils resembles the three alternative super-*kdr* mutations that were recently described in resistant whitefly (*Bemisia tabaci*) populations, where M918V, L925I and T929V mutations were found alone in individual insects without the L1014F mutation (Morin *et al*., 2002; Alon *et al*., 2006; Roditakis *et al*., 2006) and in a resistant strain of thrips, where T929I is apparently found alone (Toda and Morishita 2009).

The role of the T929 residue in the *para* sodium channel/insecticide interaction has been examined previously using a model of the membrane-

enclosed portion of the housefly sodium channel (based on the rat brain Kv1.2 potassium channel crystal structure) known as the O'Reilly *et al*. (2006) model (Long *et al*., 2005a, 2005b) (Figure 3-8).

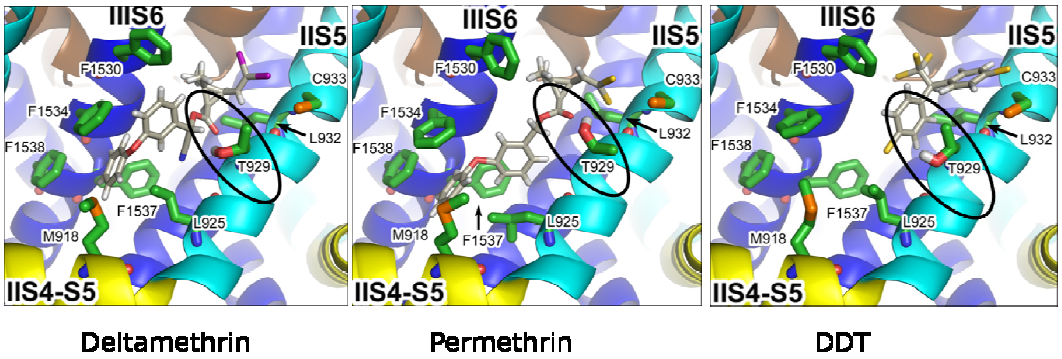

Fig. 3-8: Predicted binding sites for pyrethroids (left-hand and centre panel) and DDT (right-hand panel) on the *para* sodium channel protein. The model identifies a hydrophobic cavity that is formed between the IIS4-S5 linker, the IIS5 helix and the IIIS6 helix. Several of the residues that have been implicated in pyrethoid resistance face into this cavity (O'Reilly *et al*., 2006, *Biochemical J.* **396**, 255-263).

This model implies a binding site on *para* that accommodates a diversity of insecticidal structures in the DDT/pyrethroid series (Davies *et al*., 2007). The binding site is located within a long, narrow hydrophobic cavity, delimited by the IIS4-IIS5 linker and the IIS5/IIIS6 helices, which is accessible to lipid-soluble insecticides (Davies *et al*., 2007). The model (O'Reilly *et al*., 2006) suggests that some of the *kdr*-type mutations are located within the binding pocket, as well as the super-*kdr* T929I on the IIS5 helix. Further interpretation

of this binding site suggests that the hydrophilic T929 on the IIS5 helix may be a key residue for binding, possibly due to the natural tendency of this threonine residue to hydrogen bond, a property which is enhanced by the introduction of an α-cyano group (as in Type II pyrethroids) (Davies *et al*., 2008). Experimental evidence supporting the role of T929 as a key amino acid for the binding of both DDT and pyrethroids comes from electrophysiological studies which demonstrate that the T929I mutation makes the sodium channel highly insensitive to many insecticide compounds (DDT, type I and type II pyrethroids) (Usherwood *et al*., 2007). The super-*kdr* substitution T929I (and also M918T) both promote closed-state inactivation of the sodium channel and also increase the rate of dissociation of pyrethroids by up to 100-fold (Vais *et al*., 2003). Such studies of *kdr* and super-*kdr* type mutations have served to highlight the roles that specific sodium channel residues are likely to play, not only in conferring resistance but also in the binding of DDT and pyrethroids.

Studies of vertebrate sodium channels have identified a mutation at the same amino acid residue corresponding to the T929 of insect sodium channel α-subunit gene (T704M in human; T698M in rat) that is implicated in biophysical defects in mammalian skeletal muscle sodium channel function and results in hyperkalemic periodic paralysis, a hereditary muscle disorder (Ptacek & Griggs, 1996). Electrophysiological studies have shown that the mutation alters the voltage dependence of activation and impairs fast and slow inactivation (Cannon & Strittmatter, 1993; Cummins & Sigworth, 1996). Taken together, these data indicate that the highly conserved threonine residue in the IIS5 segment of sodium channel is a critical element not only for the modulation of pyrethroid sensitivity but also for the functional properties of the sodium channel (Lee *et al*., 2000).

Insecticide resistance is usually associated with fitness costs in the absence of insecticides (Coustau *et al*., 2000). These costs include the impairment of the reproductive performance of resistant individuals, due to resource reallocation from a basic physiological process to the protection against insecticides, favoring their survival at the expense of their reproduction (Coustau *et al*., 2000; Foster *et al*., 2000; Guedes *et al*., 2006). Recent demographic and competition studies carried out on JA and JF populations show that the JA strain does not exhibit a fitness cost while JF does (Fragoso *et al*., 2005; Guedes *et al*., 2006; Ribeiro *et al*., 2007; Oliveira *et al*., 2007). Individuals from JA strain exhibit higher respiration rate and body mass than individuals from JF and SL. Variations in respiration rate may assist in detecting stress and stress response with potential for detecting costs associated with insecticide resistance, while modifications in fat body morphology indicate the availability and mobilization of energy reserves for the individual's maintenance, leading to its survival when exposed to toxic compounds (Guedes *et al*., 2006). Although the JA population has been kept under laboratory conditions without insecticide selection, the persistence of the T929I mutation within this population may be explained by the hypothesis proposed by Guedes *et al*., (2006) and reinforced by Araujo *et al*. (2008a), that higher respiration rate may be correlated with larger size, which may help to promote greater energy storage and mitigate the costs of insecticide resistance, allowing the maintenance of the resistance mechanism without compromising reproductive performance. JF, however, was collected fairly recently from a grain mill and the persistence of the T929I mutation within this population, despite its fitness cost, may be explained by a recent study of carbohydrate and lipid-metabolizing enzymes, which suggested that part of

the high lipase activity detected in weevils from the JF population is involved in energy mobilization, partially preventing lipid accumulation and an increase in body mass while allowing the maintenance of its higher levels of insecticide resistance (Araujo *et al*., 2008).

The persistence of the super-*kdr* mutation in laboratory strains without selection pressure can also be explained by the fact that the genes that confer *kdr* are usually 'recessive', which means that only homozygous individuals (two copies of the recessive gene need to be present to result in a change in phenotype) will present this characteristic. These recessive genes can often persist at low frequency in a population without being lost, even if no selection pressure is introduced (Davies *et al*., 2008).

As pyrethroids continue to be used as a main pest control strategy, it is likely that new mutations will be revealed in other agricultural and medically important insect species.

Chapter 4

Diagnostic assays for detection of the super-*kdr* mutation in field-collected populations of *Sitophilus zeamais* from Brazil

4.1 Introduction

The main objectives of insecticide resistance management strategies are to extend the life of effective insecticides while at the same time providing continued pest control. Such strategies often rely on the sensitive detection of mutations associated with resistance (Bass *et al*., 2007a). For this purpose high-throughput DNA-based diagnostic assays are required and a number of different methods for detecting the DNA changes responsible for *kdr*-type resistance in insects have been described.

The identification of a super-*kdr* type mutation (T929I) in maize weevil laboratory strains (originally collected from the field) suggests that this amino acid substitution may also be present in field-collected populations. In order to test this, a diagnostic assay that was not dependent on DNA sequencing (which is both expensive and time consuming) was required. Different techniques have been used for rapid and sensitive detection of resistance alleles in other insect species, many of which are based on the PCR technique. The relative advantages and disadvantages (safety, cost, speed and simplicity) of each method were considered before deciding which one would be most suitable for genotyping maize weevil field populations. From a range of techniques, two high-throughputs assays based on real-time PCR, TaqMan SNP genotyping and High Resolution Melt (HRM), were selected for this purpose. Technologies based on real-time PCR are quicker and easier to perform than those based on conventional PCR as they do not require post-PCR processing. Another potential advantage of real-time PCR is the possibility of quantifying the number of resistance alleles in a sample of pooled individual

insects based on standard curves and making quantitative comparisons, which is not possible using conventional PCR (Mackay, 2004). In addition, these assays do not require agarose gel electrophoresis to process the samples, which is time consuming, restricts through-put and requires the use of the hazardous compound ethidium bromide (Bass *et al*., 2007b). However, the major disadvantage of real-time PCR assays is the capital cost of the more expensive machine required. Nevertheless, the price of real-time PCR machines is falling and is likely to become closer to standard thermo cyclers in the near future.

A standard nested PCR followed by restriction fragment length polymorphism (RFLP) analysis of amplicons was also tested to diagnose the T929I mutation. Although this last method is time-consuming, involving many laboratory intensive steps, this assay may be more suitable for laboratories that do not have access to a real-time PCR machine.

This chapter describes two methods based on real-time PCR (TaqMan and HRM) and one method based on conventional PCR (PCR RFLP). The TaqMan assay showed the best performance when diagnosing the T929I mutation in twelve field-collected populations of *S. zeamais* from Brazil. This mutation was previously identified in laboratory strains (see Chapter 3) and is responsible for a highly resistant phenotype. TaqMan and HRM were found to have a specificity and sensitivity comparable to standard PCR and performed well in a blind trial using a 96 sample reference plate containing DNAs from a variety of field-collected *S. zeamais* individuals.

The super-*kdr* mutation (T929I) represents the primary mechanism of resistance to pyrethroids in *S. zeamais.* Accurate determination of the

frequency of the *kdr*-type allele in *S. zeamais* populations is extremely important to measure resistance levels, estimate resistance potential, and genetically monitor effects of insect control strategies (Jamroz *et al*., 1998).

4.2 Diagnostic assays for insecticide resistance

4.2.1 TaqMan Assay

The presence of the super-*kdr* mutation in maize weevil populations maintained in laboratory for more than 10 years suggests that this mutation appeared many years ago and consequently it might be common in field strains. This was tested by screening weevils from field-collected populations using a fluorescence-based high-throughput assay (TaqMan). This assay is based on TaqMan single nucleotide polymorphism (SNP) genotyping and is a 'closed tube' approach that involves a single step to genotype a weevil DNA sample (Bass *et al*., 2007b).

The TaqMan assay uses oligonucleotide probes 5'-terminally labelled with a reporter fluorophor and labelled internally or 3'-terminally with a quencher (Wilhelm & Pingoud, 2003). Intact probes do not fluoresce because they are quenched. During the extension phase of PCR, the probe, which is complementary to the amplicon sequence, will bind to the single-stranded DNA target sequence flanked by the forward and reverse primer binding sites. When Taq DNA polymerase extending from the primer reaches the probe, this last is sheared and endonucleolytically cut. The quencher is hence released from the fluorophor, which now fluoresces after excitation (Heid *et al*., 1996, Holland *et al*., 1991; Gibson *et al*., 1996). By using different reporter

fluorophors, cleavage of allele-specific probes can be detected in a single PCR (Livak, 1999). In the present study, two probes were used, the first specific for the mutant allele is labelled with FAM, and the second specific for the wild type allele is labelled with VIC. Figure 4-1 shows discrimination of the resistance allele (I929) after optimization of the TaqMan assay using templates of known super-*kdr* genotype from JA and JF populations.

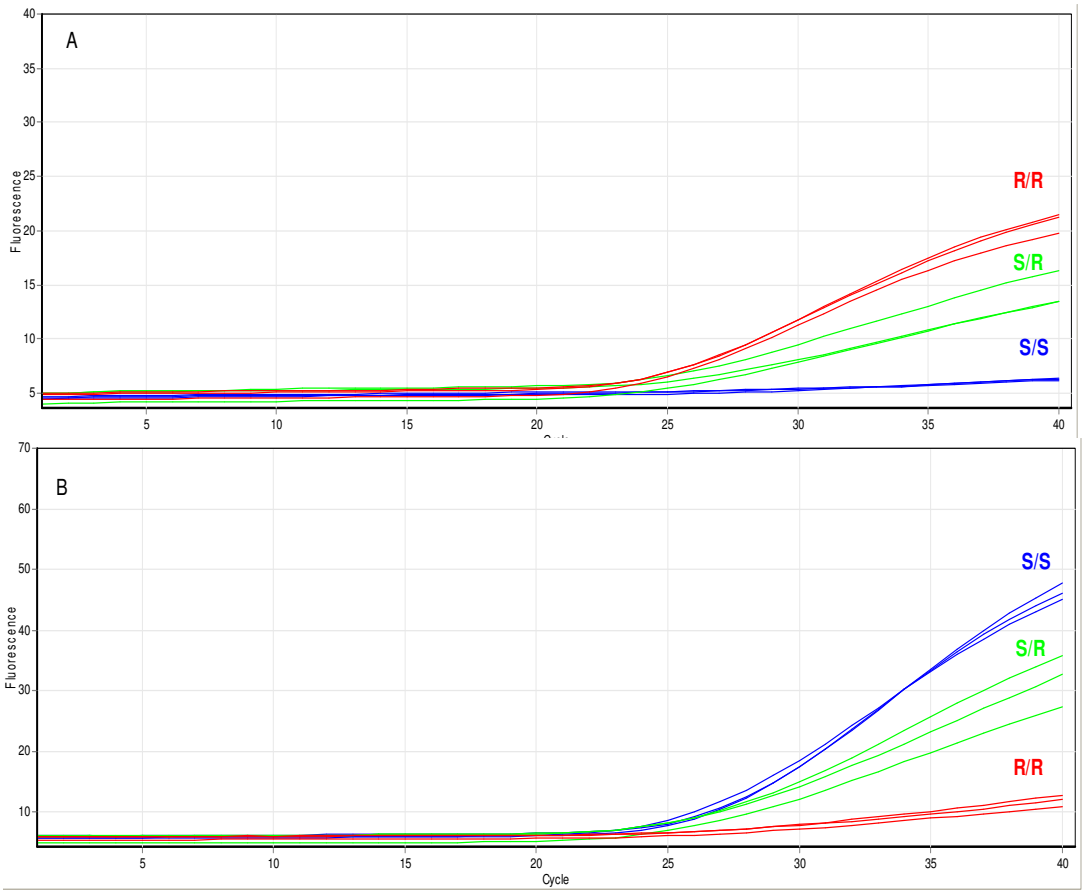

Fig. 4-1: Real-time TaqMan detection of super-*kdr* allele (I929) in JA and JF populations. A) Cycling of FAM-labelled probe specific for the super-*kdr* allele (Isoleucine). B) Cycling of VIC-labelled probe specific for the wild type allele (Threonine). Water was used as a negative control. S: wild-type allele (T929), R: resistant allele (I929).

In the assay, an increase in only FAM fluorescence indicates a homozygous mutant, an increase in only VIC fluorescence indicates a homozygous wild type, and a usually intermediate increase in both signals indicates a heterozygote. Individuals homozygous for the super-*kdr* mutation display no increase in VIC fluorescence in the wild type assay and vice versa.

After optimization, the diagnostic test was further tested using *S. zeamais* individuals from twelve field-collected populations (Machado, Espírito do Santo do Pinhal, Guarapuava, Nova Era, Sacramento, Rio Verde, Piracicaba, Viçosa, Sao João, Votuporanga, Linha Barreirinha and Sao José do Rio Pardo). Twenty individual weevils were scored from each population with a total of 240 individuals genotyped. To allow easier scoring of genotypes, the Rotor-Gene software allows endpoint fluorescence values for the two dyes to be automatically corrected for background and plotted against each other in bi-directional scatter plots (Figure 4-2).

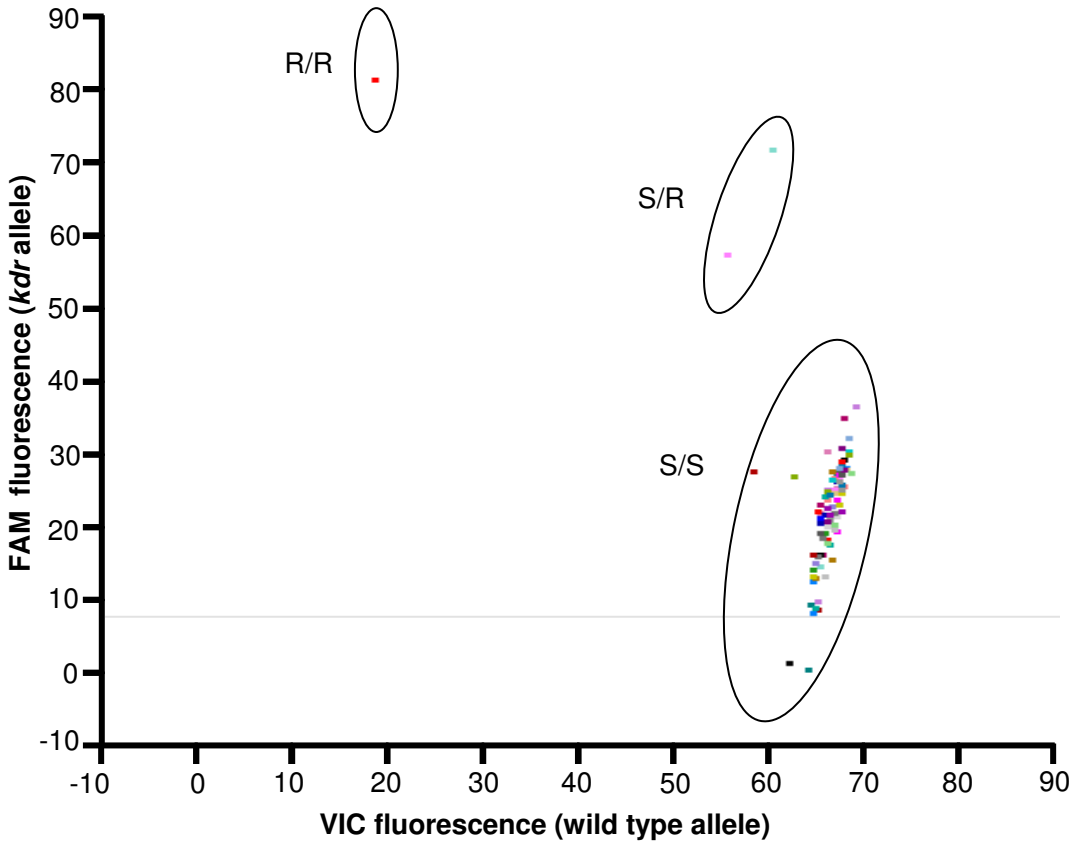

Fig. 4-2: Scatter plot analysis of TaqMan fluorescence data. Real-time PCR was carried out using 96 different DNA samples from field-collected populations. Three positive controls of known genotypes (R/R, S/R and S/S) and a negative control (water) were also used in the assay. S: wild-type allele (T929), R: resistant allele (I929).

The TaqMan assay did not show any individual weevil carrying the mutant allele in the homozygous form (R/R). In the figure above the single resistant insect displayed as R/R in the scatter plot is the positive control for this genotype. Most of the individuals in the populations screened were scored as homozygous wild type (S/S) and only the Sao Joao and Linha Barreirinha

populations showed one individual each with the mutant allele in the heterozygous form (S/R). The results of the TaqMan screening were verified by sequencing a subset of samples from each population and the results of sequencing were in complete agreement with results obtained by TaqMan. The DNA sequences from the field populations were also analyzed in an attempt to find other mutations, but no mutations and/or variations were observed in the nucleotide sequences, even within the two small introns.

4.2.2 High Resolution Melt (HRM)

A High Resolution Melt assay was also developed as a diagnostic for the super-*kdr* allele (I929) in *S. zeamais*. Like TaqMan, this assay is also a 'closed-tube' method which requires no post-PCR steps and is thus particularly suitable for high-throughput purposes.

In this assay, melting analysis of short PCR products, in the presence of a third generation fluorescent dsDNA dye, was used to genotype SNPs (Bass *et al*., 2007a). The new generation of dyes for this method (SYTO 9 (Invitrogen), LC Green (Idaho Technologies) and Eva Green (Biotium Inc)) causes less inhibition to PCR than traditional dyes, allowing them to be used at higher concentration. As a result, maximum saturation of the resulting dsDNA amplicon is achieved (Vezenegho *et al*., 2009). The use of these new intercalating dyes and improvements in instrumentation has made the HRM approach possible (Wittwer *et al*., 2003). Using a real-time PCR machine with high optical and thermal precision, a highly resolution melt step is performed

centered around the T_M of the amplicon. The dye is released when the dsDNA dissociates into single strands, and the fluorescence reduces providing a melt curve profile characteristic of the sequence of the amplicon (Liew *et al*., 2004).

The HRM assay was optimized using templates of known super-*kdr* genotype from JA and JF strains, and after PCR amplification, it was possible to discriminate the three different genotypes (R/R, S/R, S/S) (Figure 4-3).

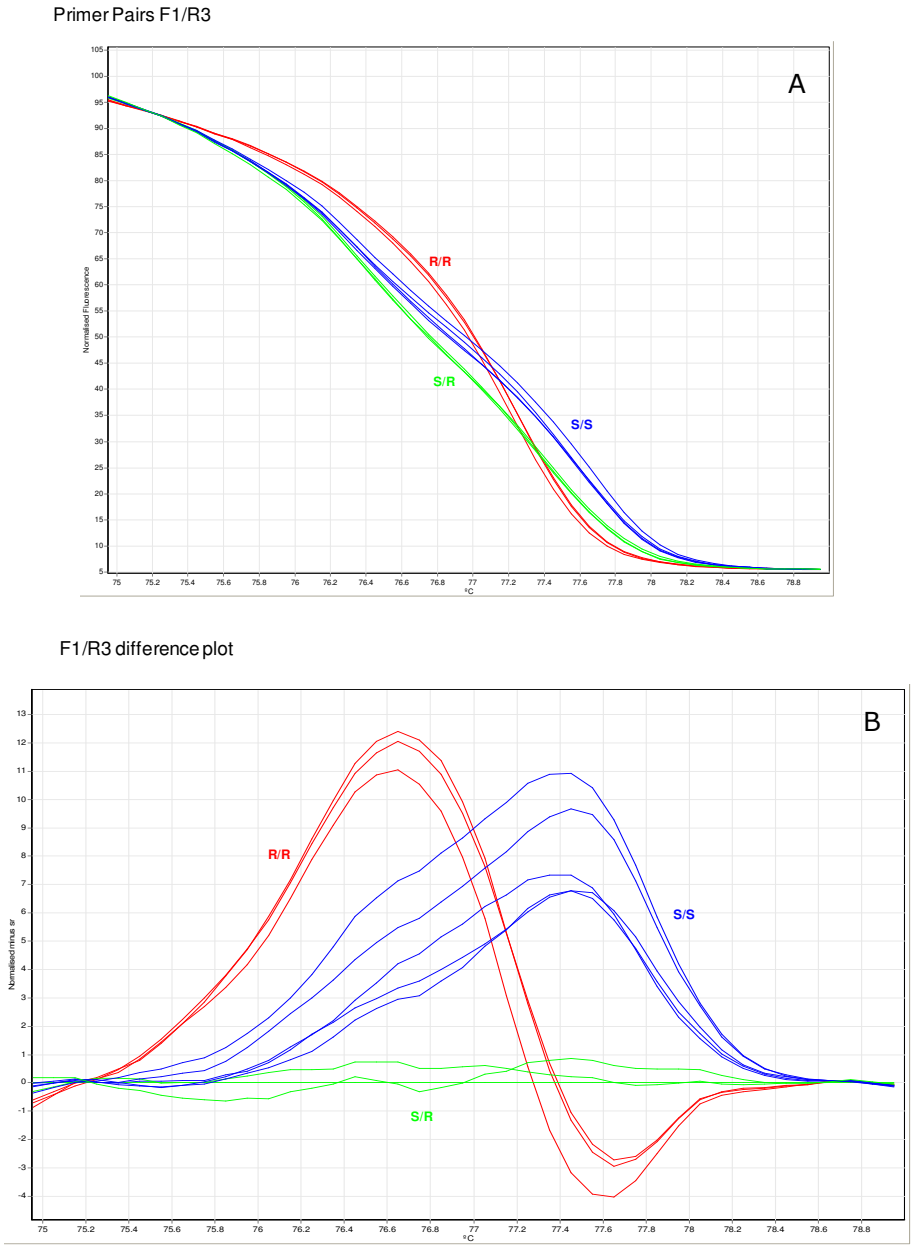

Fig. 4-3: (A) High Resolution Melt (HRM) detection of the super-*kdr* allele I929 in JA and JF populations. Water was used as a negative control; (B) Melt curve profiles plotted as a difference plot as an aid to visual interpretation: the difference in fluorescence of a sample to a selected control (in this case an S/R genotype control) is plotted at each temperature transition. S: wild-type allele (T929), R: resistant allele (I929).

As shown in Figure 4-3A, the melt curve shape of the homozygous wild-type genotype (S/S) was different from that of the homozygous mutant (R/R) genotype. These results differ from the results obtained by Bass *et al*., (2007a) when detecting *kdr* mutation in *A. gambiae*, where heterozygous individuals were characterized by a change in the shape of the melt curve and homozygous individuals presented the same melt curve profile, differing only in $T_{M.}$ Moreover, Liew *et al*., (2004), studying all possible SNP base combinations at one position, also showed that all homozygotes presented the same melt curve profile and heterozygotes produced more complex melting curves.

Although the assay was able to distinguish the three genotypes in the example above, in subsequent experiments the results with samples of known genotype were not consistent and sometimes resulted in incorrect scoring of genotypes. Attempts were made to further optimize the assay and increase the specificity by altering temperature conditions but significant improvements in specificity were not obtained.

To better score homozygous wild-type allele, the difference plot function of the Rotor-Gene software which plots the difference in fluorescence of one sample against a chosen reference (heterozygous in this case) at each temperature increment was used (Figure 4-3B).

4.2.3 PCR RFLP (Restriction Fragment Length Polymorphism)

A disadvantage of the high-throughput TaqMan approach is the initial cost of the real-time PCR machine required. An alternative assay based on conventional PCR was therefore designed that, although lower in throughput, may be more amenable to laboratories which do not currently have access to a suitable real-time PCR machine.

The single base pair substitution at position 929 of the *para* sodium channel gene results in the creation of an Mbo I restriction enzyme site in the resistant allele and serves as a marker of the resistance phenotype. Similar to the former methods, the assay was also performed using known super-*kdr* genotypes from JA and JF populations.

The PCR RFLP assay uses forward and reverse primers to amplify a 211 bp product encompassing the T929I mutation site (Figure 4-5A). Products are then digested with Mbo I which recognises a site present only in the resistant allele (I929) cleaving the amplicon into two fragments of 53 bp and 158 bp in size. As shown in Figure 4-5B, the smaller of these is too small to be clearly visible after agarose gel electrophoresis, however, the size difference in the larger fragment can be clearly distinguished from the uncut fragment of susceptible genotypes. Although this satisfactory result, the sample labeled as homozygous susceptible (S/S) is revealing two DNA fragments instead of one after the enzymatic digestion. This is likely to be a PCR contamination or an error during the labelling procedure. Like the TaqMan assay, the PCR-RFLP method is sensitive enough to identify the genotypes of individual weevils.

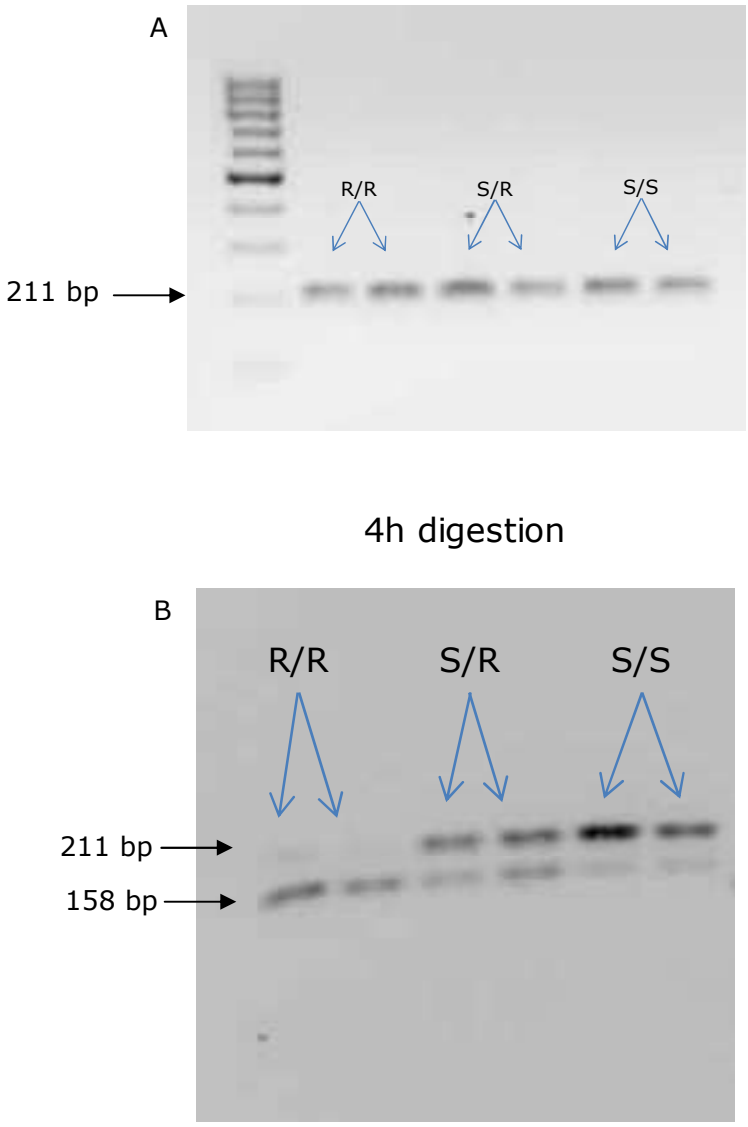

Fig. 4-5: PCR RFLP detection of the T929I mutation in *S. zeamais.* A) PCR product encompassing the T929I mutation site; B) Restriction patterns obtained by PCR RFLP after separation on a 2% agarose gel with a 100bp ladder. R/R: homozygous mutant allele, S/R: heterozygous allele, S/S: homozygous wild-type allele.

PCR RFLP method efficiently detected the super-*kdr* mutation in laboratory resistant strains of *S. zeamais* and confirmed the results obtained during the optimization of the Taqman and HRM assay.

4.3 Discussion

Currently, the main means of control against maize weevil infestations relies on the use of a range of pyrethroid formulations. The identification of the super-*kdr* mutation within laboratory strains suggest that there is a risk that these products may become ineffective in controlling these insects if the same mutation (T929I) conferring strong resistance is also widespread within field populations. To investigate the occurrence of the resistant allele I929 within field-collected strains, two high-throughput methods based on real-time PCR, Taqman SNP genotyping and High Resolution Melting, which can be used to accurately genotype large number of individual weevils for the mutation, were developed.

Of the two assays, the TaqMan platform showed the best performance for genotyping maize weevil field-collected strains, being more sensitive and robust for detection of the super-*kdr* mutation and discrimination of the genotypes. The HRM method showed promise during optimization with templates of known genotype from laboratory individuals, but subsequently did not perform well when genotyping field strains. According to Vezenegho *et al*., (2009), one explanation for this may be the presence of variable DNA quality and quantity in the samples which could lead to late amplification or failing to reach full plateau phase.

When using the Taqman assay to genotype field-collected maize weevils from twelve different sites in Brazil, it was observed that the resistance allele (I929) was not found in any population and, from 240 insects screened in the assay, only 2 individuals were scored as heterozygous (S/R). These results may be explained by the treatment history of stored grain in Brazil in the last few years. The use of insecticides in stored maize has changed significantly. At the moment, farms are using organophosphates alone or combined with pyrethoids, which may not select the super-*kdr* resistance mechanism described in this study. Although the super-*kdr* mutation was found at very low frequency, this mutation may re-emerge in the future if the more toxic organophosphates are withdrawn and farmers revert to more intensive use of pyrethroids. In addition, the T929I mutation may also occur in combination with additional resistance mechanisms and this may present a serious problem for the effective control of this pest. As the field strains have not been re-selected over many generations since collection it is also possible that the frequency of resistant individuals has fallen due to any fitness cost incurred by the resistant phenotype in the absence of insecticide selection pressure.

A standard PCR-RFLP assay was also developed as an alternative method to diagnose the super-*kdr* mutation that did not require the use of a more expensive real-time PCR machine. This method was found to be as sensitive as the TaqMan assay when genotyping *S. zeamais* laboratory strains. However, because this assay is lower throughput than the TaqMan approach it was not used to genotype maize weevil field-collected strains in this study.

The rapid identification of resistance-associated mutations is an important part of agricultural pest control strategies. High-throughput assays are an important molecular tool to monitor the frequency of resistance

conferring alleles in field-collected populations (Bass *et al*., 2007a). Thus, the spread of resistance may be prevented due to early detection of any resistance conferring mutation by implementing resistance management strategies. Control of populations that have already developed this resistance would also be improved by recommending the use of other insecticide classes or alternative control methods. Because of the ability of insects to develop multiple resistance mechanisms, the molecular assays should be used in conjunction with insecticide bioassays to establish a resistance profile for individual insects. The resistance profile will give more information about compounds which retain useful activity, based on the mechanism present (Williamson *et al*., 2003).

Chapter 5

Electrophysiological Characterization of Voltage-Gated Ion Channels in Maize Weevils

5.1 Introduction

Voltage-gated sodium channels are crucial for electrical signaling in most types of excitable cells because they are responsible for increasing the sodium ion permeability that underlies the rising phase of the action potential (Gordon *et al*., 2007). Because of this important role in membrane excitability, these proteins are the site of action of structurally diverse naturally occurring neurotoxins (Cestele & Caterrall, 2000; Blumenthal & Seibert, 2003; Wang & Wang, 2003) as well as synthetic insecticides, such as DDT and pyrethroids (Narahashi, 1988; Soderlund & Bloomquist, 1989). In the case of DDT and pyrethroids they disrupt nerve function by acting on sodium channels and causing hyper-excitation and paralysis (Denac *et al*., 2000).

The intensive use of DDT and pyrethroids over many generations has lead to the widespread development of resistance in many insect species. Amongst the resistance mechanisms that have evolved, various inherited point mutations (so called *kdr* and super-*kdr*) in the voltage-gated sodium channel, which alter the amino acid sequence of the sodium channel protein, have been shown to cause insecticide resistance.

In Chapter 3, the identification of a super-*kdr* mutation (T929I) was described in the IIS5 domain of the *para* ortholog sodium channel gene of *S. zeamais* from Brazil. This substitution was found alone in two laboratory strains (JA and JF) and is responsible for a highly resistant phenotype in these two populations.

Previous work using site-directed mutagenesis and the *Xenopus* oocyte expression system (Usherwood *et al*., 2007) has demonstrated how the T929I mutation in the *Drosophila para* gene affects sodium channel function and

reduces sodium channel sensitivity to DDT and pyrethroids. Characterization of the mutant sodium channel in neurons of super-*kdr* maize weevils, which carry the T929I mutation, provides an opportunity to study the channel in its native environment and also to determine the effect of T929I in an insect neuron in the absence of the *kdr* mutations such as L1014F which normally accompany it.

This chapter will describe the electrophysiological characterization of ion channels from *S. zeamais* neurons. Different experimental conditions were tested to optimize the methodology and isolate sodium currents for subsequent studies. After sodium currents were isolated, the effect of pyrethroid insecticides in the wild-type and mutant super-*kdr* (T929I) neurons was investigated and is reported in Chapter 6, enabling responses in insect neurons to be compared with those seen when insect sodium channels were expressed in heterologous cells such as *Xenopus* oocytes.

Light and electron microscopy was used to illustrate the external morphology of maize weevils and monitor cell isolation procedures. Three different substrates (Poly-L-lysine, Concanavalin A and Laminin) were tested for adherence of cells to 35mm Petri dishes. Finally, a variety of ion channel blockers was used to reduce the interference of other ion currents with the sodium channel activity.

5.2 Understanding the organization of the cells in the thoracic ganglia is important for isolation of neurons

Electrophysiological studies require a good yield of neuronal cell bodies. The method was modified from previous work on house fly (Thomson, 1998; Verdin, 2008) with changes intoduced to refine the technique for *S. zeamais*. Following the dissection of individual weevils and extraction of the ganglia the following steps appear to be important: a) incubation of the ganglia in collagenase and dispase enzymes in order to digest the membrane sheath as well as connective tissues which hold the cells together; b) liberation of neurons into the culture medium made by trituration through the flame-polished tip of a Pasteur pipette; c) and finally, culturing neurons overnight to allow them to recover from the stress of the isolation process and to allow the expression of voltage-gated sodium channels.

Initially, the process of enzymatic digestion was not efficient and some parts of the ganglia appeared to be intact with few cells being isolated for electrophysiological studies. Examination of the ganglia by light and electron microscopy provided information about the thickness of the ganglionic sheath and the size and organization of nerve cell bodies and highlighted the need for efficient enzyme treatment.

5.2.1 Light microscopy

Light micrographs showed that the ganglionic sheath is relatively thin and the neurons are organized around the periphery of the ganglion (Figure 5-1). This type of organization makes the dispersion of the nerve cell bodies easier after digestion with enzymes.

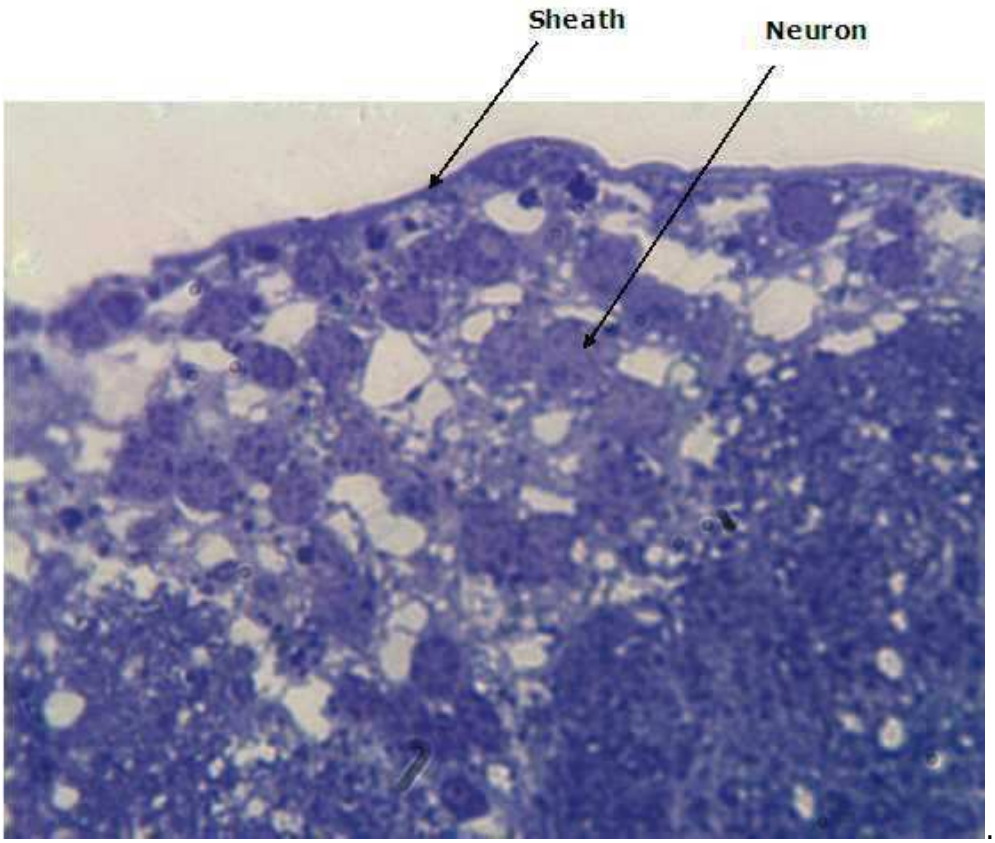

Fig. 5-1: 0.5µm epoxy resin section of *S. zeamais* ganglion stained with toluidine blue (2000x).

5.2.2 Transmission electron microscopy

The transmission electron microscope (TEM) shows more detail of the size and organization of the neurons inside the ganglion. Figure 5-2A shows that the thickness of the membrane sheath varies from 0.8 to 0.9µm. Figures 5-2A, B and D confirm the presence of the nerve cell bodies (3.2 x 4 to 4 x 6.3µm) in the periphery of the ganglion. Figure 5-2C shows the location of tracheoles in the ganglion sheath, and Figures 5-2E and F show the neuropil with a dense network of axons.

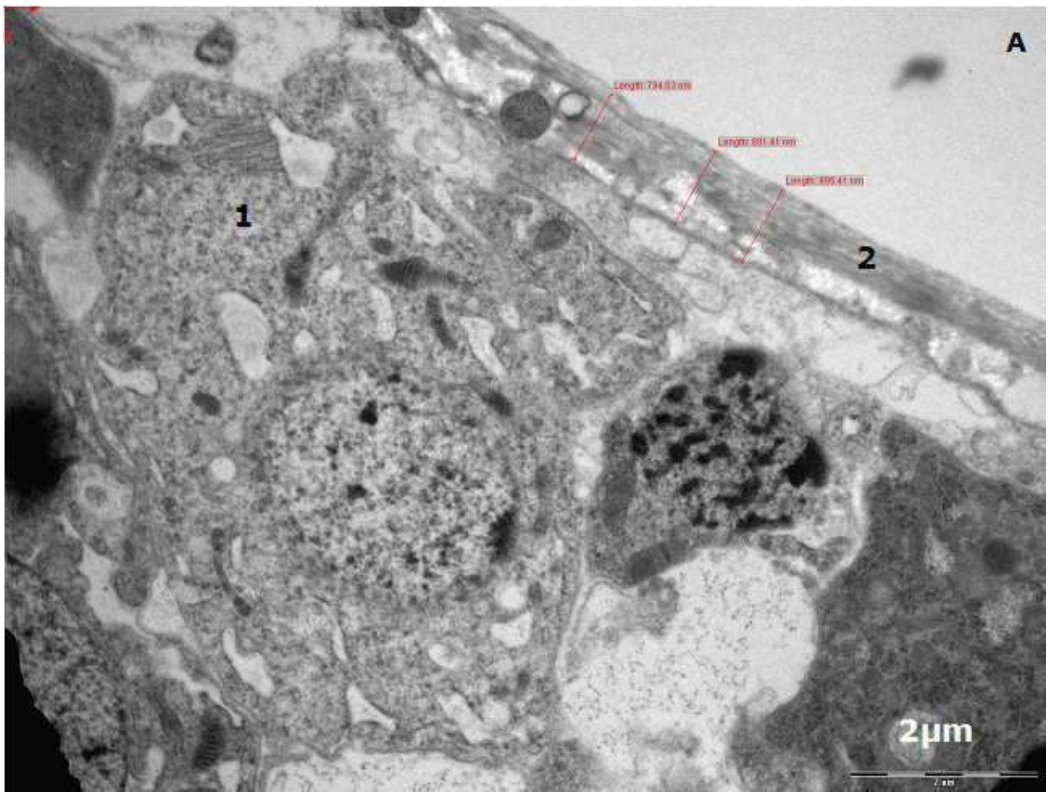

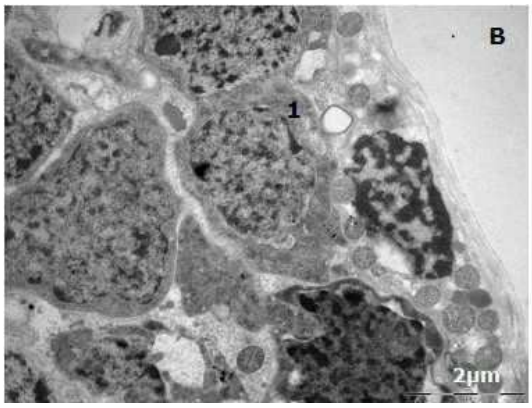
B
1
2µm

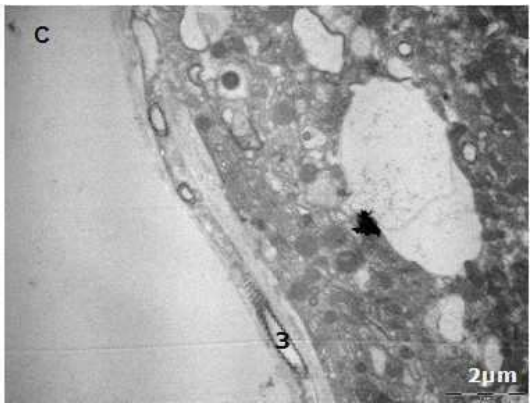
C
3
2µm

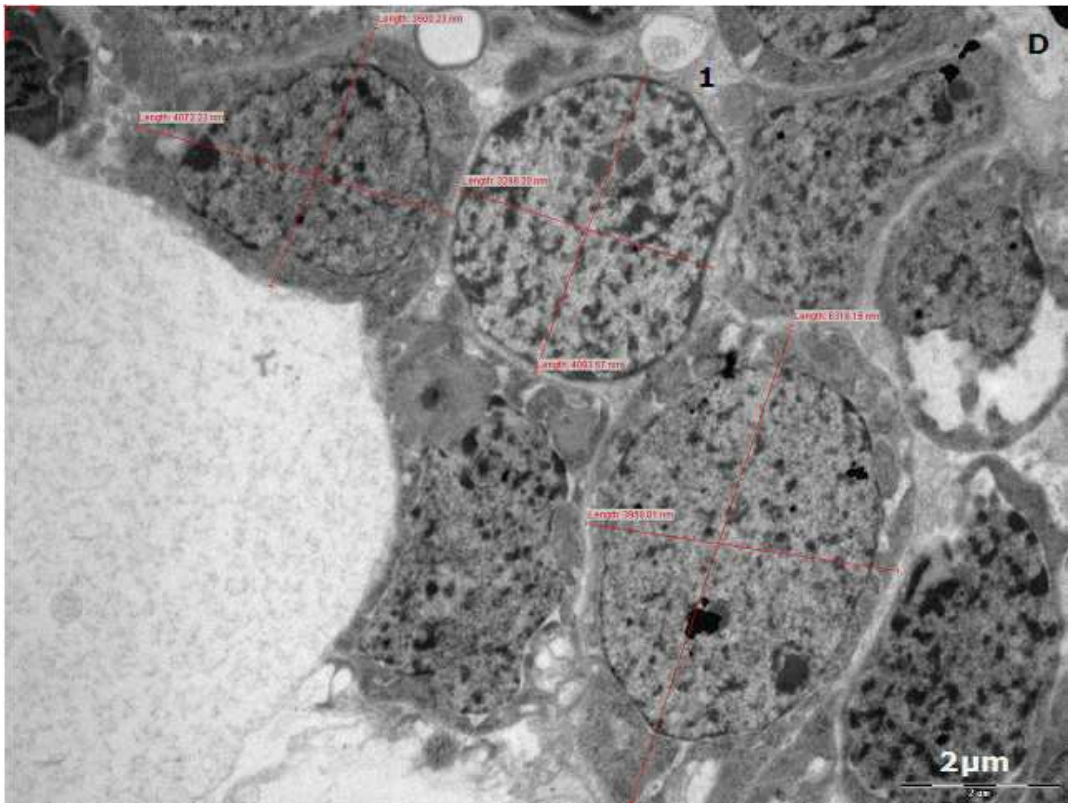
D
1
2µm

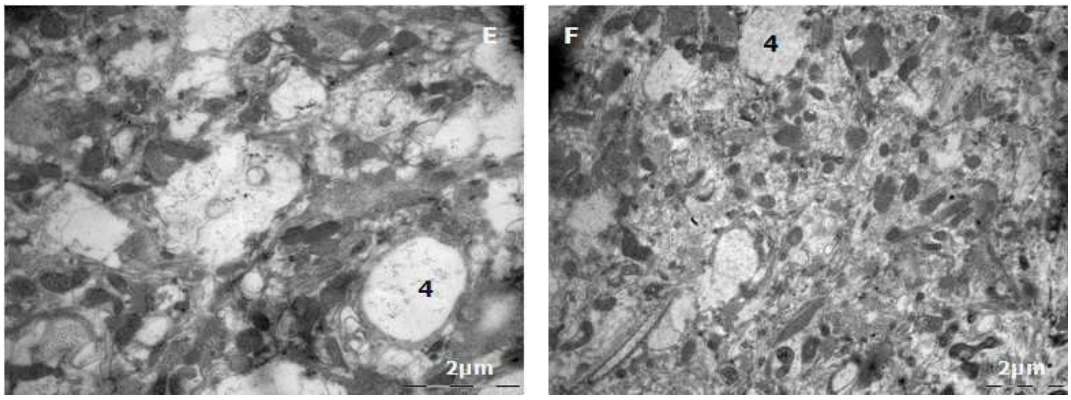

Fig. 5-2 (A-E): Transmission electron microscopy sections of *S. zeamais* ganglion. Labels indicate (1) nerve cell bodies in the periphery of the ganglion; (2) ganglion sheath surrounding the ganglion; (3) trachea in the ganglion sheath; (4) axons crossing the neuropil.

After understanding the organization of the neurons inside of the ganglia some changes were made in the isolation methodology, including the time and temperature of incubation which changed from 10min at 37ºC to 1h at room temperature (21-23ºC) to gain better control of the digestion process.

5.3 Ion channels are induced by depolarization

In this study, the whole-cell patch-clamp technique (Fenwick *et al*., 1982) was used because it permits control of intracellular ionic concentration and enables the dissection of membrane currents by external or internal ion substitutions.

Ion currents were recorded from individual cells isolated from approximately fourty thoracic ganglia removed from fifteen different maize weevils. After isolation, these neurons were placed in nine Petri-dishes, each dish representing one experiment. Isolated neurons of *S. zeamais* form a heterogeneous population with different levels of activity in response to depolarising stimuli. This heterogeneity was ameliorated by repeating experiments a number of times to obtain a population average. The neuron recorded in Figure 5-3 revealed currents characteristic of voltage-gated sodium, calcium and potassium channels in response to a depolarising stimulus. Therefore, different ion channel blockers were added to the pipette and bath solutions in an attempt to isolate the sodium channel current. These blocking agents were tested in different combinations depending on the aim of each experiment.

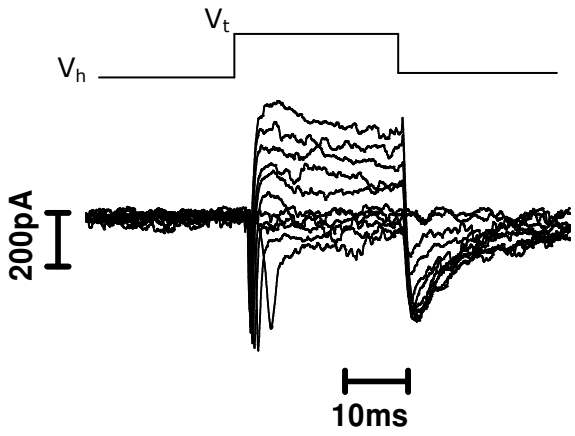

Fig. 5-3: Ion Currents in *S. zeamais* neurons were recorded by depolarizing the cell to test potentials in the range -70mV to +70mV in 10mV increments for 25ms from a holding potential of -80mV. The pipette solution contained 140mM KCl, 1.1mM EGTA, 2mM $MgCl_2$, 0.1mM $CaCl_2$, 5mM HEPES, pH 7.2 with KOH. The bath solution contained 140mM NaCl, 5mM KCl, 0.75mM $CaCl_2$, 4mM $NaHCO_3$, 1mM $MgCl_2$, 5mM HEPES, pH 7.2 with NaOH.

The current-voltage relationship of the inward current (peak current plotted against test potential) in neurons of *S. zeamais* wild-type strain is shown in Figure 5-4A. The relationship gives an activation threshold of ~-50mV and maximum activation at a membrane potential of ~-10mV. At more positive membrane potentials the size of the inward currents decreases due to increasingly positive internal membrane potential having an inhibitory effect on net ion influx. The voltage-dependence of activation in neurons from the same population is shown in Figure 5-4B. This curve was generated by plotting peak conductance amplitude in response to depolarization against the test potential and then, fitting the curve with a Boltzmann sigmoidal function. In these cells it is not possible to maintain recording conditions whilst delivering

large enough depolarizing pulses to reach the reversal potential for the inward current. Reversal potentials used in analyses were obtained by extrapolation of the I-V curve.

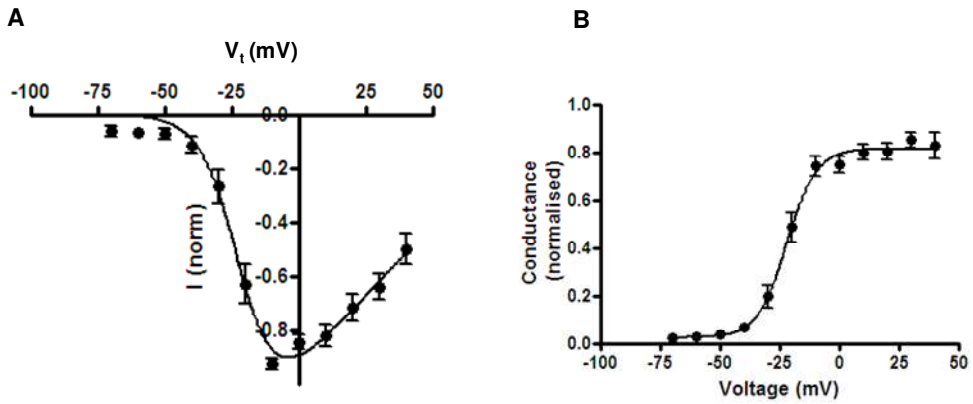

Fig. 5-4: (A) Current-voltage relationship (I-V curve) for inward currents in *S. zeamais* wild-type neurons: peak current generated from single cells using voltage protocol 1 were normalized, averaged and plotted against test potentials (V_t) to generate the I-V curve. The curve (solid line) was fit using equation 1. Extrapolated V_{rev}=88.41±10.01 mV (N=22). Points are mean ± SEM. (B) Voltage dependence of activation of inward currents in S. *zeamais* wild-type neurons: conductance was normalized to the peak conductance per cell and many cells averaged. The curve (solid line) was fitted with a Boltzmann function. V_{50}=-22.22±1.07 mV (N=22). Points are mean ± SEM.

5.4 Electrophysiological studies require efficient cell adhesion to the surface of the Petri dish

The whole-cell patch clamp technique requires good adhesion of the cells on the surface of the Petri dish, and choosing the best culture substrate for the dish is critical for this settlement to occur.

Poly-L-lysine is widely used for coating Petri dishes and glass cover slips before performing electrophysiological recordings. This synthetic cationic polypeptide (Huang, 1998) has shown to be efficient for attaching different types of nerve cells on surfaces (Deglise *et al*., 2002; Martin *et al*., 2000; Motomura & Narahashi, 2001). Poly-L-lysine, however did not mediate good adhesion of maize weevil neurons, and most of the cells were left in suspension with very few neurons suitable for electrophysiological recordings.

For this reason, two other substrates were tested: 1) Concanavalin A (Con A): a tetrameric lectin from jackbean, *Canavalia ensiformes*, which binds to specific carbohydrate residues, mannose and glucose (Goldstein *et al*., 1965) and 2) Laminin, a multidomain basement membrane glycoprotein (Green *et al*., 2009). The effect of these substrates on adhesion and evoked currents was determined.

5.4.1 Con A promotes adhesion without affecting the inward current

Experiments with uncoated Petri dishes yielded unsatisfactory results with few cells adhering to the surface of the dishes. After dishes were incubated overnight with Con A and Laminin, most cells adhered to the surface of the dish. Con A alone produced similar results. On the other hand, cells did not adhere well to the surface of dishes coated with laminin alone. Thus Con A was selected as the most useful substrate for coating the surface of dishes.

Con A has been shown to abolish the desensitization of glutamate receptors on insect muscle fibres (Mathers & Usherwood, 1976, Evans & Usherwood, 1985) and other studies have demonstrated the insecticidal effect of Con A against Coleoptera (Janzen & Juster, 1976; Gatehouse *et al*., 1984; Czapla & Lang, 1990; Murdock *et al*., 1990) and Lepidoptera (Czapla & Lang, 1990; Harper *et al*., 1995).There is no evidence that this plant lectin affects the inward current in insect neurons nevertheless the responses of cells in dishes coated with Con A were compared with cells in dishes coated with Poly-L-lysine to confirm that Con A was not affecting the responses reported here.

Inward currents from wild-type neurons were recorded by depolarizing the cell to test potentials in the range -70mV to +70mV in 10mV increments for 25ms from a holding potential of -80mV (as in Figure 5-3), generating the current-voltage relationship and voltage-dependence of activation curve (Figure 5-5).

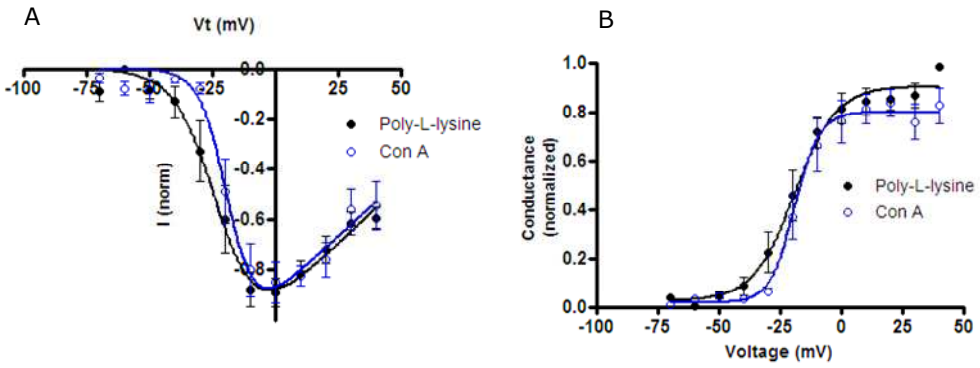

Fig. 5-5: (A) I-V curve for inward currents in *S. zeamais* wild-type neurons: peak current generated from single cells were normalized, averaged and plotted against test potentials. Poly-L-Lysine extrapolated V_{rev}=97.29±20.9 mV (N=7), Con A extrapolated V_{rev}=97.41±20.77 mV (N=8). Points are mean ± SEM. (B) Voltage dependence of activation of sodium currents in S. *zeamais* wild-type neurons: conductance was normalized to the peak conductance per cell and many cells averaged. The curve is fitted with a Boltzmann function. Poly-L-lysine V_{50}=-20.32±1.796 mV (N=7), Con A V_{50}=-18.36±1.535 mV (N=8). V_{rev} and V_{50} are not significantly different (p=0.9966 and p=0.4237, respectively; F test to compare V_{rev} and V_{50}) between the two culture substrates. Points are mean ± SEM.

There was no significant difference (p>0.05) between the extrapolated reversal potential (V_{rev}) and the voltage at which half of the maximal conductance is elicited (V_{50}), between cells grown on Poly-L-lysine and Con A (Table 5-1).

Table 5-1: Inward currents are similar in cells grown on Poly-L-Lysine and Con A.

	Poly-L-lysine	**Concanavalin A**
$\mathbf{V_{rev}}$	97.29±20.9 mV (N=7)	97.41±20.77 mV (N=8)
$\mathbf{V_{50}}$	-20.32±1.796 mV (N=7)	-18.36±1.535 mV (N=8)

Con A was used as a substrate for coating Petri dishes in subsequent experiments.

5.5 TTX blocks the inward currents

Step depolarization of *S. zeamais* neurons produces inward and outward currents simultaneously. Ideally these ion currents need to be separated in order to isolate sodium currents, the subject of this study. TTX, a heterocyclic guanidine derivative found in the ovaries and liver of puffer fish (Figure 5-6), was dissolved in DMSO (1mM stock solution) and applied to the bath solution to achieve two final concentrations (10nM and 100nM). After 3 minutes, all the inward current present in the neurons was blocked by the higher concentration, 100nM (Figure 5-7). This result reveals that *S. zeamais* neurons are TTX-sensitive and the inward current is mediated by sodium channel activity. Since calcium channel blockers were not added to the bath solution, some inward current component was expected to persist after applying TTX; however, 100nM TTX blocked all the inward current, suggesting that these neurons did not normally exhibit voltage-gated calcium channel activity. For

further characterization of sodium channels in *S. zeamais* neurons, a widely used calcium channel blocker, Co^{2+}, was added to the bath solution to prevent any small calcium currents which may be present.

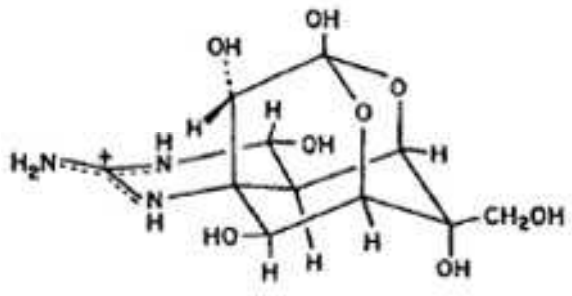

Fig. 5-6: Structure of TTX (Narahashi, 2008).

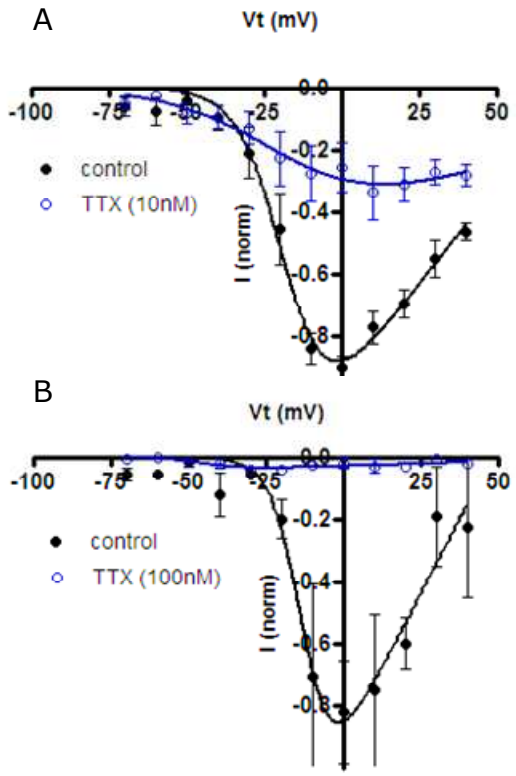

Fig. 5-7: I-V curve for inward current from maize weevil wild-type neurons in the presence of two different concentrations of TTX, (A) 10nM and (B) 100nM. Peak inward currents generated from single cells were normalized, averaged and plotted against the test potential (V_t) to generate I-V curves. The curves are fitted with a Boltzmann function. Points are mean ± SEM, (A) N=10 for control, N=10 for 10nM TTX; and (B) N=7 for control and N=7 for 100nM TTX.

5.6 Outward currents in *S. zeamais* neurons are highly resistant to blockade

5.6.1 Conventional potassium channel blockers do not completely block outward currents in *S. zeamais* neurons

The outward current evoked by depolarization normally carried by voltage-gated potassium channels is another important component which should ideally be blocked when studying sodium currents. *S. zeamais* neurons revealed outward currents similar to the voltage-gated delayed-rectifier type potassium channels, with A-current type present in a few cells. Potassium channel blockers (Cs^+, TEA and 4-AP) have been extensively used for blocking outward currents in a variety of cells (Byerly & Leung, 1988; Stankiewicz *et al*., 1995; Vignali *et al*., 2006; Standker *et al*., 2006). However, addition of these blocking agents to the pipette (140mM Cs^+) and bath solutions (30mM TEA and 1mM 4-AP), failed to abolish outward currents in *S. zeamais* neurons (Figure 5-8). Figure 5-9 shows the sensitivity of the outward currents to block by Cs^+, TEA and 4-AP.

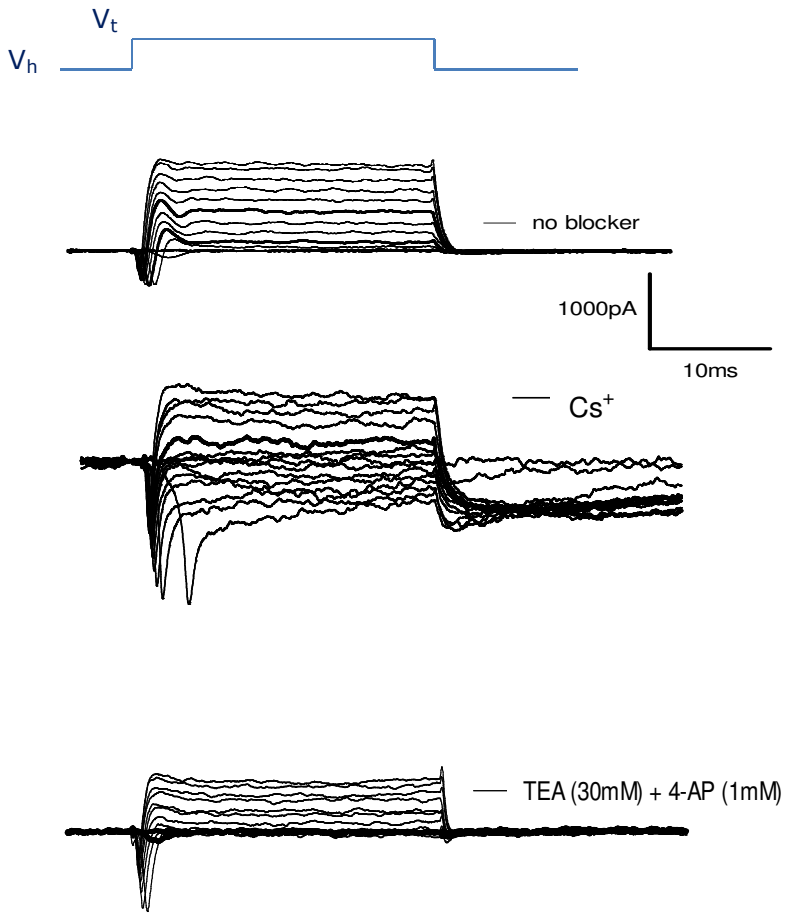

Fig. 5-8: Currents produced when a neuron is depolarised from a V_h of -80mV to V_t in the range of -70mV to +70mV in 10mV increments for 25ms. Outward current is resistant to Cs^+, TEA and 4-AP.

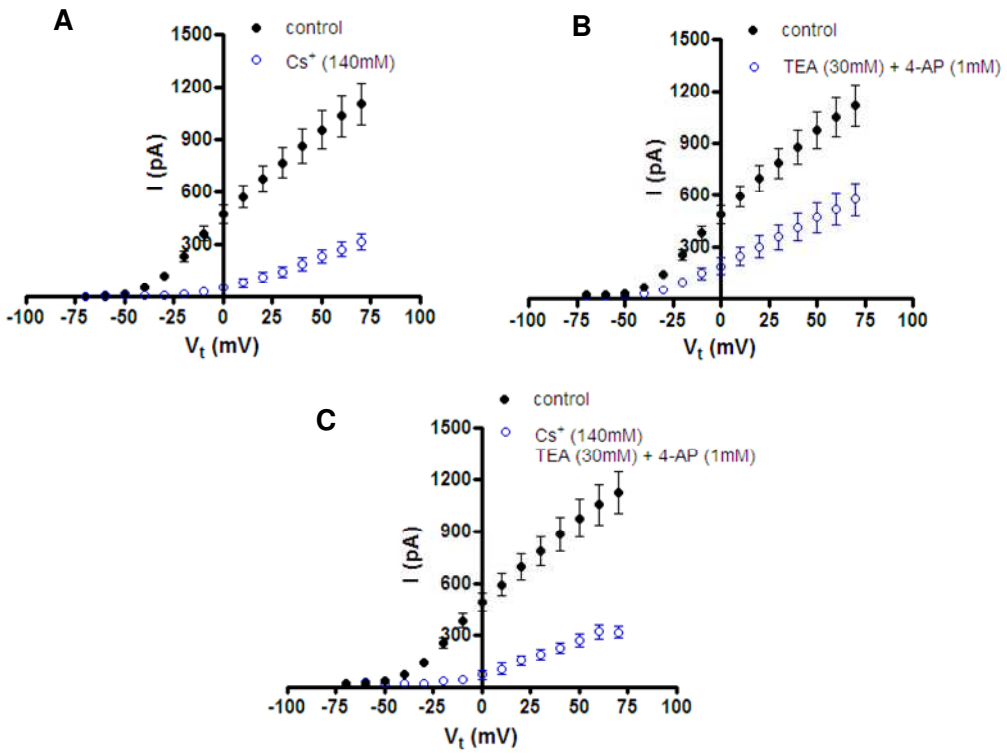

Fig. 5-9: Outward currents from maize weevil wild-type neurons recorded under control conditions, in the presence of (A) 140mM Cs^+ in the pipette solution, (B) 30mM TEA and 1mM 4-AP in the bath solution and (C) 140mM Cs^+ in the pipette solution plus 30mM TEA and 1mM 4-AP in the bath solution. Points are mean ± SEM, N=23 for control, N=18 for Cs^+, N=19 for TEA + 4-AP and N=7 for Cs^+ + TEA + 4-AP.

The action of channel blockers on the outward current was tested in three experiments, Cs^+ alone in the pipette, TEA and 4-AP in combination in the bath and all three blocking agents together. Cs^+ was more effective than TEA and 4-AP, reducing the outward current by nearly 80%. The effects of Cs^+were reduced at more positive potentials. As TEA and 4-AP did not produce

any additional inhibition of outward currents, only Cs^+ was used to block outward current in subsequent experiments.

5.6.2 Red Sea soft coral toxin does not inhibit the persistent outward current

Trigonelline hydrochloride (also called 3-carboxy-1-methyl pyridinium) (Figure 5-10), a compound derived from Red Sea soft coral species (*Sarcophyton glaucum*, *Lobophyton crassum* and *Sinularia leptoclados*) was also investigated as a blocking agent of the outward current in *S. zeamais* neurons which persists in the presence of 140mM Cs^+.

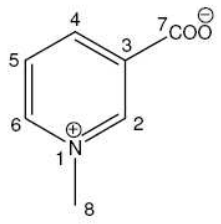

Fig. 5-10: Structure of trigonelline hydrochloride (3-carboxy-1-methyl pyridinium) (Temraz *et al*., 2006).

Previous studies on rat dorsal root ganglia (Temraz *et al*., 2006) revealed that trigonelline blocked voltage-activated potassium channels in cultured sensory neurons. Trigonelline was dissolved in distilled sterile water and applied to the bath solution to achieve two different final concentrations, 0.1mM and 1mM. After 5 minutes, the outward current was still present (Figure 5-11). Since Cs^+ (140mM) was previously found to be the best blocking agent for the outward current, this was also added to the pipette solution and used as control treatment. The sensitivity of the outward current in *S. zeamais* neurons for each concentration of trigonelline is shown in Figure 5-12.

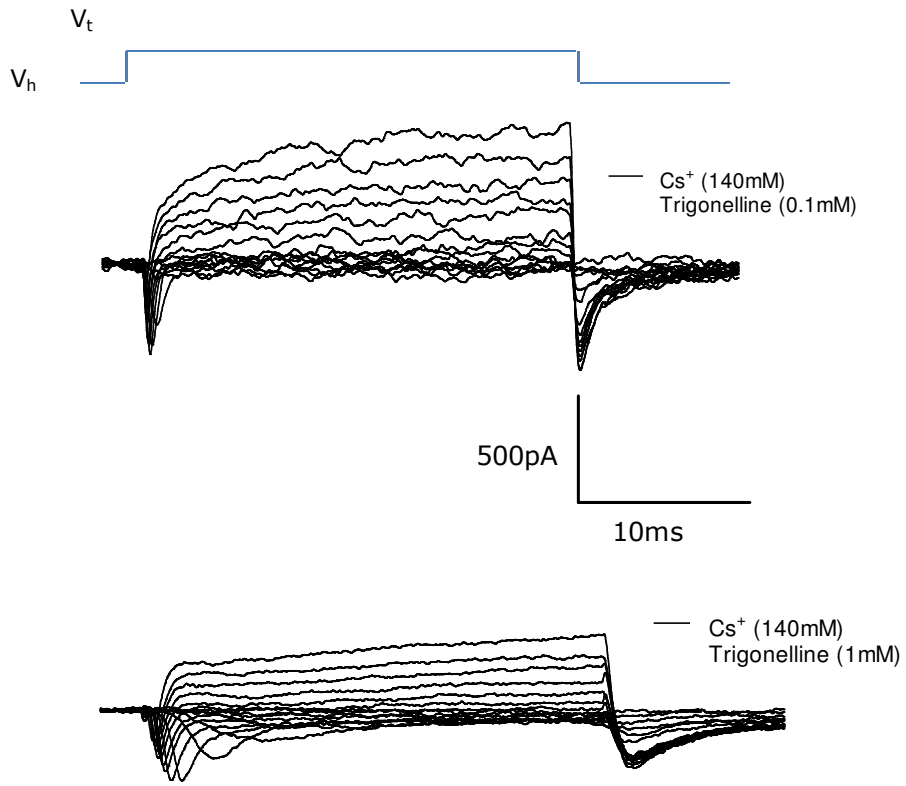

Fig. 5-11: Currents produced when a neuron is held at a V_h of -80mV and stepped to V_t in the range of -70mV to +70mV in 10mV increments for 25ms. Outward current is resistant to the Red Sea soft coral toxin trigonelline at all concentrations tested.

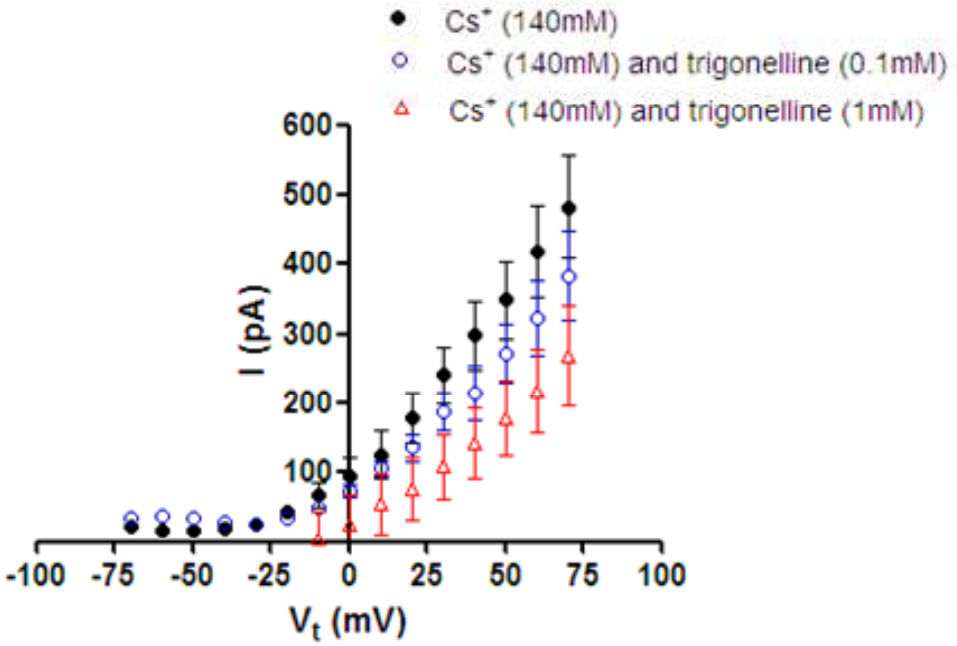

Fig. 5-12: Outward current from maize weevil wild-type neurons recorded under control conditions, in the presence of 140mM Cs^+ (**black**), 140mM Cs^+ and 0.1mM trigonelline (**blue**) and 140mM Cs^+ and 1mM trigonelline (**red**). Cs^+ was added to the pipette solution and trigonelline was applied to the bath solution. Points are mean ± SEM, N=10 for Cs^+, N=10 for Cs^+ + 0.1mM trigonelline, N=10 for Cs^+ + 1mM trigonelline.

Unfortunately trigonelline (final concentrations 0.1mM and 1mM) did not significantly add to the block of outward current due to Cs^+. In particular the outward current at more positive potentials (10mV to 40mV) was similar to that seen in Cs^+ alone.

These data suggest that the persistent outward current in *S. zeamais* neurons may not originate from unblocked voltage activated potassium channels, but may result from current flowing through chloride channels or non-selective voltage-dependent cation channels identified by Alzheimer (1994).

The activity of chloride channels in *S. zeamais* neurons was tested using Cl^- free bath solution and the electrophysiological recordings showed that the outward currents were still present. The lack of evidence for a Cl^- current suggests that the persistent outward current in *S. zeamais* neurons may be due to voltage-sensitive non-selective cation channels.

5.6.3 Persistent outward current is unaffected by other cation channel blockers

In view of the lack of success in blocking the outward current with potassium channel blockers, the presence of other cation channels such as, stretch-activated channels (SACs) and transient receptor potential (TRP) channels was investigated. SACs are involved in a variety of responses to mechanical perturbations, including gene expression, DNA synthesis, cell volume regulation, increased intracellular Ca^{2+}, cell proliferation, baro-receptor discharge, release of atrial natriuretic factor and altered cardiac electrical activity (Caldwell *et al*., 1998). TRP channels are a large family of cation-permeable channels and members of the TRPV subfamily (probably the best understood member of the TRP channel family) respond to a variety of stimuli,

including high temperatures, tissue damage and exposure to pungent compounds such as capsaicin (Szallasi & Blumberg, 1999; Caterina & Julius, 2001).

Amiloride and Gd^{3+} have been shown to block SACs in different preparations (Yang & Sachs, 1989; Lane *et al*., 1991) and ruthenium red has been extensively used as a non-selective TRP channel blocker in a variety of experiments (Bengtson *et al*., 2004; Salazar *et al*., 2008).

In this study, amiloride (5mM), Gd^{3+} (5mM) and ruthenium red (100μM) were added to the pipette solution together with Cs^{+} (140mM) and the effect of each blocking agent was tested individually. Figure 5-13 shows the level of block of the persistent outward current from *S. zeamais* neurons in the presence of each of these bolckers.

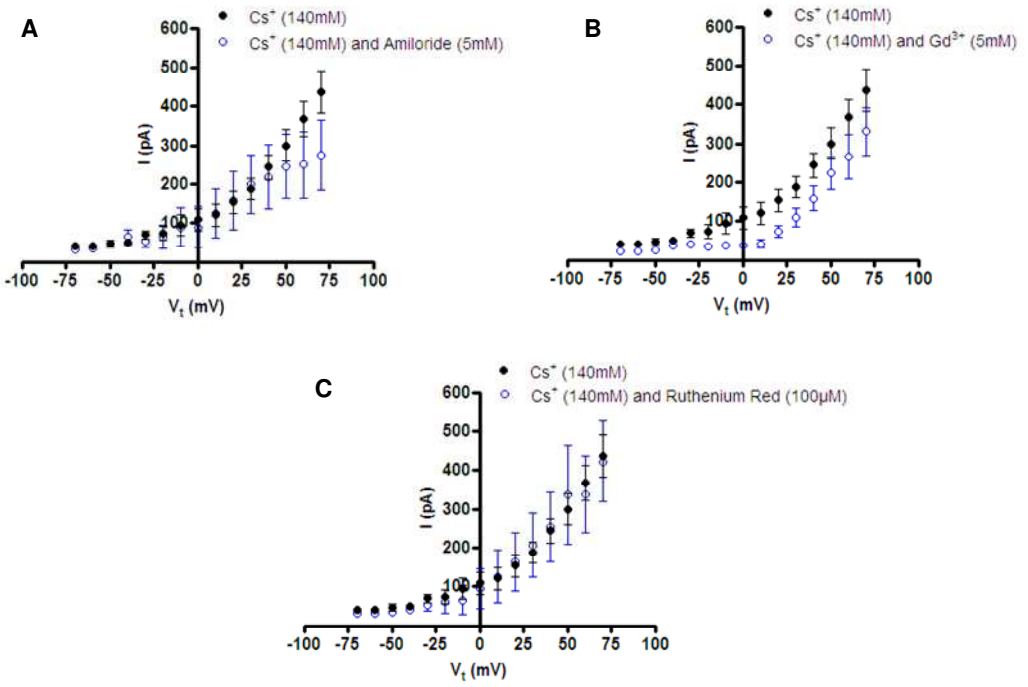

Fig. 5-13: Outward current from maize weevil wild-type neurons recorded in the presence of 140mM Cs^+ (A, B and C), and 5mM amiloride (A), 5mM Gd^{3+} (B) and 100µM ruthenium red (C). All blocking agents were added to the pipette solution. Points are mean ± SEM, N=11 for Cs^+, N=11 for Cs^+ + amiloride, N=8 for Cs^+ + Gd^{3+}, N=5 for Cs^+ + ruthenium red.

The results showed that amiloride (Figure 5-13A) and ruthenium red (Figure 5-13C) did not induce any further inhibition of the persistent outward current of *S. zeamais* neurons when compared with the treatment with Cs^+ alone. On the other hand, Gd^{3+} (Figure 5-13B) showed some additional block when added to the pipette solution with Cs^+, but only at the more negative potentials (similar to 1mM trigonelline). In conclusion, the persistent outward

current was not sensitive to block by amiloride, Gd^{3+} and ruthenium red. These compounds were not used further in electrophysiological studies.

5.7 Discussion

In this chapter, electrophysiological characterization of voltage-gated ion channels from *S. zeamais* neurons was performed in order to optimize the methodology for whole-cell patch clamp recordings. The aim of these initial investigations was to isolate as far as possible the sodium current before investigating the effect of the super-*kdr* mutation (identified in Chapter 3) on sodium channel function and sensitivity to pyrethroids (see Chapter 6).

The ganglion sheath appears to be relatively thin in transmission electron micrographs and this is confirmed by the relative ease with which it can be disrupted using a combination of enzyme and mechanical treatment. After disruption and attachment to the substrate most viable *S. zeamais* nerve cell bodies are very small (< 10μm diameter), compared to other insect species used in electrophysiological studies (Giles, 1980).

After cell dissociation, most neurons were unipolar with an axonal appendage. Early studies showed that ion channels usually occur at low abundance in cell bodies of insect neurons (Hoyle & Burrows, 1973; Goodman & Heitler, 1979) with the majority of synaptic connections taking place on the highly branched proximal axon sometimes referred to as the "dendritic tree". *S. zeamais* neurons from thoracic ganglia were dissociated and maintained in

culture for 1-2 days prior to recording, because previous studies indicated that short-term culture increases sodium currents in insect somata (Lapied *et al*., 1990; Tribut *et al*., 1991). The cells were physically separated from each other and did not project long neurites or form synaptic connections. The whole-cell patch technique was used to characterize *S. zeamais* neurons. A diverse family of voltage-gated channels (apparently similar to sodium, calcium and potassium channels) was expressed at different levels and in recordings the action of these channels was represented by inward and outward currents. Inward currents appeared after a minimum of 20 hours. It is possible that the cell isolation process selects for particular types of neuron and that other neuronal types are lost during preparation, but in the absence of cell specific markers, the type or function of cells studied could not be identified. The preparation method was standardized, as far as possible, to ensure that a consistent population of cells is prepared from each strain of insect and use of Con A increased the proportion of isolated neurons which were available for recording. The consistency of the biophysical properties of the cell population from week to week and the ubiquity of voltage-gated sodium channels makes this method appropriate for comparisons between different insect strains and between insecticide treatments.

All inward current present in *S. zeamais* neurons was completely blocked by a low concentration of TTX (100nM). This result reveals, that inward current in maize weevil neurons is mediated by TTX sensitive sodium channels.

The lack of any additional inward current after the block of sodium channels with TTX suggests the absence of voltage-gated calcium channels.

Very low calcium currents were found in olfactory receptor neurons of *Mamestra brassicae* (Lucas & Shimahara, 2002) and the same neurons in *Manduca sexta* similarly did not exhibit calcium currents (Zufall *et al*., 1991). One possible reason for the absence of calcium currents in *S. zeamais* neurons would be the down-regulation of these currents as a result of dissociation. This was reported in *Aplysia* bag-cell neurons, in which phorbol esters activate a previously silent form of calcium channels (Strong *et al*., 1987). Another explanation would be the inhibition of voltage-gated calcium channels caused by Con A, as described in the hypotrichous ciliate, *Stylonychia mytilus* (Ivens & Deitmer, 1986). In addition, according to Zufall *et al*. (1991), calcium channels could occur at a very low density in the somata and for this reason, could not be detected. The possibility that calcium currents are present in a sub-population of *S. zeamais* neurons cannot be excluded; therefore, a well known calcium channel blocker (Co^{2+}) was added to the external solution.

Good settlement of the cells is crucial for efficient whole-cell patch clamp. Three substrates were tested (Poly-L-lysine, Con A and Laminin) and evaluated according to two parameters: 1) secure attachment of cells to the bottom of the dish, 2) lack of interference with inward currents. Con A facilitated the best adherence of the cells to the surface of the dish, however previous studies have demonstrated that this lectin can affect biological processes in a variety of cells. Desensitization of L-glutamate receptors on locust skeletal muscle fibre, during repeated iontophoretic application of L-glutamate, is abolished by Con A (Mathers & Usherwood, 1976). Con A has shown insecticidal effects in different insect species, including the bruchid, *Callosobruchus maculatus* (Gatehouse *et al*., 1984); the potato leafhopper, *Empoasca fabae* (Habibi, *et al*., 1998); the western tarnished plant bug, *Lygus*

hesperus (Habibi *et al*., 2000); the tomato moth, *Lacanobia oleraceae*, (Fitches *et al*., 2001a; Fitches, *et al*., 2001b), the peach-potato aphid, *Myzus persicae* (Gatehouse *et al*., 1999), the pea aphid, *Acyrthosiphon pisum* (Sauvion *et al*., 2004) and the rice brown planthopper, *Nilaparvata lugens* (Powell *et al*., 1998). Increase of sodium permeability and intracellular sodium content of pig lymphocytes is also caused by Con A (Felber & Brand, 1983), as well as the inhibition of voltage-gated calcium channels in the hypotrichous ciliate, *Stylonychia mytilus* (Ivens & Deitmer, 1986). In this study Con A, when used as a culture substrate, did not show any effect on inward currents, producing similar results to Poly-L-lysine.

Another interesting feature of *S. zeamais* neurons was the presence of outward currents resistant to block by conventional potassium channel blockers (Cs^+, TEA and 4-AP). Cs^+ is a classical voltage-gated potassium channel blocker (Clay, 1985), and TEA and 4-AP are used to block specific types of potassium channels, including the delayed-rectifier (Stanfield, 1983; Hille, 2001) and A-current (Rudy, 1988). Although some persistent outward current was still present remained after applying these blockers, outward currents in maize weevil neurons seem to be most sensitive to Cs^+. A previous study in pyramidal neurons of rat sensorimotor cortex has demonstrated outward current also resistant to block by Cs^+, TEA and 4-AP, but with more sensitivity to TEA (Alzheimer, 1994).

Potassium channels are a very diverse group of channels and provide targets for a variety of marine and terrestrial natural toxins. Some toxins from marine invertebrates block voltage-dependent potassium currents, including sea anemone peptides (Diochot *et al*., 1998; Yeung *et al*., 2005), the

coneshell toxin k-conotoxin PVIIA (Terlau *et al*., 1996) and latruculin A from sponges and nudibranchs (Houssen *et al*., 2006). In this study, a Red Sea soft coral toxin was used in an attempt to block the persistent outward current, which might originate from potassium channels. The active compound of the toxin is 3-carboxy-1-methyl pyridinium (trigonelline hydrochloride) and, according to Temraz *et al*., (2006), 1mM of the synthetic compound inhibited 82% of the potassium current at 60mV in cultured sensory neurons of rat dorsal root ganglia. However, after applying the same concentration of trigonelline to *S. zeamais* neurons in combination with Cs^+, the outward current was only blocked at more negative potentials, with this current reappearing as soon as the potential becomes more positive.

After unsuccessful attempts to block the outward current in *S. zeamais* neurons through conventional potassium channels blockers and also a Red Sea soft coral toxin, other hypotheses were tested such as the possibility of SACs or TRP channels being the source of the persistent outward current. Three blockers (amiloride, Gd^{3+} and ruthenium red) were tested in combination with Cs^+. None of them resulted in a useful reduction in the outward current acting only at more negative potentials. The voltage dependent block obtained with amiloride is in agreement with a previous study in *Xenopus* oocytes, where the block of SACs occurs at more negative potentials (Lane *et al*., 1991). Gd^{3+} was the only blocker which showed an additional block at more positive potentials, when compared to the treatment with Cs^+ alone. However, this blocker was applied at a much higher concentration (5mM) than in other SAC studies (10μM) (Yang & Sachs, 1989). Although the initial results were promising, Gd^{3+} was not used as a recent single channel study showed, that this blocking

agent reduced the sensitivity of mutated rat sodium channels (I874M) to deltamethrin (Peng *et al*., 2009).

The attempts to inhibit this highly resistant outward current in maize weevil neurons suggests that it may originate not from voltage-gated potassium channels, SACs or TRP channels, but possibly from a class of non-specific cation channels similar to those described by Alzheimer (1994). In view of the ineffectiveness of these channel blockers when tested individually and in combination with Cs^+, only Cs^+ was added to the pipette for further electrophysiological characterization of voltage-gated sodium channels from wild-type and super-*kdr S. zeamais* neurons.

Chapter 6

Electrophysiological Investigation of Super-*kdr* Resistance in *Sitophilus zeamais* and the Action of Pyrethroids

6.1 Introduction

Pyrethroids are one of the most widely used classes of insecticides worldwide. They are potent neurotoxins that prolong the sodium channel current associated with an action potential by altering the gating kinetics of insect sodium channels (Narahashi, 1992; Soderlund & Bloomquist, 1989). Based on their distinct poisoning symptoms, effects on nerve preparations and their chemical structures, these synthetic insecticides are grouped into two categories: type I (e.g., permethrin) and type II (e.g., cypermethrin, deltamethrin) (Gammon *et al*., 1981; Lawrence & Casida, 1982).

Extensive electrophysiological and pharmacological studies on the mode of action of pyrethroids have been carried out over the past decades. These studies show that pyrethoids cause a variety of effects on sodium channels, ranging from a slowing of deactivation with the appearance of a pronounced decaying tail current upon membrane repolarisation to an inhibition of open- and closed-state inactivation and a hyperpolarizing shift in activation voltage (Narahashi, 1998; Vais *et al*., 2000a; Vais *et al*., 2000b; Soderlund & Knipple, 2003).

Amino acid substitutions at specific sites on the *para* sodium channel of *Musca domestica* (termed *kdr* and super-*kdr)* have been shown to be associated with pyrethroid resistance in insects (Farnham, 1977; Sawicki, 1978; Williamson *et al*., 1996). Initially, *kdr* resistance was associated with the L1014F mutation on domain IIS6 of the *para* channel and super-*kdr* with an additional M918T substitution in the linker connecting domain II S4 and S5

(Williamson *et al*., 1996). Further studies revealed other *kdr* and super-*kdr* mutations in other insects (Davies *et al*., 2007; Soderlund & Knipple, 2003; Dong, 2007), including the super-*kdr* substitution T929I in the domain IIS5. Chapter 3 described the identification of the T929I mutation in two pyrethroid-resistant populations of *Sitophilus zeamais* from Brazil. Previous studies have demonstrated involvement of the amino acid residue T929 in binding pyrethroids as its change to isoleucine reduces deactivation inhibition by these compounds (Vais *et al*., 2003; Schuler *et al*., 1998).

Electrophysiological characterization of the T929I mutation has been previously carried out by expressing super-*kdr para* sodium channels in *Xenopus* oocytes, however, the characterization of the mutant *para* sodium channel in its native environment, neurons of super-*kdr* maize weevils which carry the T929I mutation, has not been investigated.

Usually, super-*kdr* mutations are identified in combination with some *kdr*-type substitution. However, in *S. zeamais*, the T929I mutation was identified alone and is responsible for a highly resistant phenotype in these insects. According to previous studies, the sensitivity of *Drosophila para* sodium channel to deltamethrin is reduced by over 10,000-fold when the T929I mutation is combined with the *kdr* substitution (Vais *et al*., 2003) and by 100-fold when the same mutation is independent of any other mutation (Usherwood *et al*., 2007).

In this study, the whole cell patch clamp technique was performed to investigate whether the T929I mutation alters the biophysical properties of sodium channels in central neurons of super-*kdr* maize weevil strains. The DDT bioassay described in Chapter 2 (section 2.2.2) was performed to select

the mutant (T929I) insects. The individuals who survived to exposure of DDT (50mg/ml) were used for dissection and isolation of nerve cells. The results demonstrate that voltage-dependence of activation of sodium current is altered and sensitivity to pyrethroids is reduced. These findings suggest similarities in the interaction of pyrethroids with both neuronal and expressed sodium channels and justify studies of native sodium channels in the understanding of pyrethroid action and resistance.

6.2 Super-*kdr* sodium channels show a depolarising shift in activation voltage

Electrophysiological characterization of neuronal super-*kdr* sodium channels was carried out to evaluate if the T929I mutation alters sodium channel gating properties. The current-voltage relationship (I-V curve) (Figure 6-1A) and voltage-dependence of activation curve (Figure 6-1B) for sodium currents of wild-type and super-*kdr* neurons were generated by stepwise test pulses in the range -70mV to +70mV in 10mV increments from a holding potential of -80mV. Peak conductance amplitude in response to these depolarisations was measured and plotted against the test potential. The curve was then fitted with a Boltzman sigmoidal function.

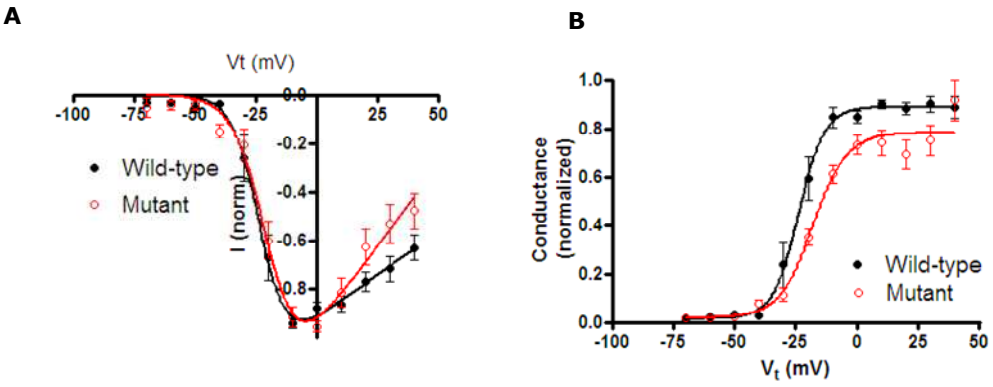

Fig. 6-1: (A) I-V curve for sodium currents in wild-type and mutant (T929I) maize weevil neurons. Peak current generated from single cells were normalized, averaged and plotted against test potential (V_t) to generate the I-V curves. (**Black**) Wild-type extrapolated V_{rev}= 127.2±22.27 mV (N=13), (**red**) mutant extrapolated V_{rev}= 71.29±7.55 mV (N=8). Points are mean ± SEM. (B) Voltage dependence of activation for sodium currents in wild-type and mutant (T929I) maize weevil neurons: conductance was normalized to the peak conductance per cell and many cells averaged. Curves were fitted with a Boltzmann function. (**Black**) Wild-type V_{50} = -23.83±1.04mV (N=13), (**red**) mutant V_{50} = -18.09±1.49mV (N=8). Points are mean ± SEM. V_{rev} and V_{50} are significantly different between wild type and mutant neurons ($p<0.05$, F test).

The V_{rev} (reversal potential), which is required to calculate conductance, was estimated by extrapolation of the I-V curve. This part of the curve is described by a linear relationship and thus extrapolation of the V_{rev} value can be considered accurate.

The T929I mutation affected channel activation and the voltage at which 50% activation of sodium channels occurs (V_{50}) is significantly shifted from -23.82mV in the wild-type to -18.09mV in the mutant cells ($p<0.05$ F test) (Figure 6-1B), i.e., the super-*kdr* sodium channel activation curve shifted ~5mV to the depolarizing potentials, indicating that channels carrying the T929I mutation require stronger depolarization for gating to occur (Zhao *et al*., 2000).

6.3 Deltamethrin causes a hyperpolarizing shift in the activation voltage in wild-type sodium channels

The sensitivity to deltamethrin of neuronal wild type and super-*kdr* sodium channels was investigated. Peak current amplitudes in response to stepwise depolarisations from -70mV to +70mV in 10mV increments from a holding potential of -80mV were transformed to show conductance and plotted against the test potentials. Thus, the voltage-dependence of activation of sodium currents in the wild type and super-*kdr* neurons was determined before and after deltamethrin treatment.

A significant ($p<0.05$) hyperpolarizing shift in the voltage-dependence of activation of sodium currents was observed in the wild type neurons after deltamethrin treatment (Figure 6-2, Table 6-1). The hyperpolarizing shift was observed after testing five concentrations of this pyrethroid insecticide, ranging from 1nM to 10μM. On the other hand, deltamethrin did not cause any

significant change in the activation curve of sodium channels which carry the mutant allele (I929).

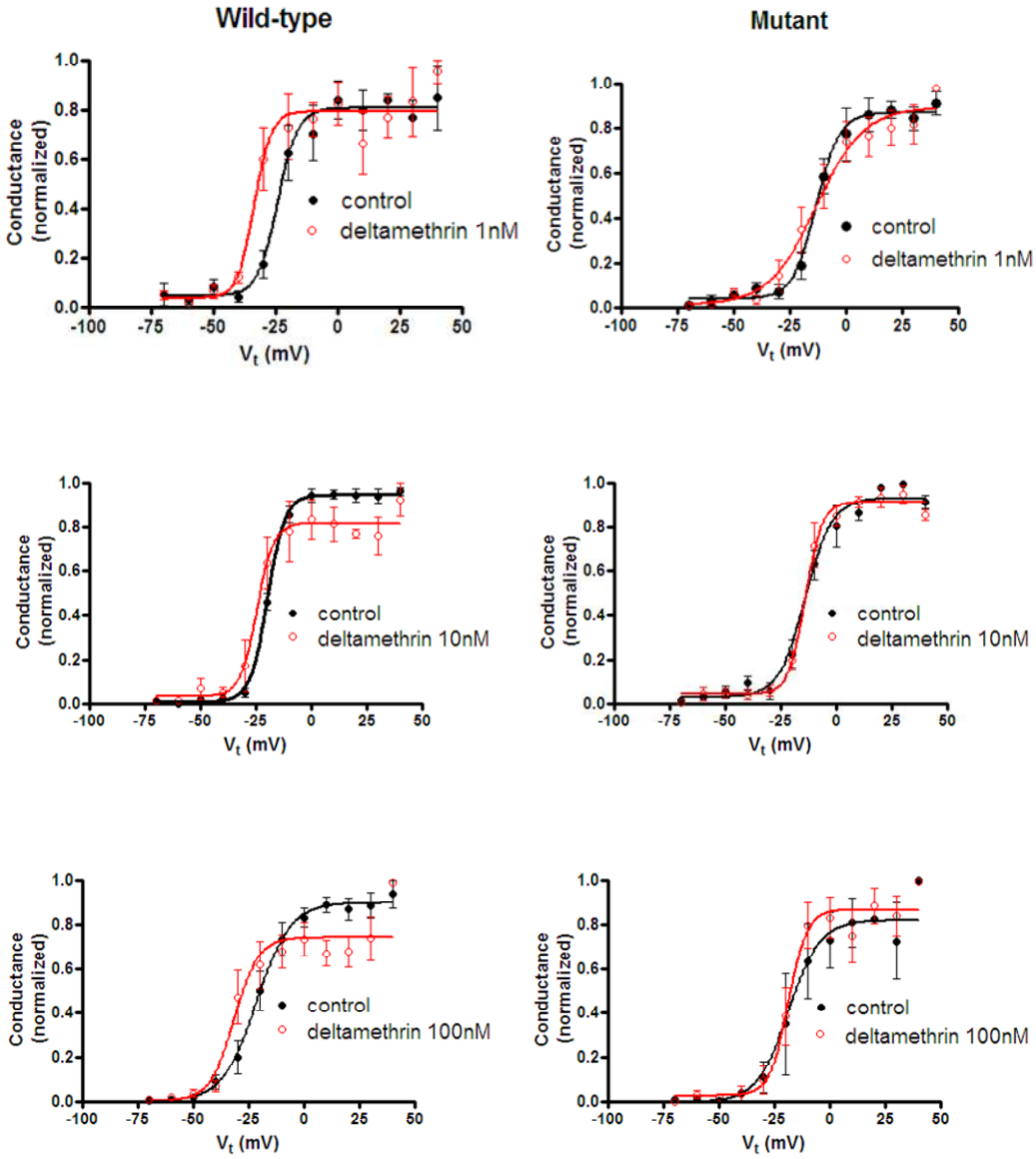

Continuing…

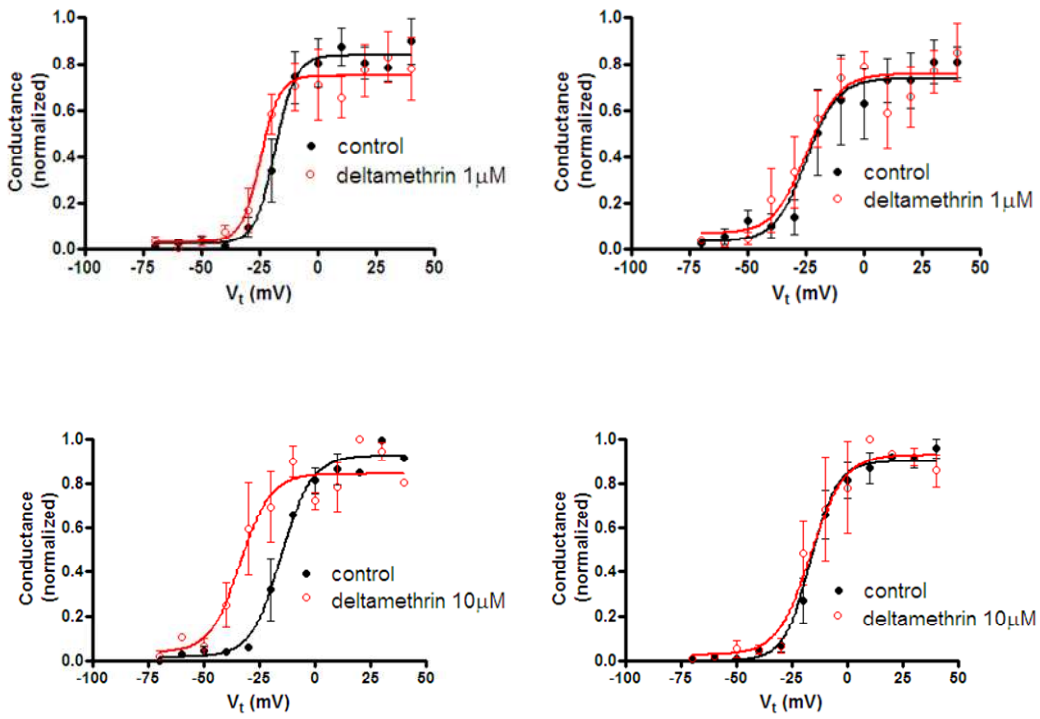

Fig. 6-2: Voltage dependence of activation for sodium currents in wild-type (left hand side) and mutant (T929I) (right hand side) maize weevil neurons, before and after deltamethrin treatment: conductance was normalized to the peak conductance per cell and many cells averaged. Curves were fitted with a Boltzmann function. In the wild-type neuron, V_{50} is significantly ($p<0.05$, F test to compare V_{50}) shifted to a more negative potential after deltamethrin treatment at all concentrations ($p<0.05$, F test). No significant shift of V_{50} was observed in the mutant (T929I) neurons. Points are mean ± SEM.

Table 6-1: Effect of deltamethrin on the voltage-dependence of activation of sodium channels in wild type and mutant (T929I) maize weevil neurons.

	V_{50} (mV)			
	Wild-type		**Mutant**	
Deltamethrin concentration	Before	After	Before	After
1nM	-24.00±1.71 N=5	-33.38±2.01* N=5	-12.79±1.33 N=4	-14.69±2.73 N=4
10nM	-19.54±0.39 N=4	-24.41±1.74* N=4	-12.67±1.16 N=4	-14.55±0.85 N=4
100nM	-21.33±1.52 N=7	-31.40±2.23* N=7	-17.53±3.28 N=3	-19.04±1.51 N=3
1µM	-18.23±1.57 N=4	-24.64±2.24* N=4	-21.69±3.50 N=5	-29.23±4.05 N=5
10µM	-15.08±1.57 N=3	-33.49±3.01* N=3	-14.86±1.31 N=3	-18.85±2.95 N=3

*V_{50} is significantly ($p<0.05$, F test to compare V_{50}) different before and after deltamethrin treatment.

6.4 Sodium channel sensitivity to deltamethrin is reduced by the super-*kdr* mutation

Previous studies have shown that deltamethrin preferentially interacts with the open state of the *Drosophila* wild type sodium channel (Vais *et al*., 1998, 2000a), prolonging the opening of the channels and resulting in the induction of a tail current associated with repolarisation (Tatebayashi & Narahashi, 1994). Theoretically, tail currents are defined as the result of inhibition of deactivation of the sodium channels, such that on repolarisation

sodium currents continue flowing into the cell under a high driving force. Not surprisingly, tail current amplitude is dependent on the sodium channel density of the plasma membrane of the cell investigated and is directly related to the peak current amplitude during the depolarising pulse under control conditions.

In this study, deltamethrin-induced tail current was measured by using the recording protocol of a 100-pulse train of 5ms depolarisations from -80mV to 0mV. The results showed that sodium currents in wild type neurons are more sensitive to deltamethrin than those in mutant (T929I) neurons. This is shown by the larger tail current amplitude observed in the wild type neuron in response to the same concentration of deltamethrin (Figure 6-3A). Five concentrations of deltamethrin were tested (1nM, 10nM, 100nM, 1μM and 10μM) and the lowest concentration was already sufficient to cause inhibition of deactivation in wild type sodium channels, resulting in a persistent tail current on repolarisation. Mutant sodium channels showed clearly reduced sensitivity to the highest concentration of deltamethrin (10μM) (Figure 6-3B). Channels in neurons from super-*kdr* insects are less sensitive to deltamethrin, because the T929I mutation reduces the availability of sodium channels by slowing activation (see Figure 6-1).

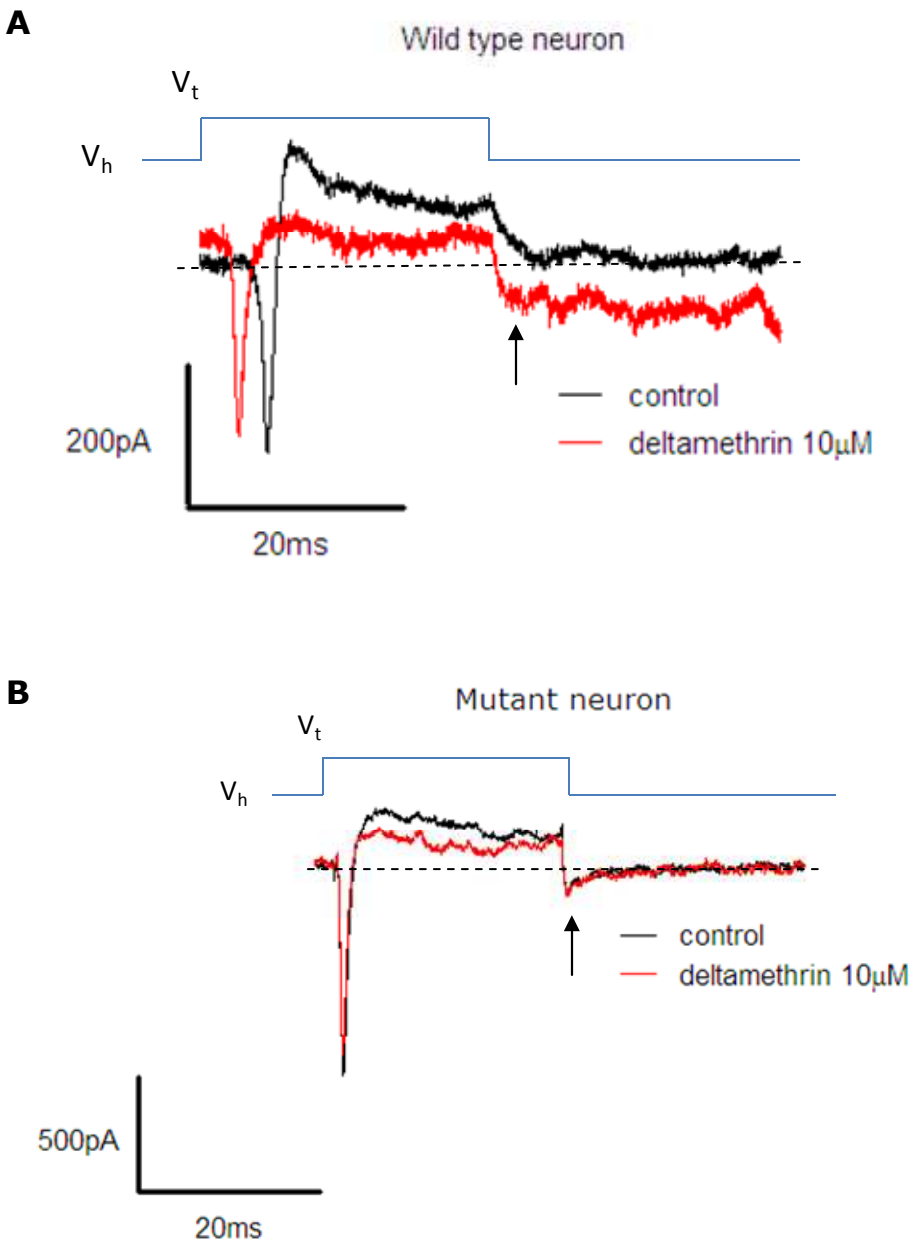

Fig. 6-3: Tail current (↑) amplitude is greater in the wild type (A) neuron than in the mutant (T929I) (B) neurons in response to 10µM deltamethrin. Currents generated by depolarizing the cell to test potentials in the range -70mV to +70mV in 10mV increments for 25ms from a holding potential of -80mV. Currents from single neurons are shown.

Pyrethroid-induced tail current has been used to quantify pyrethroid modification of the sodium channel (Lund & Narahashi, 1982; Vijverberg *et al*., 1982; Song *et al*., 1996; Lee *et al*., 1999b; Vais *et al*., 2000a). Therefore, the sensitivity to deltamethrin was evaluated by measuring the amplitudes of tail currents induced by this compound and quantifying the percentage of modified channels, as described in Chapter 2 (Tatebayashi & Narahashi, 1994). The percentage modification was plotted as a function of deltamethrin concentration (Figure 6-4).

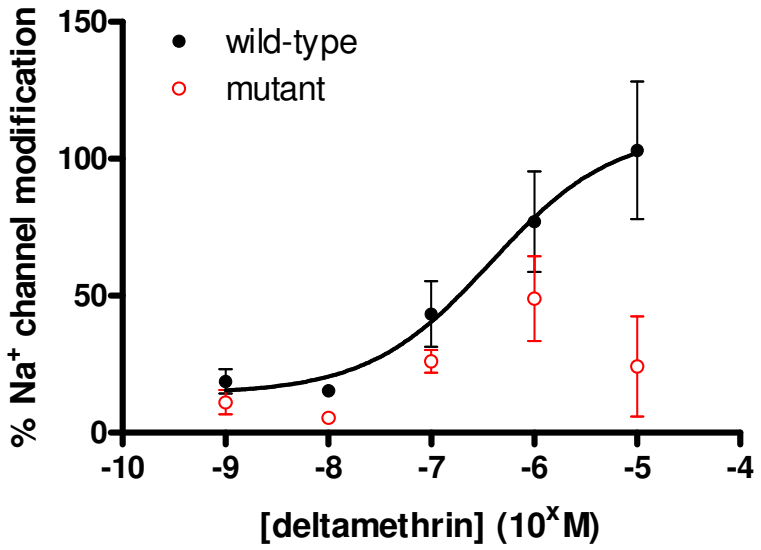

Fig. 6-4: Concentration-response relationship for deltamethrin modification of sodium currents in wild-type (**black**) and mutant (T929I) (**red**) neurons. Apparently, sodium channels in the mutant neurons are less sensitive to pyrethroid modification. Wild-type: EC_{50}=379.3nM (N=5), mutant: ambiguous fit (the data obtained with the mutant cells did not fit into the curve). Points are mean ± SEM. Data were obtained by depolarizing the neurons and measuring tail currents (sodium currents remaining after repolarisation).

Although there was a large degree of variation between responses of individual cells to deltamethrin and the mutant cells showed a higher level of variation, it is clear that deltamethrin had a much greater effect on sodium channels of wild type than mutant neurons. These results show that the T929I mutation is highly protective against pyrethroid poisoning.

The concentration of deltamethrin required to cause 50% of maximum sodium channel modification (EC_{50}) in the wild type neurons was 379.3nM (N=5). An EC_{50} could not be calculated for the mutant channels.

6.5 Fast inactivation

The decay rate of the sodium current was also determined as a measure for fast inactivation of the sodium channel. Single exponentials were fitted to the decay phase of the recorded inward currents and decay time constants (τ_{decay}) were plotted against the step depolarization. Decay rates are the reciprocal of the time constant such that smaller decay time constants indicate an increase in the rate of fast inactivation.

As membrane depolarization increased, the consistent trend was for τ_{decay} to decrease, i.e. the current decayed faster due to an increase in the rate of fast inactivation. The results obtained here followed the same pattern described above, with the decay time constant of sodium currents in wild type and super-*kdr* channels decreasing at more positive potentials (Figure 6-5). Furthermore, similar time constant (τ_{decay}) values for fast inactivation were

observed in the wild type and mutant sodium channels (Table 6-2), agreeing with the results obtained with expressed *Drosophila para* channels (Usherwood *et al*., 2007)

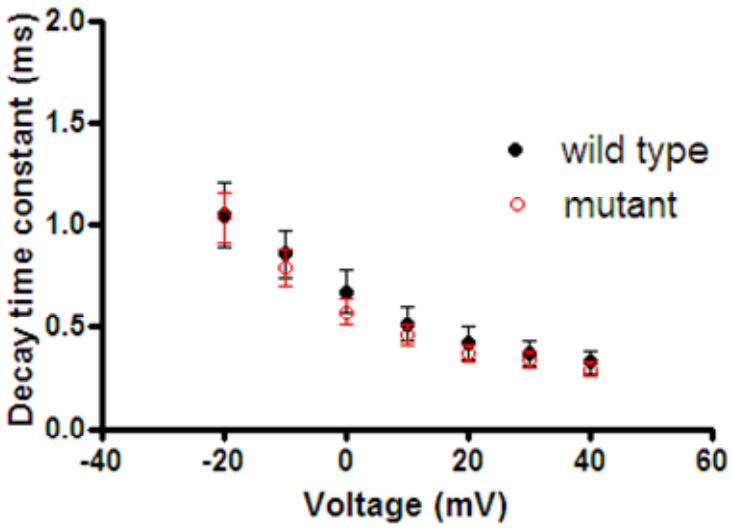

Fig. 6-5: The rate of sodium current decay for wild type (**black**) compared to the mutant (T929I) (**red**) channels. Decay phases were fitted with single exponentials giving decay time constant (τ_{decay}) values, plotted as a function of the membrane potential (mV). Points are mean ± SEM.

Table 6-2: Effects of T929I mutation on the τ_{decay} constants, the reciprocal of which defines the rate of sodium current decay, between -20mV to +40mV test depolarisations.

	Wild type	**Mutant**
	τ_{decay} (ms)	
-20mV	1.05±0.16 n=14	1.04±0.16 n=14
-10mV	0.85±0.12 n=17	0.78±0.09 n=19
0mV	0.67±0.10 n=18	0.57±0.06 n=20
+10mV	0.51±0.08 n=17	0.46±0.05 n=20
+20mV	0.42±0.08 n=16	0.37±0.04 n=19
+30mV	0.36±0.06 n=15	0.34±0.04 n=19
+40mV	0.32±0.06 n=13	0.29±0.04 n=19

Deltamethrin treatment did not result in any change in the decay time constants of wild-type and mutant neurons, suggesting that, this insecticide may not affect the fast inactivation of sodium currents in maize weevils (Figure 6-6).

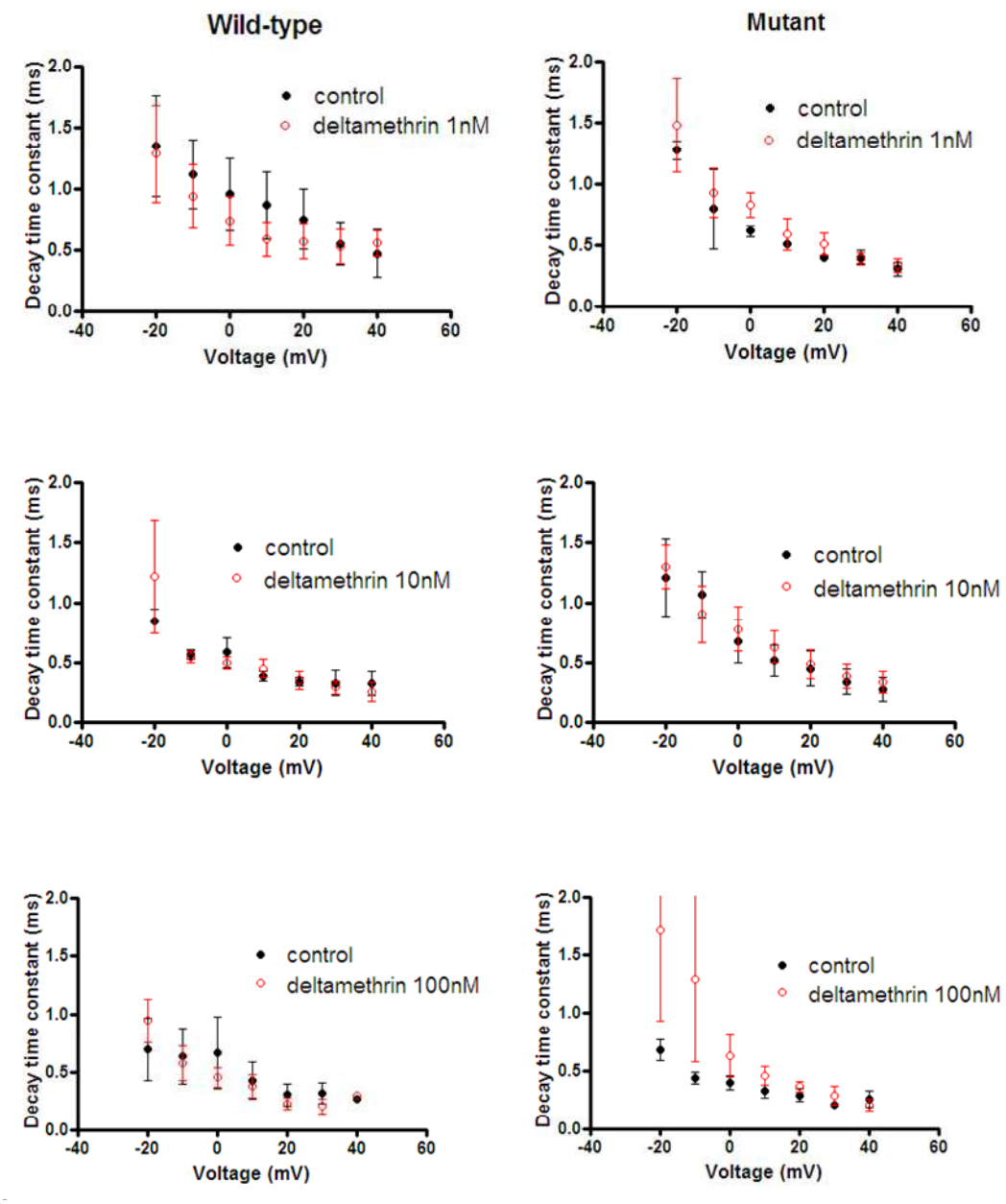
Wild-type
Mutant
control
deltamethrin 1nM
deltamethrin 10nM
deltamethrin 100nM
Decay time constant (ms)
Voltage (mV)
0.0
0.5
1.0
1.5
2.0
-40
-20
0
20
40
60

Continuing…

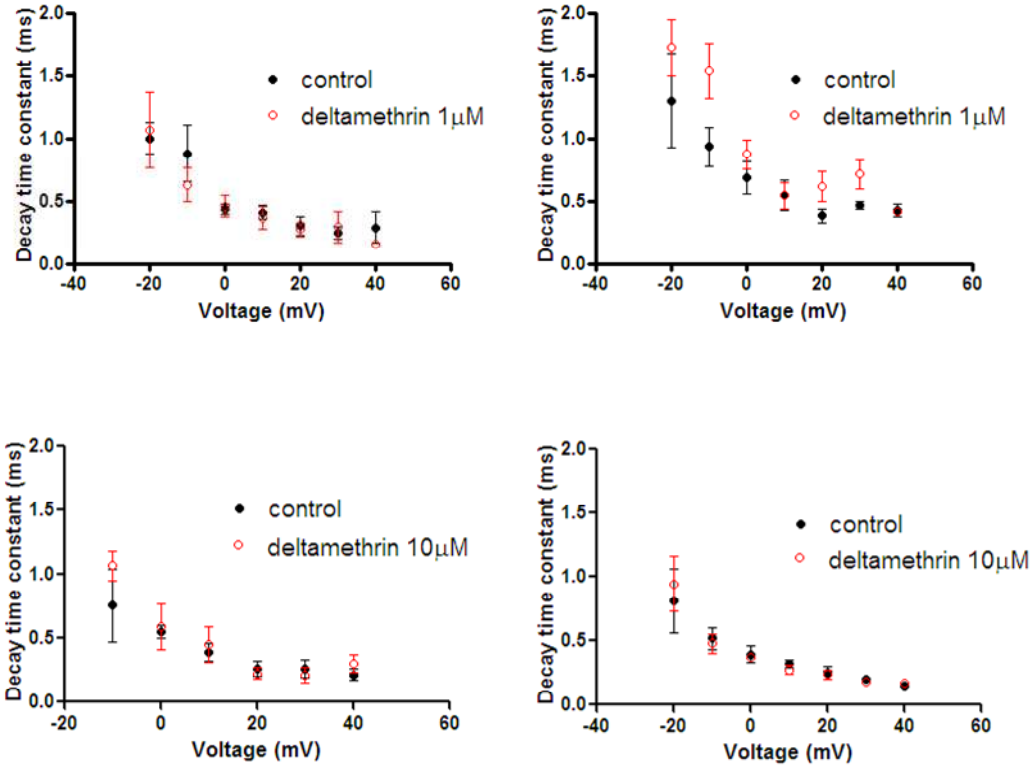

Fig. 6-6: Effect of deltamethrin (1nM, 10nM, 100nM, 1μM and 10μM) on the decay time constant of sodium currents in wild-type (left hand side) and mutant (T929I) (right hand side) sodium channels. Decay phases were fitted with single exponentials giving decay time constant (τ_{decay}) values, plotted as a function of the membrane potentials (mV). Points are mean ± SEM, wild-type: N=5 for 1nM, N=5 for 10nM, N=6 for 100nM, N=4 for 1μM, N=4 for 10μM; mutant: N=4 for 1nM, N=5 for 10nM, N=4 for 100nM, N=5 for 1μM, N=3 for 10μM.

6.6 Discussion

In this chapter, sodium channels from wild-type and super-*kdr* (T929I) maize weevil neurons were characterised electrophysiologically, enabling comparison with insect sodium channels exogenously expressed in *Xenopus* oocytes. Several studies have reported that pyrethroid resistance mutations cause a depolarising shift in voltage-dependence of activation of sodium currents, including some *kdr*-type mutations in the native environment (Lee *et al*., 1999a) or introduced in the *Drosophila para* sodium channel expressed in *Xenopus* oocytes (Zhao *et al*., 2000; Vais *et al*., 2000a; Lee & Soderlund, 2001). In maize weevil neurons, activation of super-*kdr* (T929I) currents is also shifted to more positive potentials relative to wild-type currents. However, this shift was not observed when the same super-*kdr* mutation (T929I) was introduced in the Drosophila *para* channel (Vais *et al*., 2003; Usherwood *et al*., 2007). There is evidence that heterologous expression of sodium channels may diminish the effect relative to expression in neurons (Lee *et al*., 1999a; Zhao *et al*., 2000). As an example, the V421M mutation causes a 13mV shift of voltage-dependence of activation in central neurons of *kdr Heliothis virescens*, but only a 7mV shift when expressed heterologously. Alternative splicing and/or RNA editing can yield sodium channels with different channel properties (Song *et al*., 2004; Du *et al*., 2006) and this may be the cause of the unmodified voltage-dependence of activation in heterologous expressed super-*kdr* sodium channels. It is suggested that depolarising shifts may be part of the resistance mechanism by decreasing the excitability of the nervous system so that a greater degree of depolarisation

would be required to activate sodium channels and initiate an action potential. The depolarising shift in voltage-dependence of activation may ameliorate the hyperpolarising shift in membrane potential after modification by pyrethroid and DDT (Usherwood *et al*., 2005).

Previous studies with vertebrate and marine invertebrate sodium channels have shown that pyrethroids induce channel opening at more negative potentials than normal (Narahashi, 1996). Deltamethrin has similar effects on *Drosophila para* sodium channels, but the effects are more potent and the slowing of gating transitions is more extreme (Vais *et al*., 2000a). DDT also showed the same effect on *para* channels, shifting the peak of the I-V curve and V_{50} activation towards more negative voltages (Usherwood *et al*., 2005). The results obtained with neuronal maize weevil sodium channels are consistent with the results above, with 1nM deltamethrin shifting the voltage-dependence of activation of sodium currents to a more negative potential in wild type neurons. Presumably, the same effect would be expected with DDT, since maize weevils show cross-resistance for both DDT and pyrethroids. Hyperpolarising shifts in the voltage-dependence of activation induced by pyrethroids would be expected to increase the excitability of the nervous system by producing greater activity at rest and reducing the threshold for nerve firing.

The modification of sodium channels by pyrethroids and subsequent production of sodium tail currents on repolarisation has been previously demonstrated (Vijverberg *et al*., 1982). In fact, tail current amplitude has been used in a variety of studies to quantify pyrethroid action and levels of resistance conferred by resistance mutations using calculation of percentage

modification of sodium channels (Smith *et al*., 1997; Warmke *et al*., 1997; Zhao *et al*., 2000; Vais *et al*., 2000a; Vais *et al*., 2000b; Tan *et al*., 2002a; Soderlund & Knipple, 2003; Vais *et al*., 2003; Usherwood *et al*., 2007). These studies have used different sodium channel sequences (rat, housefly and *Drosophila*) expressed heterologously in *Xenopus* oocytes.

Pyrethroid binding sites on the sodium channel were recently identified by the model of the membrane-enclosed portion of the housefly sodium channel based on the rat brain $K_v1.2$ potassium channel crystal structure (O'Reilly *et al*., 2006; Long *et al*., 2005a, 2005b). The model identified a hydrophobic cavity delimited by the DIIS4-S5 linker, DIIS5 and DIIIS6 that could potentially constitute a pyrethroid binding site. According to this model, type II pyrethroids may inhibit the normal movement of DIIIS6, which is required for deactivation. Another important step for deactivation is the movement of DIIS4 back to its resting position (Armstrong, 2006). Pyrethroids may stabilize the DIIS4-S5 linker in its activated state and, as a result, DIIS4 movement may be inhibited. If DIIS4 can move normally, this would not contribute to the movement of DIIS6 due to the lack of movement of the DIIS4-S5 linker. On repolarisation, full deactivation can be inhibited if DIIIS6 and/or DIIS6 are held in their open configuration. The channel pore could remain open and allow ion conductance, explaining the tail currents that are characteristic of pyrethroid modification.

In this study, sodium channels of maize weevil neurons are modified by deltamethrin, generating tail currents that are qualitatively similar to those seen in sodium channels expressed in oocytes. Moreover, the sensitivity of wild type sodium channels to deltamethrin was similar to that for *para*

channels expressed heterologously, in that 1nM was sufficient to see some modification (Vais *et al*., 2003). In the previous expression study, sodium channels were not modified by deltamethrin, unless the oocyte were pre-treated with ATX, a sea anemone toxin that holds the sodium channels open during depolarization and impairs fast inactivation. Here, deltamethrin modified sodium channels and produced tail currents in maize weevil neurons at low concentrations without any pre-treatment to promote channel opening. Maybe neuronal sodium channels are more susceptible to pyrethroid modification than expressed *para* channels. This lower susceptibility of expressed channels may be due to modification of channel properties when sodium channels are expressed in a non-native environment.

A reduction of pyrethroid-induced tail current amplitude in sodium channels with the T929I mutation has been demonstrated by previous studies on pyrethroid resistance, where tail currents carried by heterologously expressed sodium channels have been studied. The T929I substitution has been shown to confer a degree of resistance with regard to percentage modification of sodium channels by pyrethroids. This ranges from 100-fold, when the mutation is independent of any other substitution (Usherwood *et al*., 2007) to 10,000-fold when the same mutation is in combination with another *kdr*-type substitution (Vais *et al*., 2003). In other reports, the T929I mutation completely abolishes permethrin (SupYoon *et al*., 2008) and DDT potencies (Usherwood *et al*., 2007). The results obtained here with neuronal super-*kdr* (T929I) sodium channels are similar to those obtained with the expressed *para* channels, with the super-*kdr* channels showing less sensitivity to deltamethrin. The reduction in sensitivity to deltamethrin occurs by decreasing the time that the channel remains open once drug has bound and speeding the rate of

dissociation from open channels (Vais *et al*., 2000a). The expression studies (Vais *et al*., 2003; Usherwood *et al*., 2007) together with the neuronal study demonstrate that T929 is a key amino acid for the binding of both DDT and pyrethroids, because reductions in sensitivity were obtained with the threonine to isoleucine substitution. The importance of the T929 residue for binding was also demonstrated by the previous binding model study (O'Reilly *et al*., 2006).

An interesting hypothesis about the efficiency of deltamethrin to modify sodium channels is raised by Vais *et al*. (2000a). Once modified, sodium channels remain open after repolarisation. This process is lethal because the cell cannot repolarise completely after an action potential. This mechanism is very efficient because modification of a few channels triggers spontaneous electrical activity via the Hodgkin cycle; i.e., sodium influx is increased by sodium channel opening, which makes the cell depolarised and causes more sodium channel opening. Deltamethrin boosts this positive feedback loop because channel opening enhances deltamethrin modification, which promotes more channel opening. According to Vais *et al*. (2000a), the super-*kdr* mutation, which occurs naturally, overcomes this toxicity by reducing sodium channel opening which is enhanced by closed state inactivation and reducing the occupancy of the high affinity state for deltamethrin, as well as the number of channels that can support electrical spiking.

Another particular aspect of super-*kdr* mutations is that the effect of this substitution on sodium channels is similar to the effect of the dieldrin resistance mutation (Rdl) on γ-aminobutyric acid-gated channels (Zhang *et al*., 1994). Both mutations are repeatedly isolated in the field, indicating that the mutation can confer resistance while preserving viability. Moreover, both

mutations confer resistance by reducing the affinity of the insecticide for its receptor and modifying channel gating.

Fast inactivation of sodium channels can be assessed by measuring the rate of decay of sodium currents, the reciprocal of the time constant of the exponential fits. In maize weevil neurons, sodium currents follow the same pattern in both wild type and super-*kdr* (T929I) channels, with the decay time constants decreasing at more positive potentials. Although neuronal wild type and super-*kdr* channels revealed similar decay time constant values, a slight decrease in the rate of decay was observed in the channels carrying the T929I mutation. This suggests that substitution of a threonine to an isoleucine residue at 929 amino acid position of the *para* sodium channel is responsible for an increase in fast inactivation kinetics for the channel. According to Vais *et al*. (2000a), tail currents decay faster in the super-*kdr* channels than in the wild type, contributing to faster rate of dissociation of pyrethroids. The increase in the rate of fast inactivation may contribute to resistance by enhancing a closed state inactivation for the mutant channel and reducing the number of channels available for modification by deltamethrin (Vais *et al*., 2000b). Additionally, an increase in fast inactivation kinetics could be responsible for counteracting the typical slowed inactivation caused by pyrethroids (Lund & Narahashi, 1983). Deltamethrin treatment did not change the decay time constants of sodium currents in both wild type and super-*kdr* neurons, suggesting that this insecticide may not affect fast inactivation of sodium currents in maize weevil neurons.

In summary, this study provides the first functional analysis of super-*kdr* (T929I) sodium channels in their native environment, insect central neurons.

The results obtained here are consistent with the results in expression studies and confirm that the mutation T929I confers lower sensitivity to pyrethroids. Moreover, this mutation alters the voltage-dependence of activation and accelerates sodium current kinetics of sodium channels, which may contribute to the resistance mechanism.

Chapter 7

Conclusions and Future Directions

This study has characterized the molecular mechanism underlying pyrethroid resistance in Brazilian populations of the maize weevil, *S. zeamais*. The investigation was carried out using molecular biology and electrophysiology, focusing on the putative site of action for pyrethroids, the voltage-gated sodium channels present in the axonal membrane of the insect nervous system. Previous studies have shown that, in many cases, mutations in the sodium channel gene lead to structural changes in the sodium channel protein resulting in pyrethroid resistance, and these changes make the channel less sensitive to the effects of this insecticide. Here, it has been demonstrated that a similar mutation causes resistance in maize weevils.

7.1 Molecular characterization of the maize weevil *para* sodium channel gene

Our understanding of the interaction between pyrethroids and sodium channels at the molecular level has been elucidated significantly in the past decade due to intensive efforts to clarify the molecular mechanism of insect resistance to pyrethroid insecticides. Amino acid mutations in various regions of insect sodium channels have been detected in pyrethroid-resistant insect populations and some of these mutations have been confirmed to reduce insect sodium channel sensitivity to pyrethroids.

Here, a super-*kdr* mutation (T929I) was identified in domain II of the maize weevil *para* sodium channel gene in two resistant laboratory populations (JA and JF). Previously, the identified substitution at this residue has been

implicated in pyrethroid resistance of several other insect species. In maize weevils, the T929I mutation was identified as a single mutation and is responsible for a highly resistant phenotype. The presence of this mutation provides additional evidence that the same amino acid replacement is highly conserved across insect orders. This degree of conservation is probably explained by the necessity of the insecticide target proteins to maintain their native function.

The T929I mutation was identified in maize weevil populations that have been in laboratory culture for many years without insecticide exposure (Araujo *et al*., 2008). The persistence of this mutation suggests that these strains do not carry a fitness cost, or if they carry such cost, it is not interfering in the maintenance of the resistance mechanism. This is consistent with a previous report (Guedes *et al*., 2006) demonstrating the absence of fitness cost in the JA strain and the presence of the cost in the highly resistant JF strain. These findings are also a significant concern for pest control strategies, because the resistance allele may persist in insect populations for long periods of time, even in the absence of strong insecticide selection.

7.2 Resistance management and maize weevil control

The presence of the super-*kdr* mutation in laboratory maize weevil strains raised questions about the frequency of the same mutation within field-collected populations and the effect they might have on the efficacy of maize weevil control products. High-throughput assays based on real-time PCR,

capable of screening individual weevils for the T929I mutation, were developed and used to survey a range of weevils collected from different sites in Brazil. The results of the survey showed that the field strains do not exhibit the super-*kdr* mutation at high frequency, with the heterozygous allele being identified in only two individuals out of 240. Apparently, the super-*kdr* mutation may not be selected in some areas of Brazil due to the recent rotation of insecticides to prevent the outbreak of highly resistant strains. However, the presence of the heterozygous allele observed here could cause a degree of control failure if weevils are treated with pyrethroids alone in the future. It would be interesting to re-select these field collected strains in the lab using DDT or pyrethroid to see if the frequency of the resistance mutation can be increased.

In order to prevent a future failure in maize weevil control caused by the presence of the resistance-associated mutation, a resistance management strategy should be developed. Such a resistance management programme might prolong the effective life of the insecticides used for maize weevil control and, at the same time, avoid or slow the development of resistance. The development of appropriate strategies depends on the nature, frequency and evolution of resistance mechanisms in field populations of insect pests (Kanga *et al*., 2003) and they should be designed based on two important considerations (a) identification of the resistance mechanism and b) methods to monitor the frequency of resistance. Therefore, it is important to develop diagnostics for resistance conferring alleles in populations when they occur at low frequencies. Ideally, assays should be able to detect resistance conferring alleles in the heterozygous state (Soderlund, 1997), as was demonstrated here in the field-collected maize weevil strains. In this respect, the Taqman

assay developed in this study should provide a reliable and robust tool for quick and unequivocal genotyping of large numbers of weevils for the super-*kdr* mutation.

The sensitive detection of resistance should facilitate the development of strategies for effective chemical use, which minimises selection pressure on the insect pest and enhance the life of different insecticides used against those insects (Bass *et al*., 2004). A variety of chemical strategies could be used, including 1) the use of two or more insecticides with different modes of action simultaneously either as separate or mixed formulations; or 2) the use of classes of insecticide that are more active against strains resistant to a different class, termed negative cross-resistance (Pittendrigh & Gaffney, 2001). The first strategy has been shown to be an effective way to control maize weevils and is already being applied in Brazil (Pimentel *et al*., 2009; Pereira *et al*., 2009; Correa, 2009). The second strategy exploiting negative cross-resistance can occur through decreased fitness of the resistant strains, allosteric effects at the site of action, changes at the target site or through increased metabolic processes which activate pro-insecticides (Elliott *et al*., 1986; Hedley *et al*., 1998; Khambay *et al*., 2001).

In summary, this work has important practical implications for identifying the main mechanism of resistance in Brazilian maize weevil populations. The identification of the super-*kdr* mutation in domain II of the maize weevil *para* gene does not disprove the hypothesis that other mutations may be present in other regions of the gene (domains I, III and IV), since the *S.zeamais para* ortholog gene was not fully sequenced. Several other mutations have been previously identified outside domain II in other insect

orders and the effect of those amino acid substitutions on pyrethroid sensitivity has been confirmed in some cases (Liu *et al*., 2000; Park *et al*., 1997, Kawada *et al*., 2009). Nevertheless, the availability of PCR primers that directly amplify the genomic DNA fragment containing the domain II mutation site in *S. zeamais,* has enabled the development of a DNA-based diagnostic assay for use in monitoring programs. These assays may be used as part of a strategy for managing field resistance of maize weevils, identifying the mechanism and controlling these insects.

7.3 *S. zeamais* neurons form a heterogeneous population

A number of factors should be taken into consideration during the electrophysiological characterization of maize weevil sodium channels in their native environment. Isolated neurons of *S. zeamais* form a heterogeneous population with different levels of activity in response to depolarising stimuli. These cells do not represent the total diversity in the weevil nervous system and there remains the possibility that some factors may have interfered with the viability of some neuronal subtypes, thus the isolation procedure and length of culture before electrophysiology might benefit the survival of particular cell populations at the expense of others. The sodium currents observed are from somatic sodium channels. In the absence of cell specific markers, neurons were selected for characterization based in their size (approximately 10μm diameter) and presence of an axonal appendage. Consequently, the sodium currents recorded in this study possibly exclude

some axonal and dendritic variants, although it is unknown what ion channels are expressed in the soma as a response to injury after dissociation. It should also be noted that usable sodium currents are expressed after a minimum of 20h of culture and the cells lost their viability at about 48h. The sodium currents described in this study may reflect certain channel variants being over represented due to time-dependent expression, however this is unknown. By adopting a uniform set of protocols for dissociation and culture of cells and by standardising recording conditions it has been possible to compare properties of neurons derived from pyrethroid susceptible and pyrethroid resistant strains of maize weevils. In this study, the refinement of the isolation process and the use of Con A as culture substrate increased the proportion of cells which were available for recording. By using data, pooled and averaged from a large number of cells in most experiments, it was possible to obtain consistent data within and between individual cell isolations.

The heterogeneous population of insect neurons has been reported to express diversity in sodium channel properties, despite the fact that insect genomics suggest that insects have only one sodium channel gene – orthologs of *para*. This is demonstrated in several studies which have reported sodium current subtypes with different biophysical properties in isolated neurons (Dong *et al*., 2007). This diversity may be a result of several factors: alternative splicing and RNA editing (Dong, 2007), post-translational modification (Weston & Baines, 2007), association with accessory subunits (Feng *et al*., 1995) or regulation by other cellular components and signalling mechanisms (Li *et al*., 1992; Baines, 2003; Cantrell & Catterall, 2001); as a result, channels will express specific biophysical properties adjusted to specific cellular functions.

7.4 Electrophysiological characterization of sodium channels from maize weevil neurons

Before investigating maize weevil sodium channel function, other voltage-gated ion channels, present in *S. zeamais* neurons, were characterized aiming to reduce the interference of other ion currents with the sodium channel activity. This investigation highlighted three aspects of maize weevil neurons: a) firstly, they were found to be diverse in terms of current amplitude, with most of them revealing small sodium currents (~200pA); b) secondly, maize weevil sodium currents are TTX sensitive; c) and finally, outward currents in maize weevil neurons are highly resistant to blockage. Apparently, this outward current originates from a new class of non-selective cation channels similar to those described previously in rat neocortical neurons. The persistent outward current in maize weevil neurons was a major drawback for this study as it potentially interfered with measuring some parameters of sodium currents. So far, it has proved impossible to completely eliminate the outward current in these neurones; however, a number of features of the inward sodium current could still be reliably measured.

The effect of the super-*kdr* mutation (T929I) on sodium channel function has been previously investigated by using site-directed mutagenesis and heterologous expression of *Drosophila para* sodium channel mRNA in *Xenopus* oocyte followed by electrophysiological study using two-electrode voltage-clamp. However, this is the first characterization of this single mutation in its native environment, neuronal sodium channels of super-*kdr* maize weevils.

The results obtained here enabled comparison with expression studies revealing some differences and similarities between the two systems. The depolarizing shift observed in the voltage-dependence of activation of sodium currents in *S. zeamais* super-*kdr* channels was not observed when the same mutation was introduced in the *Drosophila para* channel (Vais *et al*., 2003; Usherwood *et al*., 2007). On the other hand, there were similarities between currents from super-*kdr* neurons and those from oocytes expressing the *Drosophila para* T929I channels, including: the lack of effect of deltamethrin on voltage-dependence of activation of sodium currents, the similarly reduced sensitivity to pyrethroids on sodium channels and the un-modified fast inactivation kinetics of sodium currents (Vais *et al*., 2000a, 2003; Usherwood *et al*., 2007)

Specific questions about sodium channel function and identification of binding sites for pharmacological agents may be better answered using heterologous expression where precise molecular changes can be made. However, some events (cited in section 7.3) which may be involved in insect sodium channel diversity emphasize the disadvantage of the heterologous expression when studying sodium channels and pyrethroid action. The isolation of these transcripts may benefit certain splice variants, providing an unrealistic picture of the natural population of sodium channels. When the transcripts are produced by cloning and specific mutations are introduced by site-directed mutagenesis, only one splice variant is usually studied. It is clear that pyrethroid action and resistance are better understood when the whole population of sodium channels is considered, and recent work has demonstrated that different housefly neurons produce currents with rapid or slow inactivation times and these neuronal populations differ in their

pyrethroid sensitivity (Verdin 2008). Therefore, heterologous expression may not give a reliable indication of the level and effect of these factors in the native environment, unless all splice variants are considered. Similarly heterologous expression systems may not assemble and modify proteins in precisely the same way as native systems, e.g. glycosylation pathways may differ between insects and amphibia or mammals. Accessory factors and subunits may also vary, and although expression of *para* genes in *Xenopus* oocytes is normally accompanied by expression of other subunits such as *TipE* this may only represent part of the protein complement giving normal function to insect sodium channels *in situ.* Studies using insect neurons together with expression studies, should give a more complete picture when analyzing environmental factors and establishing safe limits for pyrethroid use in the field, where synergism with other cellular components will be important (Verdin, 2008).

In conclusion, the results from this study provides further insight into the molecular action of pyrethroids on the sodium channel and extends the current understanding of sodium channel function in insect neuronal cells. Some important key factors contribute to the sustained value of the sodium channel as a target for future insecticides. First, the significance of sodium channel disruption as a mode of insecticidal action is amply demonstrated by the efficacy of natural toxins and insecticides (Soderlund, 2005). Second, sodium channels in insects are the products of a single gene and therefore exhibit conserved pharmacology in all neuronal tissues and insect life stages (Soderlund, 2005). Third, toxin binding sites on the sodium channel other than the pyrethroid site, seem to be unaffected by mutations that confer pyrethroid resistance (Soderlund, 2005). In this perspective, each sodium channel

binding domain can be pictured as an independent potential target for insecticide discovery and development; and the work presented here extends the field by providing knowledge of another important pest species.

- References -

Afonina, I., Zivarts, M., Kutyavin, I., Lukhtanov, E., Gamper, H., Meyer, R.B., 1997. Efficient priming of PCR with short oligonucleotides conjugated to a minor groove binder. *Nucleic Acids Research,* 25:2657-2660.

Alon, M., Benting, J., Lueke, B., Ponge, T., Alon, F., Morin, S., 2006. Multiple oringins of pyrethroid resistance in sympatric biotypes of *Bemisia tabaci* (Hemiptera: Aleyrodidae), *Insect Biochemistry and Molecular Biology*, 36: 71-79.

Alzheimer, C., 1994. A novel voltage-dependent cation current in rat neocortical neurones. *Journal of Physiology*, 479: 199-205.

Anstead, J.A., Williamson, M.S., Eleftherianos, I., Denholm, I., 2004. High-throughput detection of knockdown resistance in *Mysus persicae* using allelic discriminating quantitative PCR. *Insect Biochemistry and Molecular Biology*, 34: 871-877.

Araujo, R.A., Guedes, R.N.C., Oliveira, M.G.A., Ferreira, G.H., 2008. Enhanced activity of carbohydrate- and lipid-metabolizing enzymes in insecticide-resistant populations of the maize weevil, *Sitophilus zeamais*. *Bulletin of Entomological Research*, 98: 417-424.

Armstrong, C.M., 2006. Sodium channel inactivation from open and closed states. *Proceedings of the National Academy of Science USA*, 103: 17991-17996.

Badmin, J., 1990. IRAC survey of resistance of stored grain pests: results and progress. In: F. Fleurat-Lessard and P. Duncan, Editors, *Proc. 5th Int. Working Conf. Stored-Products Protection.* Bordeaux, pp. 973–980.

Baines, R.A., 2003. Postsynaptic protein kinase A reduces neuronal excitability in response to increased synaptic excitation in the *Drosophila* CNS. *The Journal of Neuroscience*, 23: 8664-8672.

Bass, C., Nikou, D., Donnelly, M.J., Williamson, M.S., Ranson, H., Ball, A., Vontas, J., Field, L.M., 2007a. Detection of knockdown resistance (*kdr*) mutations in *Anopheles gambiae*: a comparison of two new high-throughput assays with existing methods. *Malaria Journal*, 6: 111, doi:10.1186/1475-2875-6-111.

Bass, C., Williamson, M.S., Wilding, C.S., Donnelly, M.J., Field, L.M., 2007b. Identification of the main malaria vectors in the *Anopheles gambiae* species complex using a Taqman real-time PCR assay. *Malaria Journal*, 6: 155, doi:10.1186/1475-2875-6-155.

Bass, C., Schroeder, I., Turberg, A., Field, L.M., Williamson, M.S., 2004. Identification of mutations associated with pyrethroid resistance in the *para*-type sodium channel of the cat flea, *Ctenocephalides felis*, *Insect Biochemistry and Molecular Biology*, 34: 1305-1313.

Bengtson, C.P., Tozzi, A., Bernardi, G., Mercuri, N.B., 2004. Transient receptor potential-like channels mediate metabotropic glutamate receptor EPSCs in rat dopamine neurones. *Journal of Physiology*, 555: 323-330.

Berteau, P.E. & Casida, J.E., 1969. Synthesis and insecticidal activity of some pyrethroid-like compounds including ones lacking cyclopropane or ester groupings. *Journal of Agricultural and Food Chemistry,* 17:931–938.

Blasi, G.D., 1999. A Review of the Chemistry of Piperonyl Butoxide. *The Insecticide Synergist*, 55-70.

Bloomquist, J.R., 1996. Ion channels as targets for insecticides. *Annual Review of Entomology*, 41: 163-190.

Bloomquist, J.R., 1993. Neuroreceptor mechanisms in pyrethrpid mode of action and resistance. *Reviews in Pesticide Toxicology,* 2, pp. 185–230.

Bloomquist, J.R. & Soderlund, D.M., 1988. Pyrethroid insecticides and DDT modify alkaloid-dependent sodium channel activation and its enhancement by sea anemone toxin. *Molecular Pharmacology,* 33: 543–550.

Blumenthal, K.M. & Seibert, A.L., 2003. Voltage-gated sodium channel toxins: poisons, probes, and future promise. *Cell Biochemistry and Biophysics*, 38: 215-237.

Braga, G.C., Guedes, R.N.C., Silva, F.A.P., Castro, L.H., 1991. Avaliacao da eficiencia de inseticidas, isolados e em misturas, no controle de *Sitophilus zeamais* Motschulsky (Coleoptera: Curculionidae) em milho armazenado. *Revista Ceres*, 38: 522-528.

Brun-Barale, A., Bouvier, J.C., Pauron, D., Berge, J.B. Sauphanor, B., 2005. Involvement of a sodium channel mutation in pyrethroid resistance in *Cydia pomonella* L., and development of a diagnostic test. Pest Management Science, 61: 549-554.

Burr, S.A. & Ray, D.E., 2004. Structure–activity and interaction effects of 14 different pyrethroids on voltage-gated chloride ion channels. *Toxicological Sciences,* 77: 341–346.

Busvine, J.R., 1951. Mechanism of resistance to insecticides in houseflies. *Nature*, 168: 193-195.

Byerly, L. & Leung, H.-T., 1988. Ionic Currents of *Drosophila* Neurons in Embryonic Cultures. *The Journal of Neuroscience*, 8: 4379-4393.

Byford, R.L., Quisenberry, S.S., Sparks, T.C., Lockwood, J.A., 1985. Spectrum of insecticide cross-resistance in pyrethroids-resistant populations of *Haematobia irritans* (Diptera: Muscidae). *Journal of Economic Entomology*, 78: 768-773.

Caldwell, R.A., Clemo, H.F., Baumgarten, C.M., 1998. Using gadolinium to identify stretch-activated channels: technical considerations. *American Physiological Society*, 275: 619-621.

Campbell, J.F., 2002. Influence of seed size on exploitation by the rice weevil, *Sitophilus oryzae. Journal of Insect Behaviour*, 15: 420-445.

Cannon, S.C. & Strittmatter, S.M., 1993. Functional expression of sodium channel mutations identified in families with periodic paralysis. *Neuron*, 10: 317.

Cantrell, A.R. & Catterall, W.A., 2001. Neuromodulation of sodium channels: an unexpected form of cellular plasticity. *Nature Reviews Neuroscience*, 2: 397-407.

Casida, J.E., 2010. Michael Elliott's billion dollar chrystals and other discoveries in insecticide chemistry. *Society of Chemical Industry*. (www.interscience.wiley.com) doi 10.1002/ps.1982.

Casida, J.E. & Quistad, G.B., 1998. Golden age of insecticide research: past, present, or future? *Annual Review of Entomology*, 43: 1-16.

Caterina, M.J. & Julius, D., 2001. The vanilloid receptor: a molecular gateway to the pain pathway. *Annual Review of Neuroscience*, 24: 487–517.

Catterall, W.A., Goldin, A.L., Waxman, S.G., 2005. International Union of Pharmacology. XLVII. Nomenclature and Structure-Function Relationships of Voltage-Gated Sodium Channels. *Pharmacological Review*, 57: 397-409.

Catterall W.A., Goldin A.L., Waxman S.G., 2003. International Union of Pharmacology. XXXIX Compendium of voltage-gated ion channels: sodium channels. *Pharmacological Review*, 55:575–578.

Catterall, W.A., 2000. Structure and regulation of voltage-gated Ca^{2+} channels. *Annual Review of Cell and Developmental Biology,* 16**:** 521–555.

Cestele, S. & Catterall, W.A., 2000. Molecular mechanisms of neurotoxin action on voltage-gated sodium channels. *Biochimie*, 82: 883-892.

Chambers, J.E., Carr, R.L., Boone, J.S. & Chambers, H.W., 2001. The Metabolism of Organophosphorus Insecticides. *Handbook of Pesticide Toxicology*. Second Edition, 919-927.

Champ, B.R., & Dyte, C.E., 1978. Informe de la Prospeccion Mundial de la FAO Sobre Suscepribilidad a 10s Insecricidas de las Plagas de Granos Almacenados*.* FAO/UN, Rome.

Champ, B.R. & Dyte, C.E., 1976. Report of the FAO. Global survey of pesticides susceptibility of stored grain pests. In: *FAO Plant Protection Series n°5*, Food and Agricultural Organization of the United Nations, Rome.

Cochran, D.G., 1987. Selection for pyrethroid resistance in German cockroach (Dictyoptera: Blatellidae). *Journal of Economic Entomology*, 80: 1117-1121.

CorProtocol 6000-1-July06. High Resolution Melt Assay Design and Analysis. [http://www.corbettlifescience.net/public/Rotor-Gene%206000/hrm_corprotocol.pdf].

Correa, A.S., 2009. Resistencia Fisiologica e Comportamental de Populacoes de *Sitophilus zeamais* a Permetrina, Esfenvalerato e Esfenvalerato + Fenitrotiona. Federal University of Viçosa, Brazil. MSc thesis.

Coustau, C., Chevillon, C., ffrench-Constant, R., 2000. Resistance to xenobiotics and parasites: can we count the cost? *Trends in Ecolology and Evolution*, 15, 378–383.

Cummins, T.R. & Sigworth, F.J., 1996. Impaired slow inactivation in mutant sodium channel. *Biophysical Journal,* 71: 227.

Czapla, T.H. & Lang, B.A., 1990. Effect of plant lectins on the larval development of European Corn Borer (Lepidoptera: Pyralidae) and Southern Corn Rootworm (Coleoptera: Chrysomelidae). *Journal of Economic Entomology*, 83: 2480-2485.

Dhadialla, T.S., Retnakaran, A., & Smagghe, G., 2005. Insect Growth- and Development-Disrupting Insecticides. *Comprehensive Molecular Insect* Science, 6: 55-115.

Davies, T.G.E., O'Reilly, A.O., Field, L.M., Wallace, B.A. & Williamson, M.S., 2008. Knockdown resistance to DDT and pyrethroids: from target-site mutations to molecular modelling. *Pest Management Science*, 64: 1126-1130.

Davies, T.G.E., Field, L.M., Usherwood, P.N.R., Williamson, M.S., 2007. DDT, pyrethrins, pyrethroids and insect sodium channels. *IUBMB-Life*, 59: 151-162.

Deglise, P., Grunewald, B., Gauthier, M., 2002. The insecticide imidacloprid is a partial agonist of the nicotinic receptor of honeybee Kenyon cells. *Neuroscience Letters*, 321:13-16.

Denac, H., Mevissen, M., Scholtysik, G., 2000. Structure, function and pharmacology of voltage-gated sodium channels. *Naunyn-Schmiedeberg's Archives of Pharmacology*, 362: 453-479.

Dib-Hajj, S.D., Black, J.A., Cummins, T.R., Waxman, S.G., 2002. NaN/Nav1.9: a sodium channel with unique properties. *Trends in Neuroscience*, 25:253–259.

Diochot, S., Schweitz, H., Beress, L., Lazdunski, M., 1998. Sea anemone peptides with a specific blocking activity against the fast inactivating channel Kv3.4. *Journal of Biological Chemistry*, 273: 6744-6749.

Dong, K., 2007. Insect sodium channels and insecticide resistance. *Invertebrate Neuroscience*, 7: 17-30.

Dong, K., Valles, S.M., Scharf, M.E. Zeichner B., Bennett, G.W., 1998. The knockdown resistance (*kdr*) mutation in pyrethroid-resistant German cockroaches. *Pesticide Biochemistry and Physiology*, 60: 195-204.

Dong, K., 1997. A single amino acid change in the para sodium channel protein is associated with knockdown-resistance (*kdr*) to pyrethroid insecticides in German cockroach. *Insect Biochemistry and Molecular Biology,* 27: 93–100.

Du, Y., Liu, Z., Nomura, Y., Khambay, B., Dong, K., 2006. An alanine in segment 3 of domain III (IIIS3) of the cockroach sodium channel contributes to the low pyrethroid sensitivity of an alternative splice variant. *Insect Biochemistry and Molecular Biology*, 36: 161-168.

Ecobichon, D.J., 2001. Carbamate Insecticides. *Handbook of Pesticide Toxicology*. Second Edition, 1087-1106.

Eells, J.T., Bandettini, P.A., Holman, P.A., Propp, J.M., 1992. Pyrethroid insecticide-induced alterations in mammalian synaptic membrane potential. *Journal of Pharmacology and Experimental Therapeutics,* 262: 1173–1181.

Eleftherianos, I.G., Williamson, M.S., Foster, S.P., Denholm, I., 2002. Behavioural consequences of pyrethroid resistance in the peach-potato aphid, *Myzus persicae* (Sulzer). *Proceedings Brighton Crop Protection Conference,* 1: *745–749.*

Elliot, M., Farnham, A.W., Janes, N.F., Johnson, D.M., Pulman, D.A., Sawicki, R.M., 1986. Insecticidal amides with selective potency against a resistant (*super-kdr*) strain of houseflies (*Musca Domestica* L.). *Agricultural and Biological Chemistry* 50, 1347-1349.

Evans M.L. & Usherwood P.N.R., 1985. The effect of lectins on desensitisation of locust muscle glutamate receptors. *Brain Research,* 358: 34–39.

Farnham, A.W., Murray, A.W.A., Sawicki, R.M., Denholm, I., White, J.C., 1987. Characterization of the structure activity relationship of *kdr* and two variants of super-*kdr* to pyrethroids in the housefly (Musca domestica L.). *Pesticide Science*, 19: 209 – 220.

Farnham, A.W., 1977. Genetics of resistance of houseflies (*Musca domestica*) to pyrethroids. I. Knockdown resistance. *Pesticide Science*, 8: 631-636.

Felber, S.M. & Brand, M.D., 1983. Concanavalin A causes an increase in sodium permeability and intracellular sodium content of pig lymphocytes. Biochemical Journal, 210: 893-897.

Feng, G., Deak, P., Chopra, M., Hall, L.M., 1995. Cloning and functional analysis of TipE, a novel membrane protein that enhances *Drosophila para* sodium channel function. *Cell,* 82: 1001–1011.

Fenwick, E. M., Marty, A., Neher, E., 1982. A patch-clamp study of bovine chromaffin cells and of their sensitivity to acetylcholine. *Journal of Physiology*, 331: 577-597.

Field, L.M., Anderson, A.P., Denholm, I., Foster, S.P., Harling, Z.K., Javed, N., Martinez-Torres, D., Moores, G.D., Williamson, A.L., Devonshire, A.L., 1997. Use of biochemical and DNA diagnostics for characterizing multiple mechanisms of insecticide resistance in the peach-potato aphid, *Myzus persicae* (Sulzer). *Pesticide Science*, 51: 283-289.

Fitches, E., Ilett, C., Gatehouse, A.M.R., Gatehouse, L.N., Greene, R., Edwards, J.P., Gatehouse, J.A., 2001a. The effects of *Phaseolus vulgaris* erythro- and leucoagglutinating isolectins (PHA-E and PHA-L) delivered via artificial diet and transgenic plants on the growth and development of tomato moth (*Lacanobia oleracea*) larvae; lectin binding to gut glycoproteins in vitro and in vivo. *Journal of Insect Physiology*, 47: 1389-1398.

Fitches, E., Woodhouse, S.D., Edwards, J.P., Gatehouse, J.A., 2001b. *In vitro* and *in vivo* binding of snowdrop (*Galanthus nivalis* agglutinin; GNA) and jackbean (*Canavalia ensiformis*; Con A) lectins within tomato moth (*Lacanobia oleracea*) larvae; mechanism of insecticidal action. *Journal of Insect Physiology*, 47: 777-787.

Forcioli, D., Frey, D., Frey, J.E., 2002. High nucleotide diversity in the para-like voltage-sensitive sodium channel gene sequence in the western flower thrips (Thysanoptera: Thripidae). *Journal of Economic Entomology*, 95: 838-848.

Foster, S.P., Denholm, I., Devonshire, A.L., 2000. The ups and downs of insecticide resistance in peach-potato aphids (*Myzus persicae*) in the U.K. *Crop Protection,* 19: 873–879.

Fragoso, D.B., Guedes, R.N.C., Oliveira, M.G.A., 2007. Partial characterization of glutathione S-transferases in pyrethroid-resistant and -susceptible populations of the maize weevil, *Sitophilus zeamais*. *Journal of Stored Products Research*, 43: 167-170.

Fragoso, D.B., Guedes, R.N.C., Peternelli, L.A., 2005. Developmental rates and population growth of insecticide-resistant and susceptible populations of *Sitophilus zeamais*. *Journal of Stored Products Research*, 41: 271-281.

Fragoso, D.B., Guedes, R.N.C., Rezende, S.T., 2003. Glutathione S-transferase detoxification as a potential pyrethroid resistance mechanism in the maize weevil, *Sitophilus zeamais*. *Entomologia Experimentalis et Applicata*, 109: 21-29.

Fujitani, Y., 1909. Chemistry and pharmacology of insect powder. *Arch Exp Pathol Pharmakol*, 61: 47-75.

Gallo, D., Nakano, O., Silveira Neto, S., Carvalho, R.P.L., Batista, G.C., Berti Filho, E., Parra, J.R.P., Zucchi, R.A., Alves, S.B., 1978. Manual de Entomologia Agricola. *Agronomica Ceres*, Sao Paulo.

Gallo D., Nakano O., Wiendl F.M., Silveira Neto S., Carvalho R.P.L., 1970. Manual de Entomologia. *Agronomica Ceres*, Sao Paulo, Brazil.

Gammon, D.W., 1985. Correlations between *in vitro* and *in vivo* mechanisms of pyrethroid insecticide action. *Fundamental and Applied Toxicology*, 5:9–23.

Gammon, D.W., Brown, M.A., Casida, J.E., 1981. Two classes of pyrethroid action in the cockroach. *Pesticide Biochemistry and Physiology*, 15: 181-191.

Gammon, D.W., 1980. Pyrethroid resistance in a strain of *Spodoptera littoralis* is correlated with decrease sensitivity of the CNS *in vitro*. *Pesticide Biochemistry and Physiology*, 13: 53-62.

Gatehouse, A.M.R., Davison, G.M., Stewart, J.N., Gatehouse, L.N., Kumar, A., Geoghegan, I.E., Birch, N.E., Gatehouse, J.A., 1999. Concanavalin A inhibits development of tomato moth (*Lacanobia oleracea*) and peach-potato aphid (*Myzus persicae*) when expressed in transgenic potato plants. *Molecular Breeding*, 5: 153-165.

Gatehouse, A.M.R., Dewey, F.M., Dove, J., Fenton, K.A., Pusztai, A., 1984. Effect of seed lectin from *Phaseolus vulgaris* on the larvae of *Callosobruchus maculatus*; mechanism of toxicity. *Journal of the Science of Food and Agriculture*, 35: 373-380.

Georghiou G.P., 1990. Overview of insecticide resistance, In: *Managing Resistance to Agrochemicals*, ed. by Green MB, LeBaron HM and Moberg WK. American Chemical Society, Washington, DC, pp. 18–41.

Georghiou, G. & Taylor, C.E., 1977. Operational influences in the evolution of insecticide resistance. Journal of *Economic Entomology,* 70: 653-658.

Gibson, U.E., Heid, C.A., Williams, P.M., 1996. A novel method for real time quantitative RT-PCR. *Genome Research*, 6: 995-1001.

Giles, D.P., 1980. Studies on Insect Neurons in vitro. University of Nottingham. PhD thesis.

Goldin, A.L., 2003. Mechanisms of sodium channel inactivation. *Current Opinion in Neurobiology*, 13:284–290

Goldin, A.L., 2001. Resurgence of sodium channel research. *Annual Review of Physiology*, 63: 871–894.

Goldin, A.L., Barchi, R.L., Caldwell, J.H., Hofmann, F., Howe, J.R., Hunter, J.C., Kellen, R.G., Mandel, G., Meisler, M.H., Netter, Y.B., Noda, M., Tamkun, M.M., Waxman, S.G., Wood, J.N., Catterall, W.A., 2000. Nomenclature of voltage-gated sodium channels. *Neuron*, 28: 365–368.

Goldin, A.L., 1999. Diversity of mammalian voltage-gated sodium channels. *Annals of the New York Academy of Science*, 868: 38–50.

Goldstein, J.J., Hollerman, C.E., Smith, E.E., 1965. Protein-Carbohydrate Interaction. II. Inhibition Studies on the Interaction of Concanavalin A with Polysaccharides. *Biochemistry*, 4: 876-883.

Gonzalez-Coloma, A., Reina, M., Diaz, C.E. & Fraga, B.M., 2010**.** Natural Product-Based Biopesticides for Insect Control. *Comprehensive Natural Products II*, 3: 237-268.

Goodman, C.S. & Heitler, W.J., 1979. Electrical properties of insect neurones with spiking and non-spiking somata: normal, axotomized, and colchicines-treated neurones. *Journal of Experimental Biology*, 83: 95-121.

Gordon, D., Karbat, I., Ilan, N., Cohen, L., Kahn, R., Gilles, N., Dong, K., Stuhmer, W., Tytgat, J., Gurevitz, M., 2007. The differential preference of scorpion α-toxins for insect or mammalian sodium channels: Implications for improved insect control. *Toxicon*, 49: 452-472.

Green, R.A., Lovell, N.H., Poole-Warren, L.A., 2009. Cell attachment functionality of bioactive conducting polymers for neural interfaces. *Biomaterials*, 30: 3637-3644.

Guedes, R.N.C., Oliveira, E.E., Guedes, N.M.P., Ribeiro, B., Serrao, J.E., 2006. Cost and mitigation of insecticide resistance in the maize weevil, *Sitophilus zeamais*. *Physiological Entomology*, 31: 30-38.

Guedes, R.N.C. & Zhu, K.Y., 1998. Characterization of malathion resistance in a Mexican population of *Rhyzopertha dominica*. *Pesticide Science*, 53: 15-20.

Guedes, R.N.C., Kambhampati, S., Dover, B.A., Zhu, K.Y., 1997. Biochemical mechanisms of organophosphate resistance in *Rhyzopertha dominica* (Coleoptera: Bostrichidae) from the United States and Brazil. *Bulletin of Entomological Research*, 87: 581-586.

Guedes, R.N.C., Dover, B.A., Kambhampati, S., 1996. Resistance to chlorpyrifos-methyl, pirimiphos-methyl, and malathion in Brazilian and US populations of *Rhyzopertha dominica* (Coleoptera: Bostrichidae). *Journal of Economic Entomology*, 89: 27-32.

Guedes, R.N.C., Lima, J.O.G., Santos, J.P., Cruz, C.D., 1995. Resistance to DDT and pyrethroids in Brazilian populations of *Sitophilus zeamais* Motsch. (Coleoptera: Curculionidae). *Journal of Stored Products Research,* 31: 145-150.

Guedes, R.N.C., Lima, J.O.G., Santos, J.P., Cruz, C.D., 1994. Inheritance of deltamethrin resistance in a Brazilian strain of maize weevil (*Sitophilus zeamais* Mots.). *International Journal of Pest Management,* 40: 103-106.

Guedes R.N.C., 1993. Deteccao e heranca da resistencia ao DDT e a piretroides em *Sitophilus zeamais* Motschulsky (Coleoptera: Curcuhonidae). Universidade Federal de Vigosa, Brazil. MSc. thesis

Guedes, R.N.C., 1990. Resistencia a inseticidas: desafio para o controle de pragas de graos armazenados. *Seiva*, 50: 24-29.

Guerrero, F.D., Jamroz, R.C., Kammlah, D., Kunz, S.E., 1997. Toxicological and molecular characterization of pyrethroid-resistant horn-flies, *Haematobia irritans*: identification of *kdr* and super-*kdr* point mutations. *Insect Biochemistry and Molecular Biology*, 27, 745-755.

Habibi, J., Backus, E.A., Huesing, J.E., 2000. Effects of phytohemagglutinin (PHA) on the structure of midgut epithelial cells and localization of its binding sites in western tarnished plant bug *Lygus hesperus* Knight. *Journal of Insect Physiology*, 46: 611-619.

Habibi, J., Backus, E.A., Czapla, T.C., 1998. Subcellular effects and localization of binding sites of phytohemagglutinin in the potato leafhopper, *Empoasca fabae* (Insecta: Homoptera: Cicadellidae). *Journal of Economic Entomology*, 86: 945-951.

Hagstrum, D.W., Flinn, P.W., Howard, R.W., 1996. Ecology. In: Subramanyam, B. & Hagstrum, D.W. (Eds) *Integrated management of insects in stored products*, Marcel Dekker, New York, pp. 71-134.

Halliday, W.R. & Georghiou, G.P., 1985. Inheritance of resistance to permethrin and DDT in the Southern house mosquito (Diptera: Culicidae). *Journal of Economic Entomology*, 78: 762-767.

Harper, S.M., Crenshaw, R.W., Mullins, M.A., Privalle, I.S., 1995. Lectin binding to insect brush border membranes. *Journal of Economic Entomology*, 88: 1197-1202.

Hayashi, J.H & Hildebrand, J.G., 1990. Insect Olfactory Neurons *in vitro*: Morphological and Physiological Characterization of Cells from the Developing Antennal Lobes of *Manduca sexta*. *The Journal of Neurosciences*, 10: 848-859.

Heather, N.W., 1986. Sex-linked resistance to pyrethroids in *Sitophilus orizae* (L.) (Coleoptera: Curculionidae). *Journal of Stored Product Research*, 22: 15-20.

Hedley, D., Khambay, B.P.S., Hooper, A.M., Thomas, R.D., Devonshire, A.L., 1998. Pro-insecticides effective against insecticide-resistant peach-potato aphid (*Myzus persicae* (Sulzer)). *Pesticide Science,* 53: 201-208.

Heid, C.A., Stevens, J. Livak, K.J., Williams, P.M., 1996. Real time quantitative PCR. *Genome Research*, 6: 986-994.

Hemingway, J. & Ranson, H., 2000. Insecticide resistance in insect vectors of human disease. *Annual Review of Entomology*, 45: 371-391.

Higuchi, R., Fockler, C., Dollinger, G., Watson, R., 1993. Kinetic PCR analysis: real-time monitoring of DNA amplification reactions. *Biotechnology*, 11: 1026-1030.

Hildebrand, M.E., McRory, J.E., Snutch, T.P., Stea, A., 2004. Mammalian voltage-gated calcium channels are potently blocked by the pyrethroid insecticide allethrin. *Journal of Pharmacology and Experimental Therapeutics,* 308: 805–813.

Hille, B., 2001. Ion Channels of Excitable Membranes. Third Edition. Sunderland, Mass: Sinauer Associates.

Holland, P.M., Abramson, R.D., Watson, R., Gelfand, D.H., 1991. Detection of specific polymerase chain reaction product by utilizing the 5'-3' exonuclease activity of *Thermus aquaticus* DNA polymerase. *Proceedings of the National Academy of Science USA*, 88: 7276-7280.

Houssen, W.E., Jaspars, M., Wease, K.N., Scott, R.H., 2006. Acute actions of marine toxin latruculin A on the electrophysiological properties of cultured dorsal root ganglion neurones. *Comparative Biochemistry and Physiology C*, 142: 19-29.

Hoyle, G. & Burrows, M., 1973. Neural mechanisms underlying behavior in the locust *Schistocerca gregaria*. I. Physiology of identified motoneurons in the metathoracic ganglion. *Journal of Neurobiology*, 4: 3-41.

Huang, J., Kim, L.J., Poisik, A., Pinsky, D.J., Sander Connolly Jr., E., 1998. Does Poly-L-lysine Coating of the Middle Cerebral Artery Occlusion Suture Improve Infarct Consistency in a Murine Model? *Journal of Stroke and Cerebrovascular Diseases*, 7: 296-301.

Ingles, P.J., Adams, P.M., Knipple, D.C., Soderlund, D.M., 1996. Characterization of voltage-sensitive sodium channel gene coding sequences from insecticides-susceptible and knockdown- resistant housefly strains. *Insect Biochemistry and Molecular Biology*, 26:319–326.

Ishaaya, I. & Horowitz, A.R., 1998. Insecticides with novel modes of action: an overview. Ishaaya I. & Degheele, D. (Eds.) *Insecticides with Novel Modes of Action*. Springer, Berlin, pp. 1-24.

Isman, M.B., 2005. Chapter Six Tropical forests as sources of natural insecticides. *Recent Advances in Phytochemistry*, 39: 145-161.

Ivens, I. & Deitmer, J.W., 1986. Inhibition of a voltage-dependent Ca current by concanavalin A. *Pflugers Archiv*, 406: 212-217.

Jamroz, R.C., Guerrero, F.D., Kammlah, D.M., Kunz, S.E., 1998. Role of the *Kdr* and super-*kdr* sodium channel mutations in pyrethroid resistance: correlation of allelic frequency to resistance level in wild and laboratory populations of horn flies (*Haematobia irritans*). *Insect Biochemistry and Molecular Biology*, 28: 1031-1037.

Janzen, D.H. & Juster, H.B., 1976. Insecticidal action of the phytohemagglutinin in Black Beans on a bruchid beetle. *Science*, 192: 795-796.

Jeschke, P. & Nauen, R., 2005. Neonicotinoid Insecticides. Comprehensive Molecular Insect Science, 5: 53-105.

Kanga, L.H.B., Pree, D.J., Van Lier, J.L., Walker, G.M., 2003. Management of insecticide resistance in Oriental fruit moth (*Grapholita molesta*; Lepidoptera: Tortricidae) populations from Ontario. *Pest Management Science,* 59: 921-927.

Katsuda, Y., 1999. Development of and future prospects for pyrethroid chemistry. *Pesticide Science*, 55: 775-782.

Kawada, H., Higa, Y., Komagata, O., Kasai, S., Tomita, T., Yen, N.T., Loan, L.L., Sanchez, R.A.P., Takagi, M., 2009. Widespread Distribution of a Newly Found Point Mutation in Voltage-Gated Sodium Channel in Pyrethroid-Resistant *Aedes aegypti* Populations in Vietnam. *PLoS Neglected Tropical Disease*, 3 (10): e0000527. doi:10.1371/journal.pntd.0000527.

Keiding, J., 1975. Problems of housefly (*Musca domestica*) control due to multi-resistance to insecticides. *Journal of Hygiene, Epidemiology Microbiology and Immunology,* 19:340–355.

Khachatourians, G.G., 2009. Insecticides, Microbial. *Encyclopedia of Microbiology*. Third Edition. 95-109.

Khambay, B.P.S. & Jewess, P., 2005. Pyrethroids. In: *Comprehensive Molecular Insect Science*. (Gilbert, L.I.; Iatrow, K. & Gill, S.S. Eds), Elsevier, Oxford, pp. 1-29.

Khambay, B.P.S., 2002. Pyrethroid insecticides. *The Royal Society of Chemistry*. doi: 10.1039/b202996k.

Khambay, B.P.S., Denholm, I., Carlson, G.R., Jacobson, R.M., Dhadialla, T.S., 2001. Negative cross-resistance between dihydropyrazole insecticides and pyrethroids in houseflies, *Musca domestica*. *Pest Management Science,* 57: 761-763.

Khambay, B.P.S., Farnham, A.W., Beddie, D.G., 1994. Relationships between pyrethroid structure and level of resistance in houseflies (*Musca domestica* L.). In: *Advances in the Chemistry of Insect Control III* (Briggs, G. G. ed.), The Royal Society of Chemistry, Cambridge, UK, pp. 117–126.

Krypuy, M., Newnham, G.M., Thomas, D.M., Conron, M., Dobrovic, A., 2006. High resolution melting analysis for the rapid and sensitive detection of mutations in clinical samples: KRAS codon 12 and 13 mutations in non-small cell lung cancer. *BMC Cancer,* 6:295

Kulkarni, N.H., Yamamoto, A.H., Robinson, K.O., Mackay, T.F.C., Anholt, R.R.H., 2002. The *DSC1* channel, encoded by the smi60E locus, contributes to odor-guided behavior in Drosophila melanogaster. *Genetics,* 161:1507–1516.

LaForge, F.B. & Barthel, W.F., 1945. Constituents of pyrethum flowers. XVIII. The structure and isomerism of pyrethrolone and cinerolone. *Journal of Organic Chemistry*, 10: 114-120.

Lane, J.W., McBride, D.W., Hamill, O.P., 1991. Amiloride block of the mechanosensitive cation channel in *Xenopus* oocytes. *Journal of Physiology*, 441: 347-366.

Lapied, B., Malecot, C.O., Pelhate, M., 1990. Patch-clamp study of the properties of the sodium current in cockroach single isolated adult aminergic neurones. *Journal of Experimental Biology*, 151: 387-403.

Lawrence, L.J. & Casida, J.E., 1982. Pyrethroid toxicology: mouse intra-cerebral structure-toxicity relationships. *Pesticide Biochemistry and Physiology*, 18: 9-14.

Lee, S.H., Gao, J.R., Yoon, K.S., Mumcuogly, K.Y., Taplin, D., Edman, J.D., Takano-Lee, M., Clark, J.M., 2003. Sodium channel mutations associated with knockdown resistance in the human head louse, *Pediculus capitis* (De Geer). *Pesticide Biochemistry and Physiology*, 75: 79-91.

Lee, S.H. & Soderlund, D.M., 2001 The V410 mutation associated with pyrethroid resistance in *Heliothis virescens* reduces the pyrethroid sensitivity of house fly sodium channels expressed in *Xenopus* oocytes, *Insect Biochemistry and Molecular Biology*, 31: 19–29.

Lee, S.H., Yoon, K.S., Williamson, M.S., Goodson, S.J., Takano-Lee, M., Edman, J.D., Devonshire, A.L., Clark, J.M., 2000. Molecular analysis of *kdr*-like resistance in permethrin-resistant strains of head lice, *Pediculus capitis*, *Pesticide Biochemistry and Physiology*, 66: 130-143.

Lee, S.H., Dunn, J.B., Clark, J.M., Soderlund, D.M., 1999a. Molecular analysis of *kdr*-like resistance in a permethrin-resistant strain of Colorado potato beetle. *Pesticide Biochemistry and Physiology*, 63: 63–75.

Lee, S.H., Smith, T.J., Knipple, D.C., Soderlund, D.M., 1999b. Mutations in the housefly *Vssc1* sodium channel gene associated with super-*kdr* resistance abolish the pyrethroid sensitivity of *Vssc1/*tipE sodium channels expressed in *Xenopus* oocytes. *Insect Biochemistry and Molecular Biology*, 29: 185-194.

Li, M., West, J.W., Lai, Y., Scheuer, T., Catterall, W.A., 1992. Functional modulation of brain sodium channels by cAMP-dependent phosphorilation. *Neuron*, 8: 1151-1159.

Liew, M., Pryor, R., Palais, R., Meadows, C., Erali, M., Lyon, E., Wittwer, C., 2004. Genotyping of single-nucleotide polymorphisms by high-resolution melting of small amplicons. *Clinical Chemistry*, 50: 1156-1164.

Littleton, J.T., Ganetzky, B., 2000. Ion channels and synaptic organization: analysis of the *Drosophila* genome. *Neuron,* 26:35–43.

Liu, Z., Tan, J., Valles, S.M., Dong, K., 2002. Synergistic interaction between two cockroach sodium channel mutations and a tobacco budworm sodium channel mutation in reducing channel sensitivity to a pyrethroid insecticide. *Insect Biochemistry and Molecular Biology,* 32: 397–404.

Liu, Z., Chung, I., Dong, K., 2001. Alternative splicing of the *BSC1* gene generates tissue-specific isoforms in the German cockroach. *Insect Biochemistry and Molecular Biology*, 31: 703–713.

Liu, Z., Valles, S.M., Dong, K., 2000. Novel point mutations in the German cockroach *para* sodium channel gene are associated with knockdown resistance (*kdr*) to pyrethroid insecticides. *Insect Biochemistry and Molecular Biology,* 30: 991–997

Long, S.B., Campbell, E.B., Mackinnon, R., 2005a. Crystal structure of a mammalian voltage-dependent *Shaker* family K^+ channel. *Science*, 309: 897-903.

Long, S.B., Campbell, E.B., Mackinnon, R., 2005b. Voltage sensor of $k_v1.2$: Structural basis of electromechanical coupling. *Science*, 309: 903-908.

Longstaff, B.C., 1981. Biology of the grain pest species of the genus *Sitophilus* (Coleoptera: Curculionidae): A critical review. *Protection Ecology*, 2: 83-130.

Loughney, K., Kreber, R., Ganetzky, B., 1989. Molecular analysis of the *para* locus, a sodium channel gene in *Drosophila*. *Cell,* 58: 1143–1154.

Lucas, P. & Shimahara, T., 2002. Voltage and Calcium-activated Currents in Cultured Olfactory Receptor Neurons of Male *Mamestra brassicae* (Lepidoptera). *Chemical Senses*, 27: 599-610.

Lund, A.E. & Narahashi, T., 1983. Kinetics of sodium channel modification as the basis for the variation in the nerve membrane effects of pyrethroids and DDT analogs. *Pesticide Biochemistry and Physiology*, 20: 203-216.

Lund, A.E. & Narahashi, T., 1982. Dose-dependent interaction of the pyrethroid isomers with sodium channels of squid axon membranes. *Neurotoxicology*, 3: 11-24.

Mackay, I.M., 2004. Real-time PCR in the microbiology laboratory. *Clinical Microbiology and Infection*, 10: 190–212.

Malcolm, C.A. & Wood, R.J., 1982. Location of a gene conferring resistance to knockdown by permethrin and bioresmethrin in adults of the BKPM3 strain of *Aedes aegypti*. *Genetica*, 59: 233-237.

Mariconi, F.A.M., 1985. Inseticidas e seu emprego no combate a pragas. 7th edition. Sao Paulo, Nobel, pp. 1-305.

Mariconi, F.A. M., 1963. Inseticidas e seu emprego no combate a pragas*.* Agronomica *Ceres*, Sao Paulo, Brazil.

Martin, R.L., Pittendrigh, B., Liu, J., Reenan, R., ffrench-Constant, R., Hanck, D.A., 2000. Point mutations in domain III of a *Drosophila* neuronal Na^+ channel confer resistance to allethrin. *Insect Biochemistry and Molecular Biology*, 30: 1051-1059.

Martinez-Galera, M., Gil-Garcia, M.D., Rodriguez-Lallena, J.A., Lopez-Lopez, T., Martinez-Vidal, J.L., 2003. Dissipation of pyrethroid residues in peppers, zucchinis, and green beans exposed to field treatments in greenhouses: evaluation by decline curves. *Journal of Agricultural and Food Chemistry,* 51: 5745–5751.

Martinez-Torres, D., Chevillon, C., Brun-Barale, A., Berge, J. B. Pasteur, N., Pauron, D, 1999b. Voltage-dependent Na^+ channels in pyrethroid resistant *Culex pipiens* L mosquitoes. *Pesticide Science*, 55: 1012-1020.

Martinez-Torres, D., Foster, S.P., Field, L.M., Devonshire, A.L., Williamson, M.S., 1999a. A sodium channel point mutation is associated with resistance to DDT and pyrethroid insecticides in the peach-potato aphid, *Myzus persicae* (Sulzer) (Hemiptera: Aphididae). *Insect Molecular Biology*, 8: 339–346.

Martinez-Torres, D., Chandre, F., Williamson, M.S. Darriet, F., Berge, J.B. Devonshire, A.L. Guillet, P., Pasteur, N., 1998. Molecular characterization of pyrethroid knockdown resistance (*kdr*) in the major malaria vector *Anopheles gambiae* s.s. *Insect Molecular Biology*, 7: 179-184.

Martinez-Torres, D., Devonshire, A.L. & Williamson, M.S., 1997. Molecular studies of knockdown resistance to pyrethroids: cloning of domain II sodium channel gene sequences from insects. *Pesticide Science*, 51: 265-270.

Mason, L.J., 2003. Grain Insect Fact Sheet, E-237-W: Rice, Granary, and Maize Weevils *Sitophilus oryzae* (L.), *S. granarius* (L.), and *S. zeamais* (Motsch). Purdue University, Department of Entomology.

Mathers, D.A. & Usherwood, P.N.R., 1976. Concanavalin A blocks desensitization of glutamate receptors on insect muscle fibres. *Nature*, 259: 409-411.

McAteer, C.H., Balasubramanian, M. & Murugan, R., 2008. Pyridines and their Benzo Derivatives: Applications. *Comprehensive Heterocyclic Chemistry III*, 7: 309-336.

McKenzie, J.A., 1996. The biochemical and molecular bases of resistance: applications to ecological and evolutionary questions. In: *Ecological and Evolutionary Aspects of Insecticide Resistance* (J.A. McKenzie). Academic, Austin, pp. 123-147.

Mello, E.J.R., 1970. Constatacao de resistencia ao DDT e lindane em *Sitophilus oryzae* (L.) em milho armazenado na localidade de Capinopolis, Minas Gerais. In: *Reuniao Bras. Milho,* Porto Alegre, Brazil, pp. 131-134.

Mercer, E.H., 1963. A scheme for section staining in electron microscopy. *Journal of the Royal Microscopical Society*, 81: 179-186.

Milani, R. & Travaglino, A., 1975. Ricerche sulla resistenza al DDT in Musca domestica concatenazione del gene kdr (knockdown resistance) con due mutant morfologi. *Riv. Paras.*, 18: 199.

Miyazaki, M., Ohyama, K., Dunlap, D.Y., Matsumura, F., 1996. Cloning and sequencing of the *para*-type sodium channel gene from susceptible and *kdr*-resistant German cockroaches (*Blattella germanica*) and housefly (*Musca domestica*). *Molecular and General Genetics,* 252: 61–68.

Morgan, J.A.T., Corley, S.W., Jackson, L.A., Lew-Tabor, A.E., Moolhuijzen, P.M., Jonsson, N.N., 2009. Identification of a mutation in the *para*-sodium channel gene of the cattle tick *Rhipicephalus (Boophilus) microplus* associated with resistance to synthetic pyrethroid acaricides. *International Journal of Parasitology*, 39: 775-779.

Morin, S., Williamson, M.S., Goodson, S.J., Brown, J.K., Tabashnik, B.E., Dennehy, T.J., 2002. Mutations in the *Bemisia tabaci para* sodium channel gene associated with resistance to a pyrethroid plus organophosphate mixture. *Insect Biochemistry and Molecular Biology*, 32: 1781-1791.

Motomura, H. & Narahashi, T., 2001. Interaction of Tetramethrin and Deltamethrin at the Single Sodium Channel in Rat Hippocampal Neurons. *Neuro Toxicology*, 22: 329-339.

Murdock, L.L., Huesing, J.E., Nielsen, S.S., Pratt, R.C., Shade, R.E., 1990. Biological effects of plant lectins on the Cowpea Weevil. *Phytochemistry*, 29: 85-89.

Nakagawa, S., Okajima, N., Kitahaba, T., Nishimura, K., Fujita, T., Nakajima, M., 1982. Quantitative structure-activity studies of substituted benzyl chrysanthemates. 1. Correlations between symptomatic and neurophysiological activities against American cockroaches. *Pesticide Biochemistry and Physiology,* 17: 243-258.

Narahashi, T., 2002. Nerve membrane ion channels as the target site of insecticides. *Mini Reviews in Medicinal Chemistry,* 2: 419-432.

Narahashi, T., 1998. Chemical modulation of sodium channels. In: *Ion Channel Pharmacology* (Soria, B. and Cena, V., Eds.), Oxford University Press, Oxford, UK, pp. 23-73.

Narahashi, T., 1996. Neuronal ion channels as the target sites of insecticides. *Pharmacology and Toxicology,* 78:1–14.

Narahashi, T., 1992. Nerve membrane sodium channels as targets of insecticides. *Trends in Pharmacological Sciences*, 13: 236-241.

Narahashi, T., 1988. Molecular and cellular approaches to neurotoxicology: past, present and future. In: Lunt, G.G. (Ed.), *Neurotox '88: Molecular Basis of Drug and Pesticide Action*. Elsevier, New York, pp. 563–582.

Naumann, K., 1990. Synthetic Pyrethroid Insecticides: Structures and Properties. Springer-Verlag, Berlin, pp. 3-191.

Oliveira, E.E., Guedes, R.N.C., Totola, M.R., De Marco Jr., P., 2007. Competition between insecticide-susceptible and –resistant populations of the maize weevil, *Sitophilus zeamais*. *Chemosphere*, 69: 17-24.

O'Reilly, A.O., Khambay, B.P.S., Williamson, M.S., Field, L.M., Wallace, B.A., Davies, T.G.E., 2006. Modelling insecticide-binding sites in the voltage-gated sodium channel. *Biochemical Journal*, 396: 255-263.

Pacheco, I.A., Sartori, M.R., Bolonhezi, S., 1990. Resistance to malathion, pirimiphos-methyl and fenitrothion in Coleoptera from stored grains. In: *Proceeding 5th International Working Conference on Stored-Product Protection*. (Edited by Fleurrat-Lessard, F. & Ducom, P.), Bordeaux, France, pp. 1029-1037.

Park, Y. & Taylor, M.F., 1997. A novel mutation L1029H in sodium channel *hscp* associated with pyrethroid resistance for *Heliothis virescens* (Lepidoptera: Noctuidae). *Insect Biochemistry and Molecular Biology,* 27: 9–13.

Park, Y., Taylor, M.F., Feyereisen, R., 1997. A valine421 to methionine mutation in IS6 of the *hscp* voltage-gated sodium channel associated with pyrethroid resistance in *Heliothis virescens* F. *Biochemical and Biophysical Research Communications*, 239: 688-691.

Peng, F., Mellor, I.R., Williamson, M.S., Emyr Davies, T.G., Field, L.M., Usherwood, P.N.R., 2009. Single channel study of deltamethrin interactions with wild-type and mutated rat $Na_v1.2$ sodium channels expressed in *Xenopus* oocytes. *Neuro Toxicology*, 30: 358-367.

Pereira, C.J., Pereira, E.J.G., Cordeiro, E.M.G., Della Lucia, T.M.C., Totola, M.R., Guedes, R.N.C., 2009. Organophosphate resistance in the maize weevil *Sitophilus zeamais*: Magnitude and behaviour. *Crop Protection*, 28: 168-173.

Pfeiffer, W.D., 2008. 1,3,4-Oxadiazines and 1,3,4-Thiadiazines. *Comprehensive Heterocyclic Chemistry III*, 9: 401-455.

Pimentel, M.A.G., Faroni, L.R.D'A., Guedes, R.N.C., Sousa, A.H., Totola, M.R., 2009. Phosphine resistance in Brazilian populations of *Sitophilus zeamais* Motschulsky (Coleoptera: Curculionidae). *Journal of Stored Products Research*, 45: 71-74.

Pittendrigh, B.R. & Gaffney, P.J., 2001. Pesticide resistance: Can we make it a renewable resource? *Journal of Theoretical Biology,* 211, 365-375.

Plapp, F.W., 1976. Biochemical genetics of insecticide resistance. *Annual Review of Entomology*, 21: 179-197.

Powell, K.S., Spence, J., Bharathi, M., Gatehouse, J.A., Gatehouse, A.M.R., 1998. Immunohistochemical and development studies to elucidate the mechanism of action of the snowdrop lectin on the rice brown planthopper, *Nilaparvata lugens* (Stal). *Journal of Insect Physiology*, 44: 529-539.

Priester, T.M. & Georghiou, G.P., 1980. Cross-resistance spectrum in pyrethroid-resistant *Culex quinquefasciatus*. *Pesticide Science*, 11: 617-624.

Ptacek, L. & Griggs, R.C., 1996. Familial periodic paralysis, In: *Molecular Biology of Membrane Transport Disorders* (Schultz, S.G., Ed.), Plenum, New York, pp. 625-642.

Ranson, H., Jensen, B., Vulule, J.M., Wang, X., Hemingway, J., Collins, F.H., 2000. Identification of a point mutation in the voltage-gated sodium channel gene of Kenyan *Anopheles gambiae* associated with resistance to DDT and pyrethroids. *Insect Molecular Biology*, 9: 491-497.

Ray, D., 2010. Organochlorine and Pyrethroid Insecticides. *Comprehensive Toxicology*, 13: 445-457.

Ray, D.E., 2001. Pyrethroid insecticides: mechanisms of toxicity, systemic poisoning syndrome, paresthesia and therapy, 2nd Edition. In: Kreiger R., editor. *Handbook of Pesticide Toxicology*, vol. 2. San Diego, CA: Academic Press, pp. 1289–303.

Ray, D.E., Sutharasan, S., Forshaw. P.J., 1997. Action of pyrethroid insecticides on voltage-gated chloride channels in neuroblastoma cells. *Neuro Toxicology*, 18: 755–60.

Rees, D.P., 1996. Coleoptera. In: Subramanyam, Bh. & Hagstrum, D.W. (Eds) *Integrated Management of Insects in Stored Products*. New York, Marcel Dekker, pp. 1-39.

Ribeiro, B., Guedes, R.N.C., Correa, A.S., Santos, C.T., 2007. Fluctuating Assimetry in Insecticide-Resistant and Insecticide-Susceptible Strains of the Maize Weevil, *Sitophilus zeamais* (Coleoptera: Curculionidae). *Archives of Environmental Contamination and Toxicology*, 53: 77-83.

Ribeiro, B.M., Guedes, R.N.C., Oliveira, E.E., Santos, J.P., 2003. Insecticide resistance and synergism in Brazilian populations of *Sitophilus zeamais* (Coleoptera: Curculionidae). *Journal of Stored Product Research*, 39: 21-31.

Riskallah, M.R., Abd-Elghafar, S.F., Abo-Elghar, M.R., Nassar, M.E., 1983. Development of resistance and cross-resistance in fenvalerate and deltamethrin selected strains of *Spodoptera littoralis* (Boisd.). *Pesticide Science*, 14: 508-512.

Roditakis, E., Tsagkarakou, A., Vontas, J., 2006. Identification of mutations in the *para* sodium channel of *Bemisia tabaci* from Crete associated with resistance to pyrethroids, *Pesticide Biochemistry and Physiology*, 85: 161-166.

Roush, R.T., Mckenzie, J.A., 1987. Ecological genetics of insecticide and acaricide resistance. *Annual Review of Entomology*, 32: 361–380.

Rudy, B., 1988. Diversity and ubiquity of K^+ channels. *Neuroscience*, 25: 729-749.

Salazar, H., Llorente, I., Jara-Oseguera, A., Garcia-Villegas, R., Munari, M., Gordon, S.E., Islas, L.D., Rosenbaum, T., 2008. A single N-terminal cysteine in TRPV1 determines activation by pungent compounds from onion and garlic. *Nature Neuroscience*, 11: 255-261.

Salkoff, L., Butler, A., Wei, A., Scavarda, N., Giffen, K., Ifune, C., Goodman, R., Mandel, G., 1987. Genomic organization and deduced amino acid sequence of a putative sodium channel gene in *Drosophila*. *Science,* 237: 744–748.

Santos, J.P., Maia, J.D.G., Crux I., 1990. Efeito da infestacao pelo gorgulho *(Sitophilus zeamais) e* traca *(Sirotroga cerealella)* sobre a germinacao de sementes de milho. *Pesquisa Agropecuaria Brasileira*, 25*:* 1687-1692.

Santos J.P., Bitran, E., Nakano 0., 1988. Avaliacao residual de diversos inseticidas para a protecao de sementes de miiho contra insetos durante o armazenamento. In: *Anais 16º Congresso Nacional de Milho,* Brasilia, Brazil, pp. 268-275.

Sauvion, N., Nardon, C., Febvay, G., Gatehouse, A.M.R., Rahbe, Y., 2004. Binding of the insecticidal lectin Concanavalin A in pea aphid, *Acyrthosiphon pisum* (Harris) and induced effects on the structure of midgut epithelial cells. *Journal of Insect Physiology*, 50: 1137-1150.

Sawicki, R.M., 1978. Unusual response of DDT-resistant house-flies to carbinol analogues of DDT. *Nature*, 275: 443-444.

Schneider, I. & Blumenthal, F., 1978. Drosophila cell and tissue culture. In: *The Genetics and Biology of Drosophila Vol IIa* (M. Ashburner and Wright, T.R.F., eds.). Academic Press Inc., New York, pp. 265-315.

Schuler, T.H., Martinez-Torres, D., Thompson, A.J., Denholm, I., Devonshire, A.L., Duce, I.R. & Williamson, M.S., 1998. Toxicological, Electrophysiological, and Molecular Characterization of Knockdown Resistance to Pyrethroid Insecticides in the Diamondback Moth, *Plutella xylostella* (L.). *Pesticide Biochemistry and Physiology*, 59: 169-182.

Scott, J.G., Croft, B.A., Wagner, S.W., 1983. Studies on the mechanism of permethrin resistance in *Amblysius fallacies* (Acarina: Phystoseiidae) relative to previous insecticide use on apple. *Journal of Economic Entomology*, 76: 6-10.

Shafer, T.J., Meyer, D.A., Crofton, K.M., 2005. Developmental Neurotoxicity of Pyrethroid Insecticides: Critical Review and Future Research Needs. *Environmental Health Perspectives*, 113: 123-136.

Shafer, T.J. & Meyer, D.A., 2004. Effects of pirethroids on voltage-sensitive calcium channels: a critical evaluation of strengths, weaknesses, data needs and relationship to assessment of cumulative neurotoxicity. *Toxicology and Applied Pharmacology*, 196: 303-318.

Sharifi, S. & Mills, R.B., 1971. Radiographic studies of *Sitophilus zeamais* Mots. in wheat kernels. *Journal of Stored Products Research*, 7: 195-206.

Smith, A.G., 2010. Toxicology of DDT and Some Analogues. *Hayes' Handbook of Pesticide Toxicology*. Third Edtition. 1975-2032.

Smith, T.J., Lee, S.H., Ingles, P.J., Knipple, D.C., Soderlund, D.M., 1997. The L1014F point mutation in the house fly *Vssc1* sodium channel confers knockdown resistance to pyrethroids. *Insect Biochemistry and Molecular Biology,* 27: 807–812.

Soderlund, D.M., 2005. Comprehensive Molecular Insect Science. In: Gilbert, L.I.; Iatrow, K. & Gill, S.S. (Eds), vol. 5. Elsevier Pergamon, San Diego, pp. 1-24.

Soderlund, D.M. & Knipple, D.C., 2003. The molecular biology of knockdown resistance to pyrethroid insecticides. *Insect Biochemistry and Molecular Biology,* 33: 563–577.

Soderlund, D.M., Clark, J.M., Sheets, L.P., Mullin, L.S., Piccirillo, V.J., 2002. Mechanism of pyrethroid nerotoxicity: implications for cumulative risk assessment. *Toxicology*, 171: 3-59.

Soderlund, D.M., 1997. Molecular mechanisms of insecticide resistance. In: *Molecular mechanisms of resistance to agrochemicals* (Ed. V. Sjut), Springer-Verlag, Heidelberg *,* pp. 21-56.

Soderlund, D.M. & Bloomquist, J.R., 1990. Molecular mechanisms of insecticide resistance. In: Roush R. T. & Tabashnik, B. E. (eds) *Pesticide resistance in arthropods*. Chapman and Hall, New York, pp. 58-96.

Soderlund, D.M. & Bloomquist, J.R., 1989. Neurotoxic actions of pyrethroid insecticides. *Annual Review of Entomology*, 34: 77-96.

Song, J.H., Nagata, K., Tatebayashi, H. & Narahashi, T., 1996. Interactions of tetramethrin, fenvalerate and DDT at the sodium channel in rat dorsal root ganglion neurons. *Brain Research,* 708: 29–37.

Song, W., Liu, Z., Tan, J., Nomura, Y., Dong, K., 2004. RNA editing generates tissue-specific sodium channels with distinct gating properties. *The Journal of Biological Chemistry*, 279: 32554-32561.

Standker, L., Beress, L., Garateix, A., Christ, T., Ravens, U., Salceda, E., Soto, E., John, H., Forssmann, W.-G., Aneiros, A., 2006. A new toxin from the sea anemone Condylactis gigantea with effect on sodium channel inactivation. *Toxicon*, 48: 211-220.

Stanfield, P.R., 1983. Tetraethylammonium ions and the potassium permeability of excitable cells. *Reviews of Physiology, Biochemistry and Pharmacolology*, 97: 1-67.

Stankiewicz, M., Grolleau, F., Lapied, B., Borchani, L., El Ayeb, M., Pelhate, M., 1995. Bot IT2, a Toxin Paralytic to Insects from the Buthus occitanus tunetanus Venom Modifying the Activity of Insect Sodium Channels. *Journal of Insect Physiology*, 42: 397-405.

Staudinger, H. & Ruzicka, L., 1924. Insektentotende stoffe. I-IV and VIII-X. *Helvetica Chimica Acta*, 7: 177-458.

Storey, C.L., 1987. Effect and control of insects affecting corn quality. In: Watson, S.A., Ramstad, P.E. (Eds.), *Corn Chemistry and Technology*. American Association of Cereal Chemists, St. Paul, pp. 185–199.

Strong, J.A., Fox, A.P., Tsien, R.W., Kaczmarek, L.K., 1987. Stimulation of protein kinase C recruits covert calcium channels in *Aplysia* bag cell neurons. *Nature*, 325: 714-717.

Subramanyam, B.H. & Hagstrum, D.W., 1996. Resistance measurement and management. In: Subramanyam, Bh. & Hagstrum, D.W. (*Eds*) *Integrated Management of Insects in Stored Products*. New York, Marcel Dekker, pp. 331-397.

SupYoon, K., Symington, S.B., Lee, S.H., Soderlund, D.M., Clark, J.M., 2008. Three mutations identified in the voltage-sensitive sodium channel α-subunit gene of permethrin-resistant human head lice reduce the permethrin sensitivity of housefly *Vssc1* sodium channels expressed in *Xenopus* oocytes. *Insect Biochemistry and Molecular Biology*, 38: 296-306.

Symington, S.B. & Clark, J.M., 2005. Action of deltamethrin on N-type ($Ca_V2.2$) voltage sensitive calcium channels in rat brain. *Pesticide Biochemistry and Physiology*, 82: 1–5.

Szallasi, A. & Blumberg, P.M., 1999. Vanilloid (capsaicin) receptors and mechanisms. *Pharmacological Reviews*, 51: 159-212.

Tabarean, I.V. & Narahashi, T., 1998. Potent modulation of tetrodotoxin-sensitive and tetrodotoxin-resistant sodium channels by the type II pyrethroid deltamethrin. *Journal of Pharmacological and Experimental Therapeutics.,* 284: 958–965.

Takayama, C., 2008. History of insecticides and the transition of their production and sales. *Chudoku Kenkyu*, 21:123-31.

Tan, J.G., Liu, Z.Q., Nomura, Y., Goldin, A.L., Dong, K., 2002a. Alternative splicing of an insect sodium channel gene generates pharmacologically distinct sodium channels*. Journal of Neuroscience,* 22: 5300-5309.

Tan, J., Liu, Z., Tsai, T.-D., Valles, S.M., Goldin, A.L. Dong, K., 2002b. Novel sodium channel gene mutations in *Blattella germanica* reduce the sensitivity of expressed channels to deltamethrin. *Insect Biochemistry and Molecular Biology,* 32: 445–454.

Tatebayashi, H. & Narahashi, T., 1994. Differential mechanism of action of the pirethroid tetramethrin on tetrodotoxin-sensitive and tetrodotoxin-resistent sodium channels. *Journal of Pharmacology and Experimental Therapeutics,* 270: 595-603.

Temple, W. & Smith, N.A., 1996. Insecticides. *Human Toxicology*, 541-550.

Temraz, T.A., Houssen, W.E., Jaspars, M., Woolley, D.R., Wease, K.N., Davies, S.N., Scott, R.H., 2006. A pyridinium derivative from Red Sea soft corals inhibited voltage-activated potassium conductances and increased excitability of rat cultured sensory neurones. *BMC Pharmacology*, 6:10, doi:10.1186/1471-2210-6-10.

Terlau, H.K., Shon, M., Grilley, M., Stocker, W., Stuhmer, W., Oliveira, B.M., 1996. Strategy for rapid immobilization of prey by a fish-hunting marine snail. *Nature*, 381: 148-151.

Thompson, A.J., 1998. Actions of pyrethroids on sodium channels. University of Nottingham. PhD thesis.

Throne, J.E., 1994. Life history of immature maize weevils (Coleoptera: Curculionidae) on corn stored at constant temperatures and relative humidities in the laboratory. *Environmental Entomology*, 23: 1459–1471.

Toda, S. & Morishita, M., 2009. Identification of Three Point Mutations on the Sodium Channel Gene in Pyrethroid-Resistant *Thrips tabaci* (Thysanoptera: Thripidae). *Journal of Economic Entomology*, 102: 2296-2300.

Tomita, T., Yaguchi, N., Mihara, M., Takahashi, M., Agui, N., Kasai, S., 2003. Molecular analysis of a *para* sodium channel gene from pyrethroid-resistant head lice, *Pediculus humanus capitis* (Anoplura: Pediculidae). *Journal of Medical Entomology*, 40: 468-474.

Tribut, F., Lapied, B., Duval, A., Pelhate, M., 1991. A neosynthesis of sodium channels is involved in the evolution of the sodium current in isolated adult DUM neurons. *Pflugers Archives*, 419: 665-667.

USDA, 1980. Stored-Grain Insects. Washington, DC, ARS-USDA, 43 pp.

Usherwood, P.N.R., Davies, T.G.E., Mellor, I.R., O'Reilly, A.O., Peng, F., Vais, H., Khambay, B.P.S., Field, L.M., Williamson, M.S., 2007. Mutations in DIIS5 and the DIIS4-S5 linker of *Drosophila melanogaster* sodium channel define binding domains for pyrethroids and DDT. *FEBS Letters*, 581: 5485-5492.

Usherwood, P.N.R., Vais, H., Khambay, B.P.S., Davies, T.G.E., Williamson, M.S., 2005. Sensitivity of the *Drosophila para* sodium channel to DDT is not lowered by the super-*kdr* mutation M918T on the IIS4-S5 linker that profoundly reduces sensitivity to permethrin and deltamethrin. *FEBS Letters*, 579: 6317-6325.

Vais, H., Atkinson, S., Pluteanu, F., Goodson, S.J., Devonshire, A.L., Williamson, M.S., Usherwood, P.N.R., 2003. Mutations of the *para* sodium channel of *Drosophila melanogaster* identify putative binding sites for pyrethroids. *Molecular Pharmacology*, 64: 914-922.

Vais, H., Williamson, M.S., Devonshire, A.L., Usherwood, P.N.R, 2001. The molecular interactions of pyrethroid insecticides with insect and mammalian sodium channels. *Pest Management Science,* 57: 877–888.

Vais, H., Williamson, M.S., Goodson, S.J., Devonshire, A.L., Warmke, J.W., Usherwood, P.N.R., Cohen, C.J., 2000a. Activation of *Drosophila* sodium channels promotes modification by deltamethrin. Reductions in affinity caused by knock-down resistance mutations. *Journal of General Physiology,* 115: 305–318.

Vais, H., Atkinson, S., Eldursi, N., Devonshire, A.L., Williamson, M.S., Usherwood, P.R.N., 2000b. A single amino acid change makes a rat neuronal sodium channel highly sensitive to pyrethroid insecticides. *FEBS Letters*. 470: 135-138.

Vais, H., Williamson, M.S., Devonshire, A.L., Warmke, J,W., Usherwood, P.R.N., Cohen, C.J., 1998. Knock-down resistance mutations confer insensitivity to deltamethrin on *Drosophila para* sodium channels. *Biophysical Journal*, 74: A149.

Van der Berg, H., 2009. Global Status of DDT and Its Alternatives for Use in Vector Control to Prevent Disease. Environmental Health Perspectives, 117: 1656-1663.

Verdin, P.S., 2008. Molecular Interactions of Pyrethroid Insecticides with Insect Ion Channels. University of Nottingham. PhD thesis.

Verhaeghen, K., Bortel, W.V., Trung, H.D., Sochantha, T., Coosemans, M., 2009. Absence of knockdown resistance suggests metabolic resistance in the main malaria vector of the Mekong region. *Malaria Journal*, 8:84, doi:10.1186/1475-2875-8-84.

Verschoyle, R.D. & Aldridge, W.N., 1980. Structure–activity relationships of some pyrethroids in rats. *Archives of Toxicology*, 45:325–9.

Vezenegho, S.B., Bass, C., Puinean, M., Williamson, M.S., Field, L.M., Coetzee, M., Koekemoer, L.L., 2009. Development of multiplex real-time PCR assays for identification of members of the *Anopheles funestus* species group. *Malaria Journal*, 8: 282.

Vignali, S., Leiss, V., Karl, R., Hofmann, F., Welling, A., 2006. Characterization of voltage-dependent sodium and calcium channels in mouse pancreatic A- and B-cells. *Journal of Physiology*, 572: 691-706.

Vijverberg, H.P.M., van der Zalm, J.M., van der Bercken, J., 1982. Similar mode of action of pyrethroids and DDT on sodium channel gating in myelinated nerves. *Nature*, 295: 601-603.

Vijverberg, H.P. & van den Bercken, J., 1979. Frequency-dependent effects of the pyrethroid insecticide decamethrin in frog myelinated nerve fibres. *European Journal of Pharmacology,* 58: 501–504.

Xu, Q., Liu, H. Zhang, L., Liu, N., 2005. Resistance in the mosquito *Culex quinquefasciatus*, and possible mechanisms for resistance. *Pest Management Science*, 61: 1096-1102.

Wang, R., Huang, Z.Y., Dong, K., 2003. Molecular characterization of an arachnid sodium channel gene from the varroa mite (*Varroa destructor*). *Insect Biochemistry and Molecular Biology,* 33: 733–739.

Wang, S.-Y. & Wang, G.K., 2003. Voltage-gated sodium channels as primary targets of diverse lipid-soluble neurotoxins. *Cellular Signalling*, 15, 151-159.

Ware, G.W., 1994. Insecticides. In: *Pesticide Book* (4th edition). Thomson Publ., Fresno, CA, 41-54.

Warmke, J.W., Reenan, R.A., Wang, P., Qian, S., Arena, J.P., Wang, J., Wunderler, D., Liu, K., Kaczorowski, G.J., Van der Ploeg, L.H., Ganetzki, B., Cohen, C.J., 1997. Functional expression of *Drosophila para* sodium channels. Modulation by the membrane protein *tipE* and toxin pharmacology. *Journal of General Physiology,* 110: 119–133.

Weston, A.J. & Baines, R.A., 2007. Translational regulation of neuronal excitable properties. *Invertebrate Neuroscience*, 7: 75-86.

White, N.D.G. & Leesch, J.G., 1996. Chemical control. In: Subramanyam, Bh. & Hagstrum, D.W. (*Eds*) *Integrated Management of Insects in Stored Products*. New York, Marcel Dekker, pp. 287-330.

Wilhelm, J. & Pingoud, A., 2003. Real-Time Polymerase Chain Reaction. *ChemBioChem*, 4: 1120-1128.

Williamson, M.S., Anstead, J.A., Devine, G.J., Devonshire, A.L., Field, L.M., Foster, S.P., Moores, G.D., Denholm, I., 2003. Insecticide resistance: from science to practice. In: *Proc Br Crop Prot Conf-Crop Sci and Technol*, BCPC, Farnham, Surrey, UK, pp. 681-688.

Williamson, M.S., Martinez-Torres, D., Hick, C.A., Devonshire, A.L., 1996. Identification of mutations in the housefly *para*-type sodium channel gene associated with knockdown resistance (*kdr*) to pyrethroid insecticides. *Molecular and General Genetics*, 252: 51–60.

Wittwer, C.T., Reed, G.H., Gundry, C.N., Vandersteen, J.G., Pryor, R.J., 2003. High-resolution genotyping by amplicon melting analysis using LCGreen. *Clinical Chemistry,* 49: 853-860.

Wittwer, C.T., Herrmann, M.G., Moss, A.A., Rasmussen, R.P., 1997. Continuous fluorescence monitoring of rapid cycle DNA amplification. *BioTechniques*, 22: 130-131, 134-138.

Yamamoto, R., 1925. On the insecticidal principle of insect powder. *Inst Phys Chem Res Tokyo*, 3: 193.

Yamamoto, R., 1923. The insecticidal principle in *Chrysanthemum cinerariaefolium*. Part II and III. On the constitution of pyrethronic acid. *Journal of the Chemistry Society of Japan*, 44: 311-330.

Yang, X.-C. & Sachs, F., 1989. Block of stretch-activated ion channels in *Xenopus* oocytes by gadolinium and calcium ions. *Science*, 243, 1068-1071.

Yeung, S.Y.M., Thompson, D., Wang, Z., Fedida, D., Robertson, B., 2005. Modulation of K_v3 subfamily potassium currents by the sea anemone toxin BDS: significance for CNS and biophysical studies. *Journal of Neuroscience*, 25: 8735-8745.

Yoon, K. S., 2006. Detection and mechanism of pediculicide resistance in the human head louse, *Pediculus capitis*. University of Massachussetts. PhD Thesis.

Yu, F.H., Catterall, W.A., 2003. Overview of the voltage-gated sodium channel family. *Genome Biology*, 4:207, doi:10.1186/gb-2003-4-3-207.

Zhang, H.-G., ffrench-Constant, R.H., Jackson, M.B., 1994. A unique amino acid of the *Drosophila* GABA receptor with influence on drug sensitivity by two mechanisms. *Journal of Physiology*, 479: 65-75.

Zhao, Y., Park, Y., Adams, M.E., 2000. Functional and Evolutionary Consequences of Pyrethroid Resistance Mutations in S6 Transmembrane Segments of a Voltage-Gated Sodium Channel. *Biochemical and Biophysical Research Communications*, 278: 516-521.

Zhou, W., Chung, I., Liu, Z., Goldin, A.L., Dong, K., 2004. A Voltage-Gated Calcium-Selective Channel Encoded by a Sodium Channel-like Gene. *Neuron*, 42: 101–112.

Zufall, F., Stengl, M., Franke, C., Hildebrand, J.G., Hatt, H., 1991. Ionic currents of cultured olfactory receptor neurons from antennae of male *Manduca sexta*. *Journal of Neuroscience*, 11: 956-965.

Appendix I

External morphology of *S. zeamais* is revealed by scanning electron microscopy

For Scanning Electron Microscopy, six maize weevils were collected and serially dehydrated in ethanol (70% for 2h; 90 and 100% for 30min each). They were dried using liquid carbon dioxide in a Polaron E3000 Critical Point Drying Apparatus, stuck on aluminium stubs with Quick Drying Silver Paint, coated with gold using a Polaron E5100 Coating Unit and examined using a Jeol JSM840 scanning electron microscope (Pictures A-H).

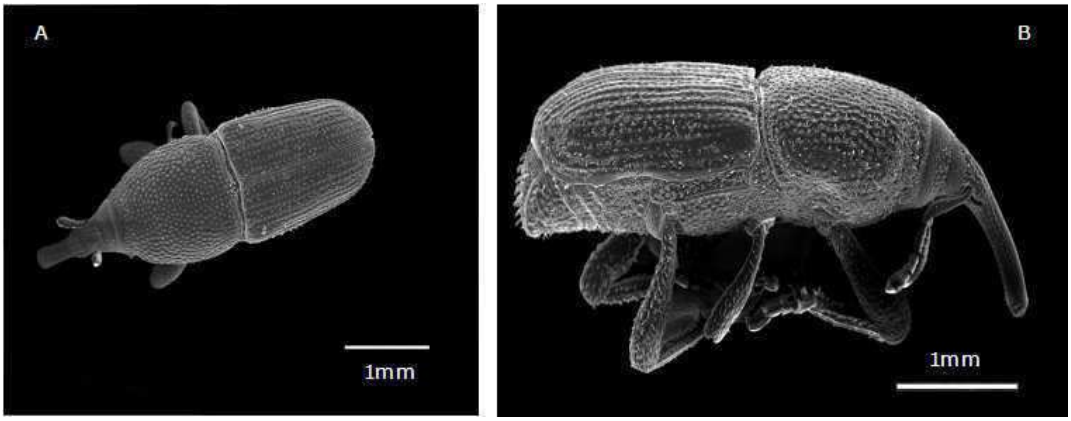

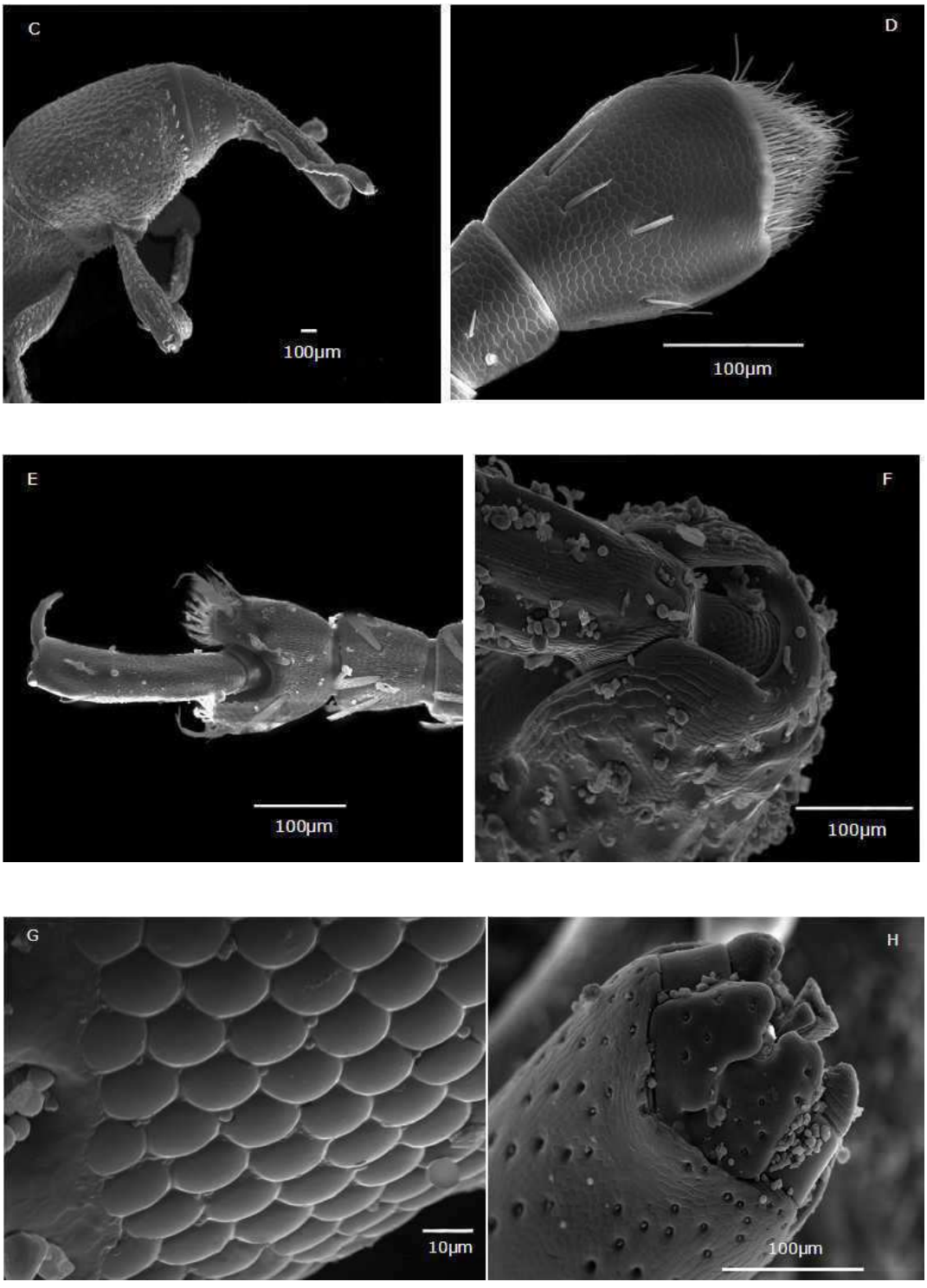

A-H: Scanning electron microscopy of *S. zeamais* adult. (A) dorsal view; (B) lateral view; (C) head of *S. zeamais*; (D) detail of the antennae; (E) detail of the claw; (F) detail of the leg joint; (G) detail of the eye; (H) detail of the snout.

Images A, B and C show this insect in different positions with a very hard exoskeleton covering the body. Details of the antennal sensillae appear in image D and details of the claw and joint leg are showed in the images E and F. The group of ommatidia composing the eye of *S. zeamais* appears in image G and image H shows details of the snout with all of the buccal components that constitute the mouth.

Scanning electron microscopy illustrated that weevils are covered with a very robust exoskeleton to protect them against mechanical injuries and loss of water. These insects live within the stored maize grain, a very dry environment with an average humidity of 13%. Their legs and claws are highly articulated, allowing them to move quickly and to gain access to maize kernels. The well developed mouthparts help the insect to cut ingest and chew the maize grain.